Chemical Simulation of Hydrogen Generation in a Plasma Fuel Reformer

by

Nuria Margarit Bel

Diploma in Chemical Engineering
Chemical Institute of Sarria, Ramon Llull University, 2001

SUBMITTED TO THE DEPARTMENT OF MECHANICAL ENGINEERING
IN PARTIAL FULFILLMENT OF THE DEGREE OF

MASTER OF SCIENCE IN AERONAUTICS AND ASTRONAUTICS
at the

MASSACHUSETTS INSTITUTE OF TECHNOLOGY

February 2004

Signature of Author .....
Department of Aeronautics and Astronautics
January 2004

Certified by .....
John B. Heywood
Sun Jae Professor of Mechanical Engineering
Thesis Supervisor

Accepted by .....
Edward M. Greitzer
H.N. Slater Professor of Aeronautics and Astronautics
Chair, Committee on Graduate Students

Chemical Simulation of Hydrogen Generation in a Plasma Fuel Reformer

by

Nuria Margarit Bel

Submitted to the Department of Aeronautics and Astronautics
January, 2004 in Partial Fulfillment of the
requirements for the Degree of Master of Science
at the Massachusetts Institute of Technology

ABSTRACT

A model for a plasma fuel reformer or plasmatron has been developed. The model was based in a series of experiments realized at the Plasma Science and Fusion Center with such a plasmatron. The device is set up to produce syngas (hydrogen and carbon monoxide gas mixture) from partial oxidation of any hydrocarbon. We studied the behavior of methane as fuel and used the GRI methane combustion mechanism in our simulations. The goal was to characterize the reactor to be able to understand and predict its performance for a wide range of operating conditions, such as different flow rates, air to fuel flow ratio or power supply.

The simulation tool used for this purpose was CHEMKIN 3.7. The fuel reformer was designed as a reactor where combustion is initiated by an electric discharge due to ohmic heating of the arc region. Two different types of reactors were used to model the plasmatron. The Plug Flow Reactor (PLUG) assumed a homogenous zero-dimensional closed system. The Partially Stirred Reactor (PASR) considered random mixing determined by a frequency mixing parameter, which is directly dependant of the system fluid dynamic properties.

Experimental results with methane generated 6%-7% molar of hydrogen and 5% of carbon monoxide. Hydrogen and oxygen balance evidenced that water and carbon dioxide are important co-products, obtaining respectively 10% and 3% at the exhaust. Also 15%-20% of methane and 3%-5% of oxygen remained unreacted. From discharge observations, energy estimations and model simulations, it was found that the electric arc initiates combustion by locally rising the temperature and then propagating the reaction by heat and mass transfer/mixing to the surroundings. Simulation results demonstrated that there is an optimum characteristic mixing time for each residence time, depending on the initial temperature reached at the arc. It was also found that the more spread the energy is, or the more mass is heated to a moderate temperature, the better the performance results.

Thesis Supervisor: John B. Heywood
Title: Sun Jae Professor of Mechanical Engineering

ACKNOWLEDGMENTS

First of all, I would like to thank Professor Heywood and Dr. Leslie Bromberg. Their wisdom and support have been of great assistance on my research. They taught me how to develop my reasoning skills and how to ask for help when required. This thesis has been possible thanks to their unconditional trust and guidance.

Alex Rabinovich and all the scientist working in the PSFC developing the plasmatron provided me with the knowledge and the data I needed for this project to go on. Thanks to them all.

My friends in the Sloan Automotive Laboratory and at MIT contributed to my well-being during the graduate student years, but above them all, I want to thank Jennifer Topinka, because she has always been a wonderful mate.

Finally, I would like to thank my family and friends back in Spain, because I owe them being here. They always encouraged me to come to MIT and now I am glad I listened to them!

This research was supported by Arvin Meritor. Thanks to their interest in computation I have been able to finish this work.

To Ernesto, for being there, for little things...

Chapter 1

INTRODUCTION TO PLASMA FUEL REFORMING

The technology for a plasma fuel reformer has been developed at the MIT Plasma Science and Fusion Center (PSFC). This specific device, also called a plasmatron, is the subject of study in this present thesis. Its posterior use and benefits onboard of engine-driven vehicles are briefly commented on as an introduction. An outline of the plasmatron functioning mode and the purpose of modeling it are reported as well in this chapter.

1.1 Hydrogen benefits in Spark Ignition (SI) Internal Combustion Engines (ICE)

Hydrogen gas (H_2) is a small molecule with particular properties. Its size, its low density and its rapid diffusivity confer it the ability to rapidly dissipate. As a direct consequence, hydrogen as fuel has a very high flame speed. When mixed with other fuels, helps increase flame speed and improve engine combustion stability as proved by [Tully, 2002]. Due to higher flame stability for fuel-hydrogen mixtures, the possibility for engines to run effectively ultra-lean arises, engines can burn mixtures with low fuel content without misfire.

Running the engine ultra-lean provides several advantages. Lean operation means higher engine efficiency, lower combustion temperature and hence, important reduction in NOx emissions. An engine working with hydrogen addition can be redesigned to have a higher compression ratio and thus, higher efficiency can be achieved. Due to the higher heat capacity of the new mixture inside the cylinder, combustion reaches more moderate temperatures. When having lower combustion temperatures, the engine will produce less NOx, because nitric oxide formation is directly related to temperature conditions [Bromberg, 2000].

However, mixing hydrogen with fuel in SI engines is not always feasible. One of the main issues with H_2 gas is the difficulty of handling and storage. Therefore, being able to generate hydrogen onboard of vehicles results in a positive solution for ICE use.

When burning any hydrocarbon (HC) in a combustor with low content in oxygen (O_2) or air, we say we are reforming the fuel. Instead of achieving complete combustion of the hydrocarbon into water (H_2O) and carbon dioxide (CO_2), we can ideally obtain a gas mixture of hydrogen and carbon monoxide (CO). This mixture is often referred as synthesis gas mixture or syngas. The actual gas mixture that is produced in the plasmatron and routed to the ICE together with more gasoline is close to this ideal mixture.

The presence of CO in addition to pure hydrogen has been proved to be beneficial in hydrogen-enhanced engines [Topinka, 2003]. The CO-H_2 mixture helps inhibit knock by slowing the autoignition reactions and by accelerating the flame speed (mainly due to H_2 presence, as commented before). Carbon monoxide is a molecule with chemical energy content that can be combusted into CO_2 releasing heat and also be counted as a dilutant in terms of lean operation.

The plasmatron is in fact a small combustor (20 cm to 30 cm long) that can be placed onboard. Besides, it requires low energy supply (200 W to 900 W power source) and it is directly feed by the same fuel used in the vehicle, producing syngas as it is required.

In order to control the syngas diverted to the plasmatron, we need to understand how the device functions and responds to any change in conditions. Thus, a comprehensive model than can predict such behavior would be specially useful.

1.2 Objectives of modeling effort

A model is a representation of an object or device. Its main goal is to schematically describe the system for its known or inferred properties for further study of its characteristics. For our particular system we required a simulation tool capable of reproducing the

behavior of the plasma fuel reformer or plasmatron. Once this first step is achieved, the same tool must be able to predict the plasmatron performance under different conditions.

The plasmatron is a combustor, i.e., a very specific type of chemical reactor. Knowing the geometrical characteristics of the same, we opted to use CHEMKIN to perform our modeling task. CHEMKIN is a software system for solving complex chemical kinetics problems. The program consists of a collection of applications. Each application represents a different chemical reactor model. In particular we are interested in two types of reactors: the Plug Flow Reactor (PFR or PLUG) and the Partially Stirred Reactor (PASR). We will describe their particular characteristics in Chapter 3.

1.2.1 Study of device performance

The first step in the modeling process is the study of the object or device performance. Being the model of a real system, we are interested in the particular behavior of such item for a wide range of operation. Also, we need to understand the geometry and setup of the whole.

The researchers at the PSFC provided us with experimental data for different plasmatron tests using methane as fuel. They ran experiments varying input parameters such as air flow rate, oxygen content in air, fuel flow rate and oxygen to fuel flow ratio. They also supplied information about the geometry of the plasmatron, the energy supplied to the system, the number of streams entering the reactor and images of the arc plasma discharge. All the various parameters and results will be described in detail in Chapter 2.

1.2.2 Prediction of behavior

The idea of having a faithful representation of the system is necessary to predict the plasmatron performance in a broad variety of conditions. The model is already based on a wide operation range.

The steps to create a model involve:

- first, understand the physical and chemical behavior of the system,
- second, reproduce the experimental results,
- then, perform parametric variations,
- and finally, validate the model for predicted values.

When these four steps are completed, the model can be utilized: either to predict behaviors for different setups, or the opposite, to optimize setups to obtain desired behaviors.

In our particular case, only the first two steps were accomplished. We ran experiments/ simulations to check the modeling software. This allowed us to understand the correct use of CHEMKIN and its applications, since the source code was not available for viewing by the user. Next, we ran simulations to match the experimental results, using equal setups and conditions than those of the experiments. Because the simulation results only reproduced the experimental results partially, no further steps were pursued.

1.3 Model description

In order to model the plasmatron, we first need to understand the main factors that have an influence in the reactor performance. To adapt the model to the real plasma reformer, we need to abstract specific domains. The experimental plasmatron was divided into sections to simplify the task of modeling.

1.3.1 Plasmatron design

A simple schematic of the plasmatron fuel reformer is shown next in Figure 1.1. This sketch represents the initial step in the reactor operation, where the electric discharge takes place and where combustion initiation occurs. Downstream of the plasma reactor (upper part of the drawing), there is an extension that allows reaction to complete (Reaction extension cylinder). The downstream section length and diameter may vary.

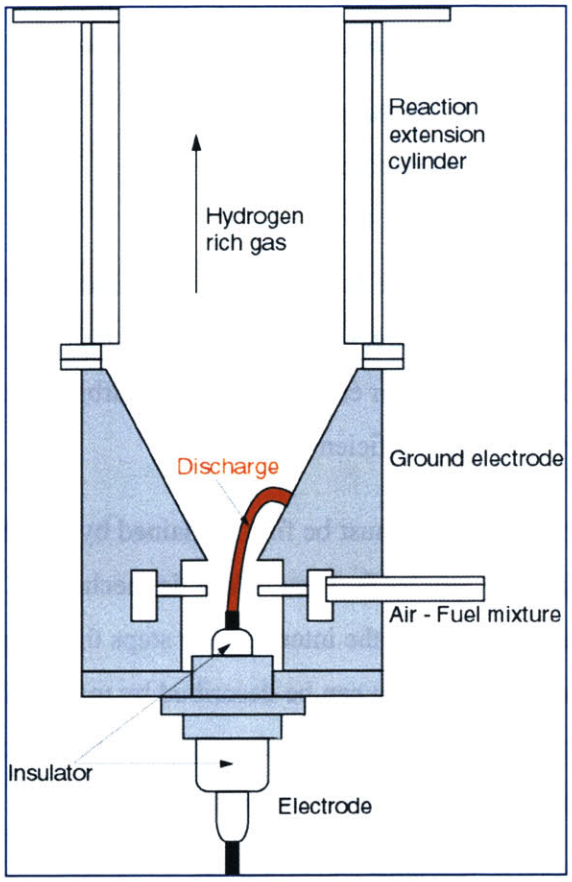

Figure 1.1 Sketch of the Plasmatron Design

As the plasmatron is still in development process and many different versions of it have been tested along the course of this thesis work, we decided to concentrate on one specific design, for which the largest amount of data using methane as fuel had been obtained.

We focussed our modeling effort on the plasmatron discharge region, putting less effort on the chemical and mechanical processes that take place afterwards in the downstream region. When any calculations in this thesis relate to the downstream section, it will be so indicated. A more specific description of the plasmatron will be given in Chapter 2, since the geometry and other characteristics of the device will be correlated to the experimental results.

1.3.2 Thermodynamic, chemical and fluid dynamic models

The main factors to be described in the fuel reformer model are:

1. Thermodynamic behavior of the system.
2. Chemical behavior: equilibrium and kinetics.
3. Fluid dynamics within the reactor.

The thermodynamic properties define the state of the gaseous mixture. The behavior of each species under changes in pressure, temperature or heat transfer effects are determined based on a series of polynomial fits for each property. The arbitrary-order polynomials are formulated from their respective coefficients.

The chemical behavior of a process must be first explained by a global reaction. The species A is transformed into the species B. Then, a kinetic mechanism, which is a collection of elementary reactions, describes all the intermediary steps that must be taken in order to convert A into B. Each global reaction can be described by many different kinetic mechanisms. Our job is to find which mechanism is the most suitable for our case. An independent elemental reaction within the kinetic mechanism is defined by:

- The species involved: reactants and products.
- The rates of the forward and reverse reactions.

The various possible mechanism and its structure are further developed in Chapter 3.

The fluid mechanics is a very important factor in a reactor. Evidently, the molecules of different species must mix at the molecular level in order to react. The rate at which the species mix directly depends on the turbulent mixing process within the reactor, which depends on the turbulence intensity in it. Either computational fluid dynamics (CFD) calculations or laboratory experiments with the plasma reformer can be used to study the degree of mixing caused by the fluid motion into and within the reactor. The results of those studies are shown in Chapter 3.

1.3.3 Methane versus other fuels

As previously commented, the plasmatron is intended for use onboard of vehicles that mainly use SI engines. The hydrocarbon conducted through the fuel reformer in that case is gasoline. Gasoline is primarily a mixture of long chain paraffinic and aromatic hydrocarbons such as iso-octane and toluene. Combustion processes for such species have been studied, however, the chemical mechanisms that represent their oxidation are especially complex, e.g. [Curran, 1998] and [Curran, 2002]. In addition, rich combustion of gasoline is not as well known as stoichiometric or lean combustion. Thus, trying to simulate the plasma reformer with gasoline as fuel becomes an important challenge.

A simpler alternative could be the use of propane in the model, as it is the shortest hydrocarbon molecule that illustrates most of the gasoline properties and behavior. But again, its rich combustion has not been extensively studied. The appropriate hydrocarbon partial oxidation mechanism is yet to be developed.

A more straightforward approach is to model the rich combustion of methane, the smallest possible hydrocarbon molecule. Its combustion process has been comprehensively studied. However, methane behaves differently than gasoline. Its small size and symmetric structure give the molecule specific properties. It is a very stable molecule. At atmospheric temperatures, methane reacts so slowly with oxygen that it is considered unreactive. Ignition is more difficult with methane than with other hydrocarbons, since the first oxidation step, extraction of one H radical, takes about 40 kJ more. Anyhow, being the plasmatron able to run with this fuel, we decided to model the reformer burning methane on a first step.

Chapter 2

PLASMATRON EXPERIMENTAL RESULTS

A series of experiments carried out at the Plasma Science and Fusion Center (PSFC) using methane as fuel are the basis for the plasmatron study and further modeling.

2.1 Plasmatron description

As seen in the previous chapter, the plasmatron is a complex device with several input parameters. In this section we explore the reactor performance.

2.1.1 Geometry and input streams

Several versions or generations of the plasmatron have been developed within a short period of time. We concentrated our measurements and tests to a single setup which is schematically described in Figure 2.1.

The main reactor chamber consists of a cylinder shaped duct with two annular electrodes (in red), one on the top, closer to the fuel injector, and one on the bottom, next to the dow-stream reactor zone, both across from an air inlet ring. The chamber has a 3-cm inner diameter and it is 6.5 cm long. The zone limited by the two electrodes is the discharge zone and it comprises 6 cm in length, from the top of one electrode to the bottom of the other one. Here is where combustion initiation takes place, primarily because of the plasma generation by the electric discharge between electrodes.

The system has two main inlet streams: one for fuel and one for air, both at ambient tem-perature. The reactor is fed by more than two inlets. Fuel is pressure-driven in through one

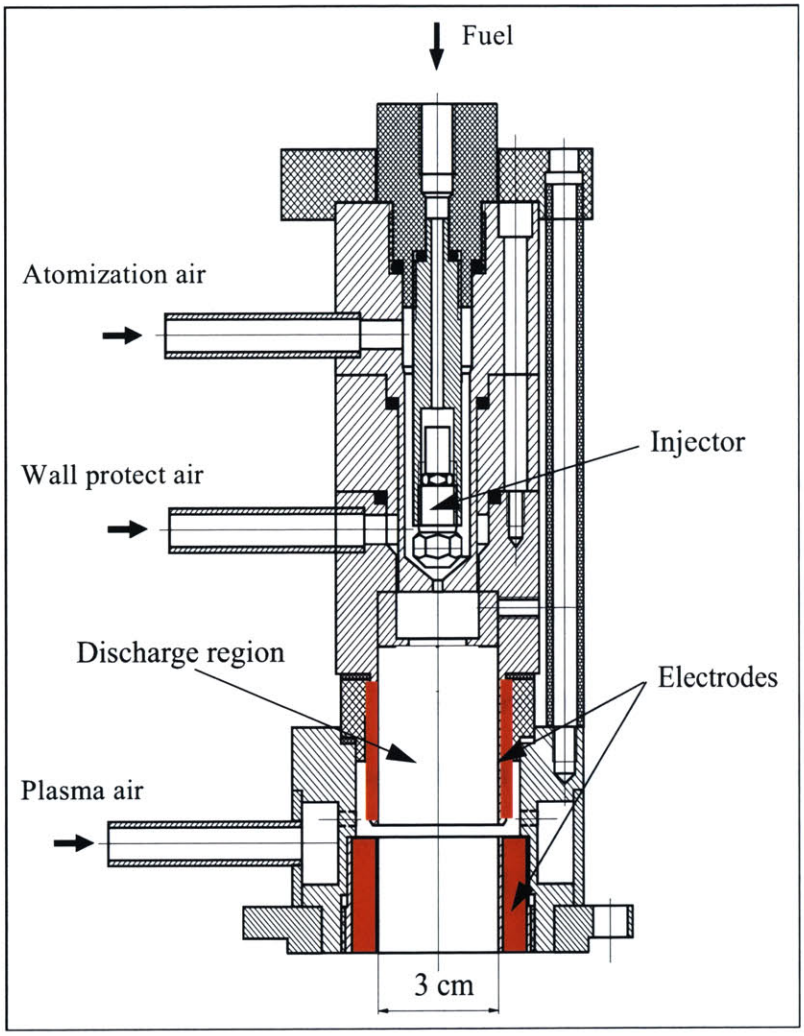

Figure 2.1 Drawing of the Plasmatron Design Tested

channel and is directly injected into the discharge region. On the other hand, there are three different paths for the air to enter the plasmatron:

1. Premixed with the fuel, and injected into the center of the plasma region (Atomization air).
2. Flowing next to the walls (Wall protect air).
3. Creating swirl in the discharge region (Plasma air).

Therefore, when we account for air flow rate coming into the plasmatron, we are referring to the sum of the three air streams. The fuel mass flow rate may oscillate between 0.5 g/s and 1.0 g/s, while the air flow is measured in volumetric rate and it varies from 30 l/min to 250 l/s at standard conditions, which corresponds in mass rate to a range from 0.50 g/s to 3.50 g/s. These latter values are obtained from experimental data rather than from molecular gas correlation, since in some cases, the air flow input is a mixture of air and pure oxygen.

Figure 2.2 illustrates the different sections found in the reactor core: in green and yellow, the plasma air distribution; in purple, the wall protect air and the centrally injected fuel and atomization air; in red, the main discharge region and swirl generating pipes.

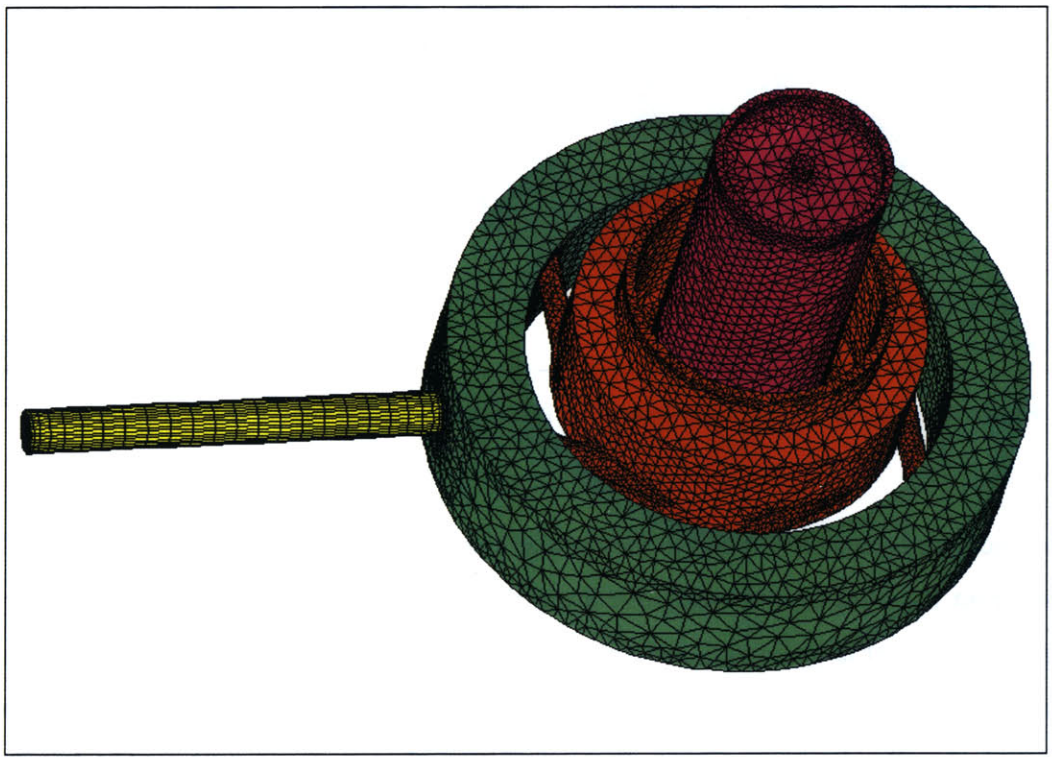

Figure 2.2 3-D Mesh used to Simulate the Fluid Dynamics in the Plasmatron using FLUENT: Wall and Atomization Air (purple), Plasma Air (yellow and green), Core of the Discharge Region (red)

A cross-sectional image of the core reactor and the plasma air distribution perpendicular to the vertical direction (y) is presented in Figure 2.3.

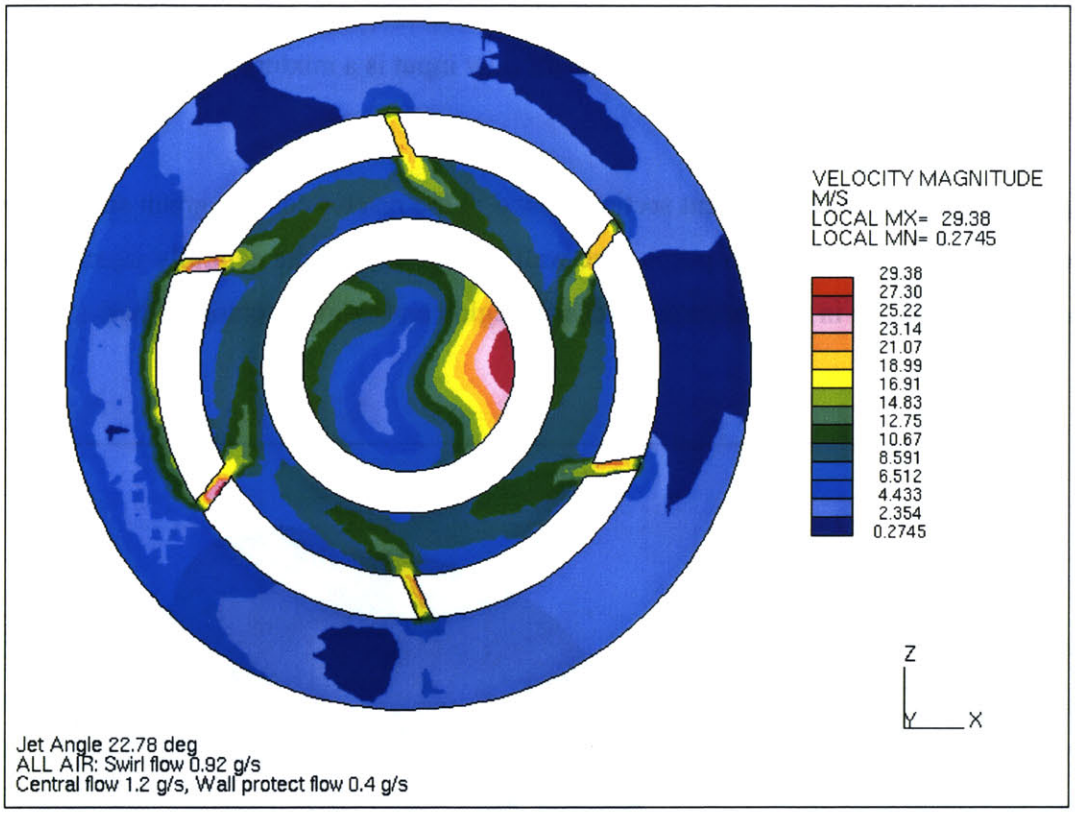

Figure 2.3 View of the Discharge Zone of the Plasmatron along the Vertical Direction (Example of Fluid Dynamics Calculation using FLUENT)

The uncolored rings correspond to the annular electrodes. The central circle represents the flow from the injector and wall protect air, the inner ring corresponds to the discharge zone where swirl is generated, and finally, the outer ring corresponds to the distribution channel for the plasma air. The downstream region, usually wider than the plasma region, is attached to the discharge region. It can operate with or without catalyst. The length is not a fixed parameter, but it ranges from 25 to 30 cm.

2.1.2 Characteristics of the discharge

One critical aspect of the plasma fuel reformer is the arc discharge. Its characteristics, such as energy supplied, current through the arc, frequency of the discharge and even shape and length, are a useful source of knowledge. We try to obtain as much information as possible from the study of the plasma arc in this section.

Discharge visualization

A useful way to examine the arc behavior is to look at the image that generates. Movies contain information about flame size and shape, location, contact areas, as well as volume and radius. Although the latter cannot be accurately measured from a 2-D image, they are still of qualitative interest.

A series of movies were taken using a Redlake MASD monochrome high-speed video camera, with up to 12,000 images per second framing capability. An example of arc images in a sequence is shown in Figure 2.4. The picture is a view of the discharge in the y direction from the plasmatron exit. When the pictures were taken, the plasmatron was running with only air, so the light seen is produced by the electric discharge. It is not combustion related.

From Figure 2.4, we observe how the arc curls, grows and moves around the reactor volume from its start up to its end. The arc reappears with a certain frequency, measured to be in average 350 Hz. The contact zone with the electrodes cannot be appreciated because it happens to be an alternated current discharge.

The figure window size measures 4 cm. Using this scale, we estimated that the average length of the arc is 3.5 cm, growing from 2 cm at start up to 5 cm before extinction (see length of the arc measured along time in Figure 2.5). Pictures also showed that the diameter of the arc ranges from 0.5 mm to 0.7 mm. That covers a total volume of $7\text{x}10^{-9}$ m^3 to $1\text{x}10^{-8}$ m^3 (7μl-10μl). It is important to note that all this information was obtained from a 2-D picture, and therefore, we had no sense of depth from the image. However, knowing

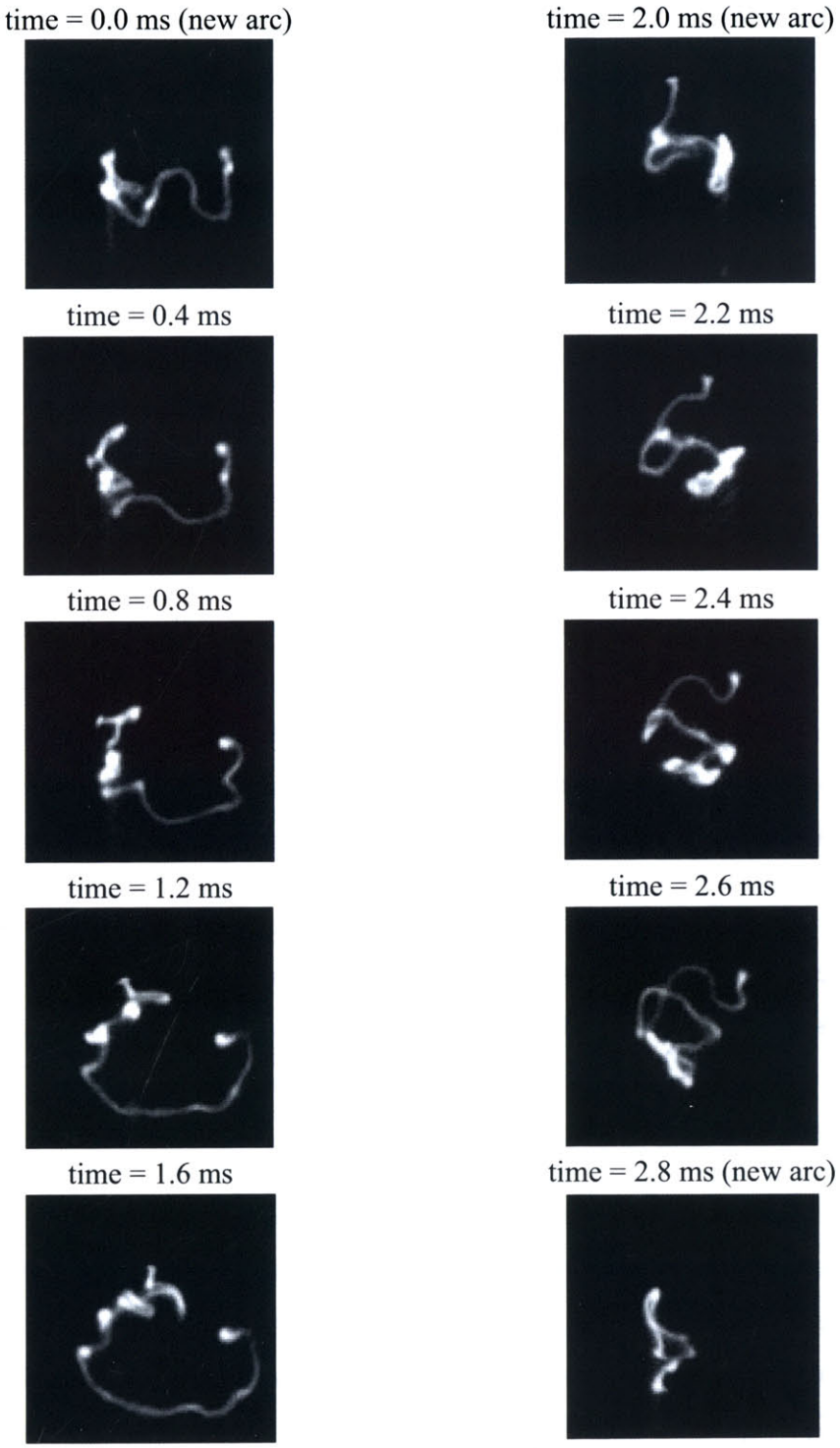

Figure 2.4 View of the Discharge Region along the y Direction from the Plasmatron Exit. The Sequence of Images along Time includes Two Complete Discharges and a Third Arc Initiation

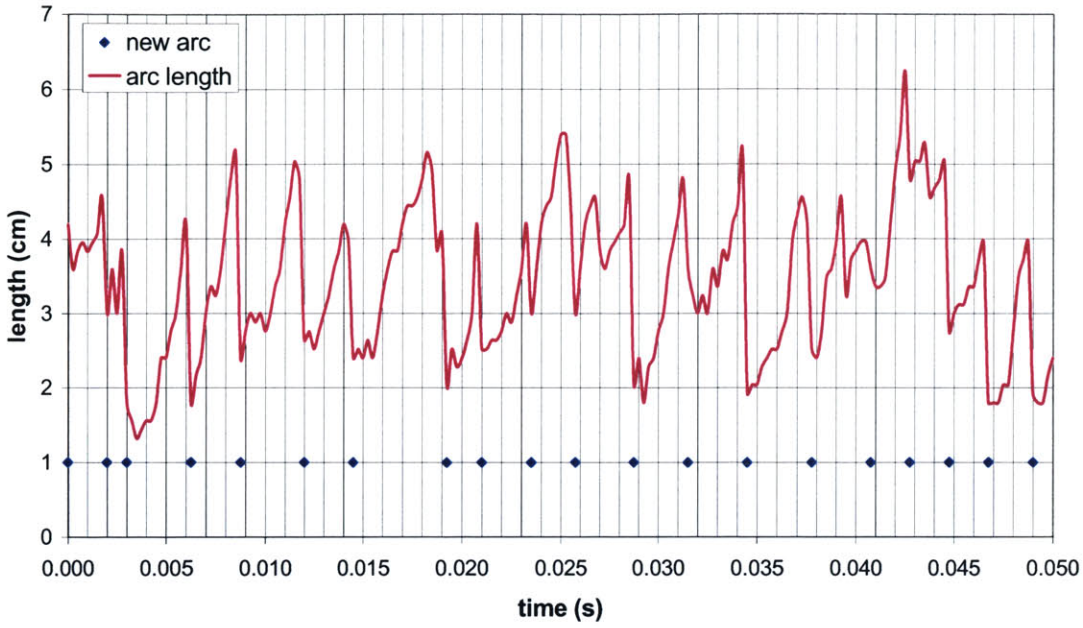

Figure 2.5 Characterization of the Length and Duration of the Arc of the Plasmatron with a 600-W Power Supply

the distance between electrodes and assuming that the arc is confined between those, we can state the following:

- the average length of the arc must be larger than the distance between electrodes,
- the curves and wider parts of the arc represent the arc traveling in the y (vertical) direction, which we accounted for twice as much as the thinner ones.

The movies besides evidenced that the discharge was restarting approximately every 3 ms, being the apparent frequency of strike equal to 350 Hz (see dots in Figure 2.5). The discharge duration is found to be similar to the residence time of the reactor.

Electrical characterization

Simultaneous to the image taking moment, measurements of the current and voltage traces were recorded with a Tektronics Digital Scope TDS 3032B oscilloscope. Figures 2.6 and

2.7 show the actual current and voltage traces measured, while Figure 2.8 represents the equivalent instantaneous power P, result of the current I and voltage V product:

$$P = I \times V \tag{2.1}$$

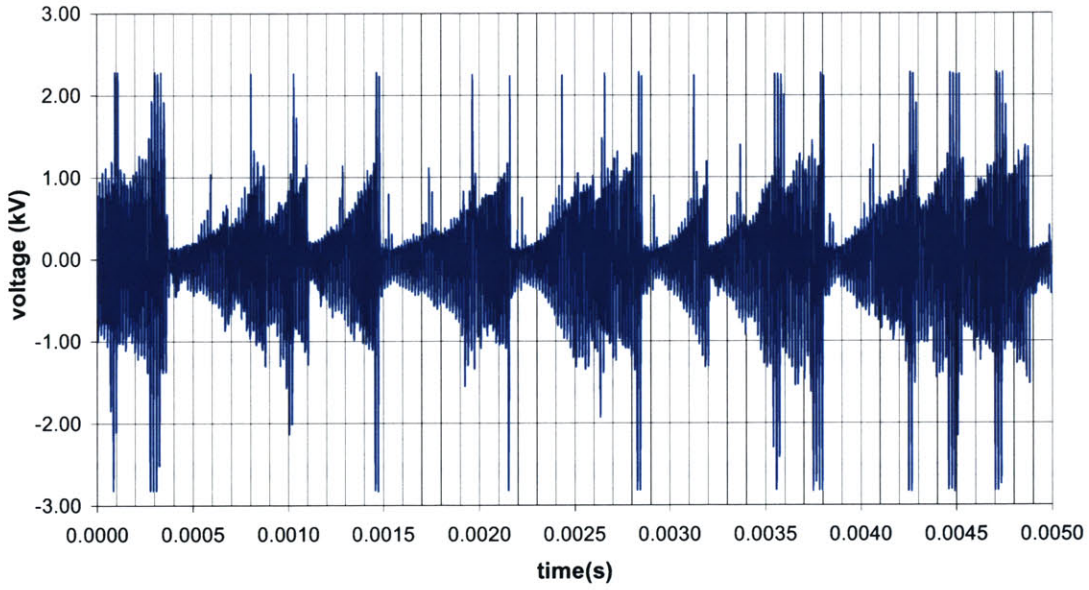

Figure 2.6 Arc Voltage Trace along Time Measured for the running Plasmatron with a 600-W Power Supply

Although we may observe random high peaks in the instantaneous power estimation, the average instantaneous power supplied to the arc is equivalent to 200 W. From the voltage and current traces we draw a new apparent frequency for the arc strike. On average, every 0.5 ms the power drops and immediately reappears, which is a different frequency for the arc strike than the visually observed discharge frequency. The power-measured frequency is considered to correspond to the breakdown of the arc and its posterior new formation, while the visual-measured frequency is assumed to be correlated to the residence time of high temperature gas mixture within the arc discharge region.

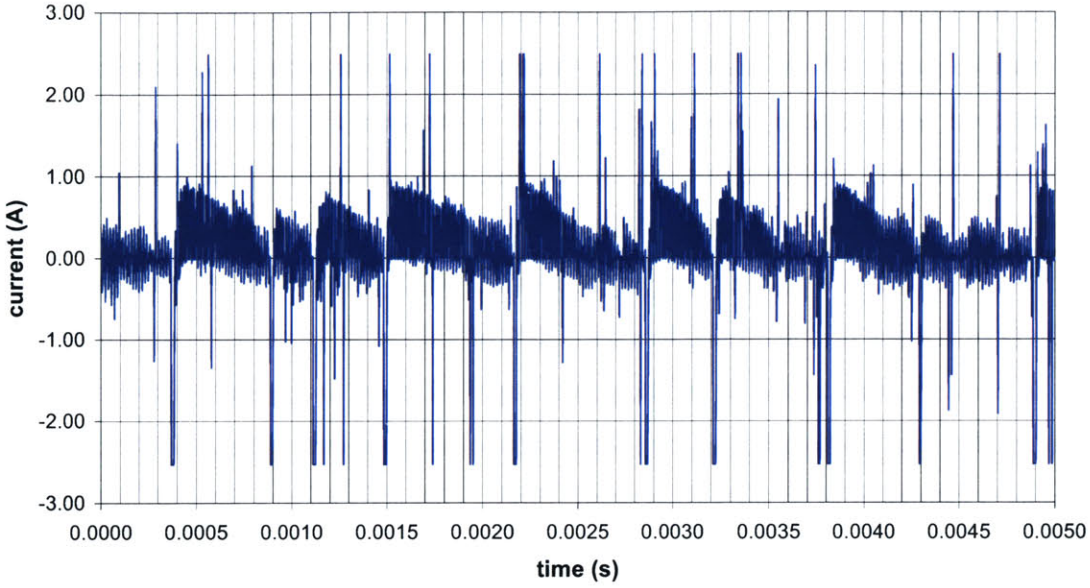

Figure 2.7 Arc Current Trace along Time Measured for the running Plasmatron with a 600-W Power Supply

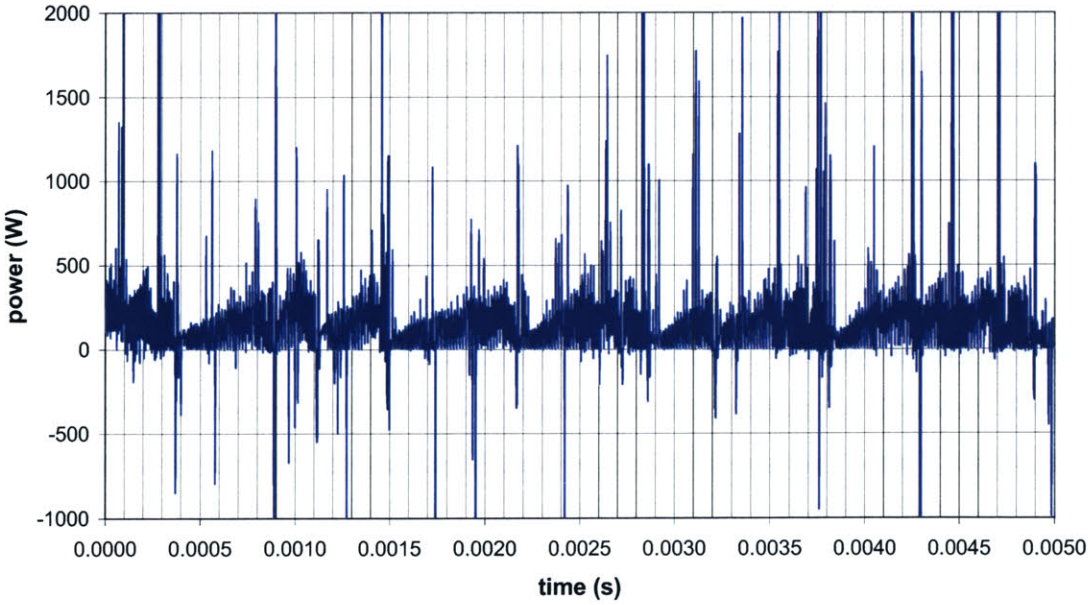

Figure 2.8 Arc Instantaneous Power Calculated from the Measured Voltage and Current Traces with a 600-W Power Supply

The plasmatron functions with an alternate current (AC) power supply whose power ranges from 200 W to 900 W. The frequency of the power supply is 200 kHz and the voltage varies between 0.6 kV and 0.7 kV. From current and voltage traces measured with the oscilloscope when using a power supply of 600 W, we were able to integrate the amount of energy that was delivered through the arc discharge per second. The average current was 0.40 A and the average voltage, 0.62 kV, which gives us a total mean power of 250 W. This indicates that the power supply system is not ideal, and that it has an approximate delivery efficiency of 50%, since less than 50% of the available power is driven into the arc. In addition, only a fraction of the power supplied to the arc is transmitted to the gas mixture. For arc discharges, the total loss to the electrodes due mainly to dissipation in sheaths is estimated to be 50% [Heywood, 1988]. This adds up to a total of 75% energy loss from the power supply to the gas mixture (equivalent to an efficiency of 25%). In conclusion, the real power dissipated in the discharge must be about 150 W.

From the real power input in the system P, we can determine the amount of energy dissipated E per second within the arc discharge which is converted into thermal energy Q. An ohmic heating process is assumed. This process produces a differential temperature increase dT on a specific mass m for each time differential dt. The equation that represents this energy conservation process is:

$$P = \frac{\mathrm{d}Q}{\mathrm{d}t} = m \times c_p \times \frac{\mathrm{d}T}{\mathrm{d}t} \tag{2.2}$$

which is derived from the first law of thermodynamics at constant pressure. For that reason, we work with the heat capacity of the mixture c_p at constant pressure as a function of temperature T only. The calculation can be completed through multiple ways, depending on the hypothesis for time τ, mass m or real power P implied on each case. The discharge energy E to be converted into thermal energy Q, may be estimated using the equation:

$$E = Q = \int_{\tau} \eta \times I \times V dt \tag{2.3}$$

where I is the current through the arc, V the voltage difference and η the efficiency of the electrodes, previously estimated to be 50%. The integration must be over a time τ which is still undetermined. Then, using Equations 2.2 and 2.3 we can draw the expression:

$$\eta \times I \times V \times dt = m \times c_p \times dT \tag{2.4}$$

Using Equation 2.4 eliminates the uncertainty about the real power P supplied to the arc. However, we still need to make assumptions for τ and m. Instead of working with mass, we rewrote Equation 2.4 as:

$$\eta \times I \times V \times dt = \rho \times v \times c_p \times dT \tag{2.5}$$

From the discharge visual study in Section 2.1.2, we concluded that the arc volume v varies from $7\text{x}10^{-9}$ m^3 at formation to $1\text{x}10^{-8}$ m^3 at extinction. Density ρ may be estimated using the equation of state of an ideal gas:

$$\rho = \frac{p \times MW}{R \times T} \tag{2.6}$$

where the pressure of the system p is atmospheric, R is the constant of ideal gases, and MW is the molecular weight of the gas mixture.

Equation 2.5 must be integrated over τ, the time during which the power is supplied. We estimated the discharge duration is in average equal to 0.5 ms, as observed from the voltage and current traces. But we also observed, from discharge visualizations, that the arc extinguishes every 3 ms, which is of the order of the reactor residence time. Whether we use the residence time or the arc duration for τ, the hypothesis will procure very different results. The first hypothesis assumes that the arc is almost continuos and is heating the same mass of gas for the total amount of time this mass is inside the reactor (residence time). The second hypothesis assumes that the power is supplied through the discharge

only for a certain period that corresponds to the duration of the arc (from its formation to its breakdown).

To integrate Equation 2.5 we have already specified the variables that are constant: the electrodes efficiency, the pressure in the reactor and the ideal gas constant. The remaining involved variables are dependant on either time or temperature as follow:

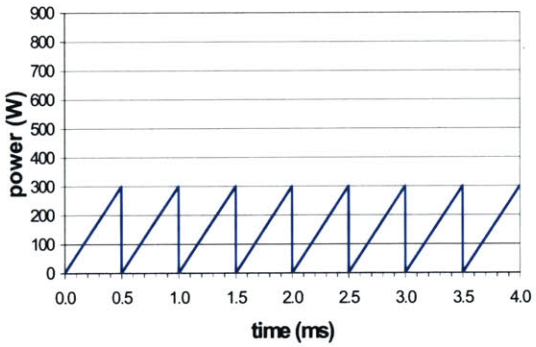

Figure 2.9 Power Supplied to the Gas Mixture under the Arc along Time

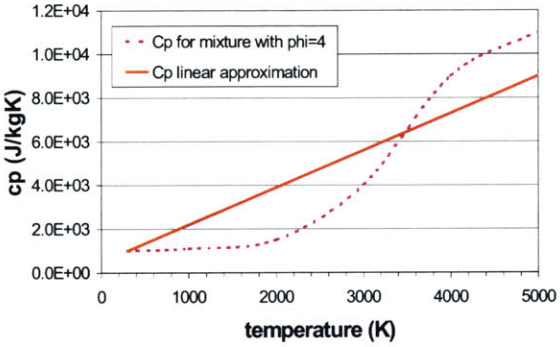

Figure 2.10 Heat Capacity of the Gas Mixture under the Arc as a Function of Temperature and Corresponding Used Linear Approximation

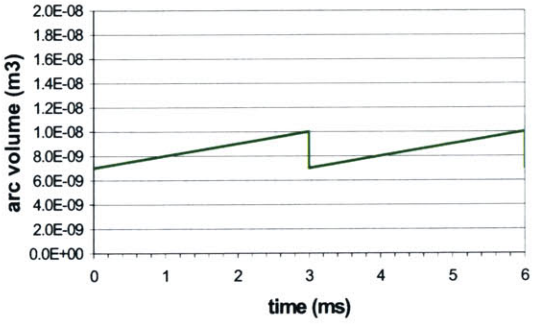

Figure 2.11 Volume of the Arc along Time

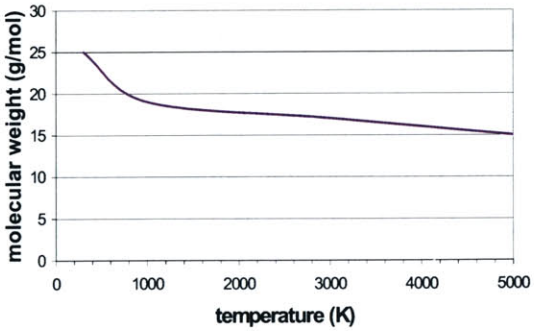

Figure 2.12 Molecular Weight of the Gas Mixture under the Arc as a Function of Temperature

For each time interval of integration, the power supplied and the volume of the arc were assumed to be constant and equal to their averages 200 W and 9×10^{-9} m^3 respectively. The

molecular weight was assumed to be constant and equal to 17 g/mol, and the heat capacity function for the gas mixture was substituted by a linear correlation of type c_p = a + bT. Based on these assumptions, Equation *2.5* became:

$$\int \frac{a+bT}{T} \times MW dT = \int \eta \times I \times V \times \frac{R}{v \times p} dt \tag{2.7}$$

An analytical integration of Equation 2.7 is now possible and gives:

$$\frac{\eta \times I \times V \times R}{MW \times v \times p} \times \Delta t = a \ln\left(\frac{T_{final}}{T_{initial}}\right) + b(T_{final} - T_{initial}) \tag{2.8}$$

Iterating for the final temperature (the initial temperature is set to 300 K) provides us with the temperature increase of the arc due to ohmic heating by the discharge. Schematically shown in Table 2.1, we obtain two different levels of gas mixture temperature rise for each one of the arc duration times determined $\tau=\Delta t$. When assuming the energy release heats up only the arc contained mass during a period equal to the discharge duration, the temperature increase estimation is of the order of 3,000 K. However, if we consider that the discharge is almost continuous and affects the mass comprised inside the total volume of the arc for a period equal to its residence time in the reactor, then the temperature rise is of the order of 13,000 K.

TABLE 2.1 Temperature Increase Estimation of the Gas Mixture Mass under the Electric Discharge Effect for two Different Arc Duration Times

	Residence Time	**Arc Duration**
Arc duration time (s)	0.003	0.0005
Arc volume (m^3)	$9x10^{-9}$	$9x10^{-9}$
Efficiency x Power (W)	150	150
Temperature (K)	13,000	3,000

So distant numbers are caused by the lack of knowledge on the time during which the gas mixture is affected by the same current discharge. [Pischinger, 1989] states that in the arc discharge breakdown phase, a small amount of plasma is generated, such that its peak temperature reaches 60,000 K. This will initiate combustion, that will afterwards continue even if the spark is extinguished. His value is higher than our estimates. Pischinger worked with spark plugs of different characteristics. However, the initiation and propagation processes of combustion are thought to be the same. Note also that these initially very high temperatures at the discharge core rapidly decrease due to thermal conduction and dissipation [Thiele, 2002].

Our calculations suggest that the temperature increase due to dissipation within the electric arc lies somewhere in between 3,000 K and 13,000 K. It is unreal to assure that all power is transformed into thermal energy. The discharge generates plasma, and therefore, part of the dissipated electric energy is used to ionize the gas (breaking up molecular bonds) at the same time that is heating it up. From [Suris, 1985] we found that between 2 kWh/m^3 and 8 kWh/m^3 are necessary to heat up to 5,000 K and dissociate any two-atom molecule of gas. Then, considering that the plasmatron arc volume varies between $7x10^{-9}$ m^3 and $1x10^{-8}$ m^3, we calculated that we need from 0.1 J to 0.3 J to generate plasma and raise the temperature of the arc to 5,000 K. The plasmatron electric discharge contains between 0.1 J and 0.6 J of available energy, depending on which time interval is used for a 200-W power release: residence time or arc duration time. It is thus plausible to have the discharge energy to be converted into both thermal energy (ohmic heating) and chemical energy (dissociation), since we are dealing with the same order of magnitude power densities.

2.2 Performance of the plasmatron

When producing experimental data with the plasmatron, a series of measurement structured on a table are generated. For each run, the following type of data is taken and noted:

- fuel and air flow rates,

- power input,
- opacity in the reactor,
- temperature at sample points,
- composition at sample points.

From these measurements, other interesting values can be computed:

- the rate of moles of each species entering and exiting the plasmatron,
- the O/C ratio, which is the number of atoms of oxygen going in, divided by the number of carbon atoms,
- the conversion efficiency of the system,
- the energy conversion.

The composition of the flow, at different points of the reactor was sampled using a gas chromatograph (GC) Hewlett Packard Micro GC model M20011. Since the column is set up for non-polar species, such device does not accept polar substances in the samples, so the first step consists of removing water from the sampled flow. Therefore, no water measurement can be directly performed. Other various comments, such as catalyst information, characteristics of the flow or soot formation, are also reported for each experiment run.

Since the measurements were taken using a GC equipped with an apolar gas chromatograph column, it was necessary to convert all experimental results from a dry basis to a wet basis. We implemented an elements balance (C, H and O) based on the measured composition results. First, we checked that the carbon balance was satisfied. Then, we used the H balance to estimate the amount of water (H_2O) that must be present. Finally, we matched the amount of oxygen present in the calculated water with the global balance of the O atom. The calculated difference resulted in an average relative error of less than 5%.

In Figures 2.13 to 2.16, the exact results obtained from the GC are shown as measured along the plasmatron in a molar dry basis. Next we used the species balance to estimate the amount of water present in each sample.

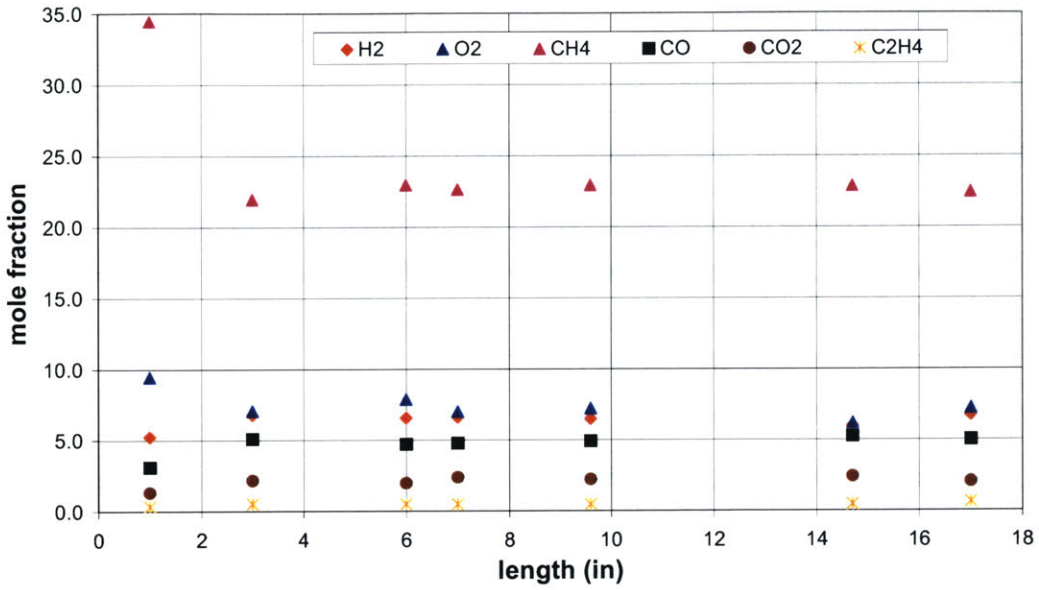

Figure 2.13 Molar Composition of the Gas Mixture along the Plasmatron for Methane Partial Oxidation with O/C = 1.01, 23% O_2 Enrichment in Air and a 700-W Power Supply (Dry Basis)

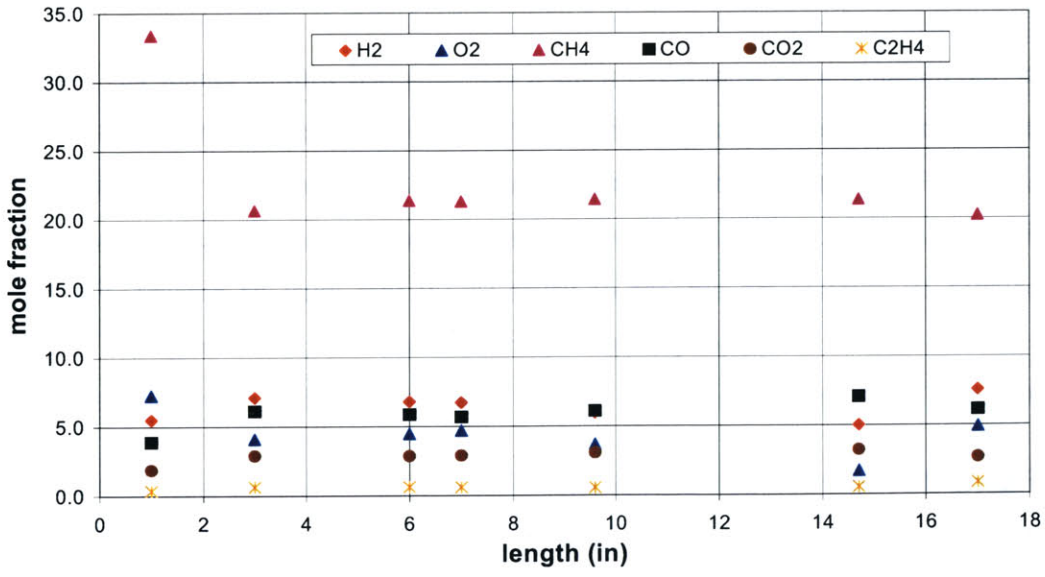

Figure 2.14 Molar Composition of the Gas Mixture along the Plasmatron for Methane Partial Oxidation with O/C = 1.06, 23% O_2 Enrichment in Air and a 700-W Power Supply (Dry Basis)

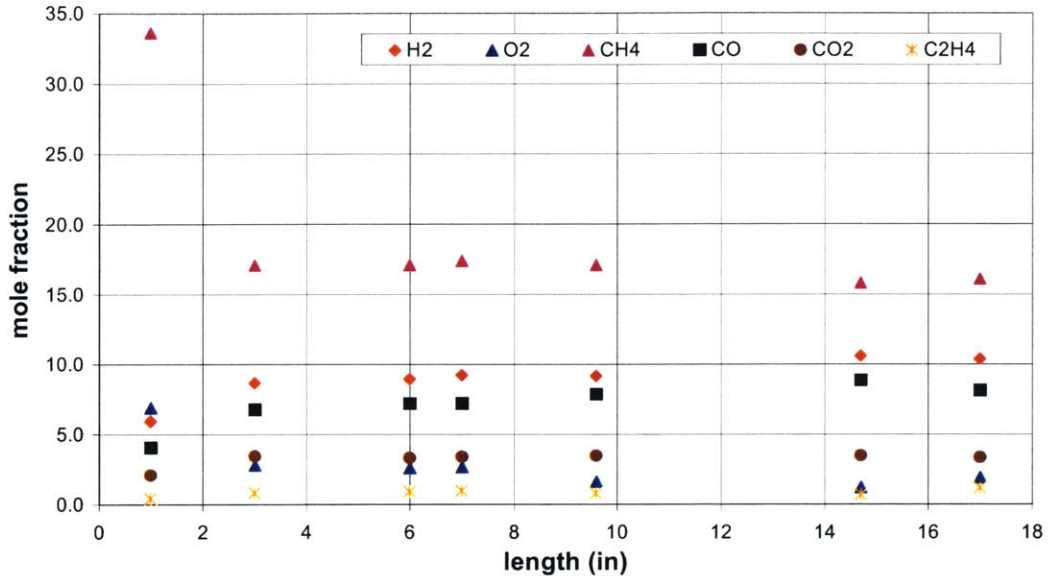

Figure 2.15 Molar Composition of the Gas Mixture along the Plasmatron for Methane Partial Oxidation with O/C = 1.11, 23% O_2 Enrichment in Air and a 700-W Power Supply (Dry Basis)

Figures 2.16, 2.17 and 2.18 show the molar composition in wet basis of the gas mixture for combustion of methane at different O/C ratios. Water molar fraction represents between a 10% and a 15% of the gas mixture composition, which is a significant fraction of the hydrogen.

From this graphs we can observe that the maximum hydrogen yield is as low as 6%-7%. At this conditions, most of the methane is not combusted (about 15% or more remains). In fact, almost 5% oxygen remains unreacted. This could be explained by poor mixing in the reactor. If that is the case, we could have zones in which the O/C ratio for the gas mixture is not equal to the global one, but lower or in some cases much higher. Consequently, we would be dealing with local lean mixtures that allow part of the oxygen to go through.

High temperatures at the exhaust of the plasma region (over 1,200 K) may indicate than even higher temperatures are achieved at the combustion core, however complete methane conversion does not occur. This may also be considered as an indirect indicator of inadequate local mixing, since some regions are thought to be at higher temperature than others.

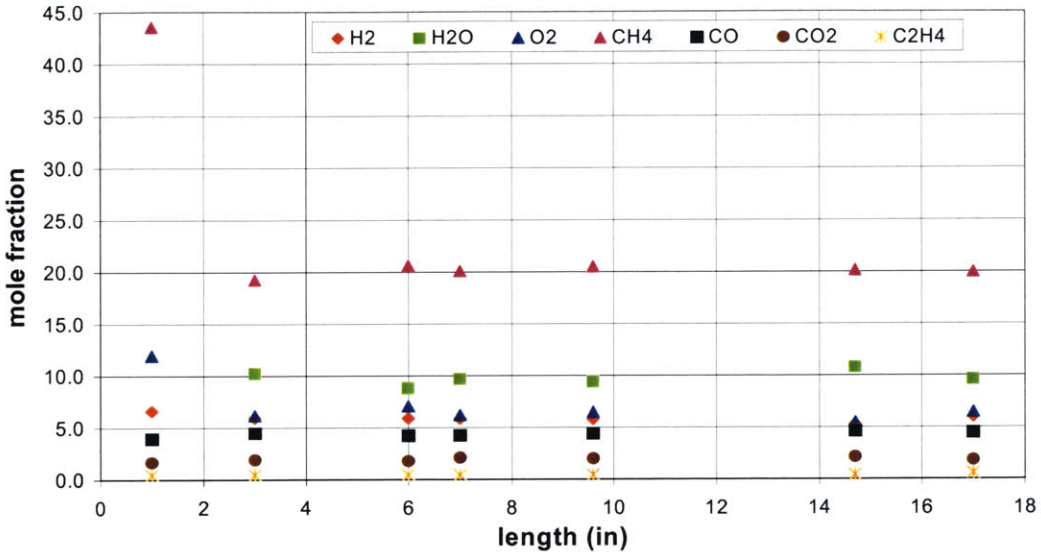

Figure 2.16 Molar Composition of the Gas Mixture along the Plasmatron for Methane Partial Oxidation with O/C = 1.01, 23% O_2 Enrichment in Air and a 700-W Power Supply (Wet Basis)

It is known that all light alkanes homogeneously pyrolyze around 1,000 K. Nevertheless, methane is the least reactive and has a conversion time of hours at such temperatures, thus the only cause of methane conversion at our conditions must be driven by oxidation.

In Figures 2.19 to 2.24 we present a series of experiments in which only one gas sample at the exhaust of the discharge region was taken. The results are presented as separate plots for each measured species. In addition, mole fractions were converted to mass fractions, to simplify subsequent comparisons between the experimental results and the model solutions. Figure 2.24 shows the methane conversion experienced through the plasma reformer.

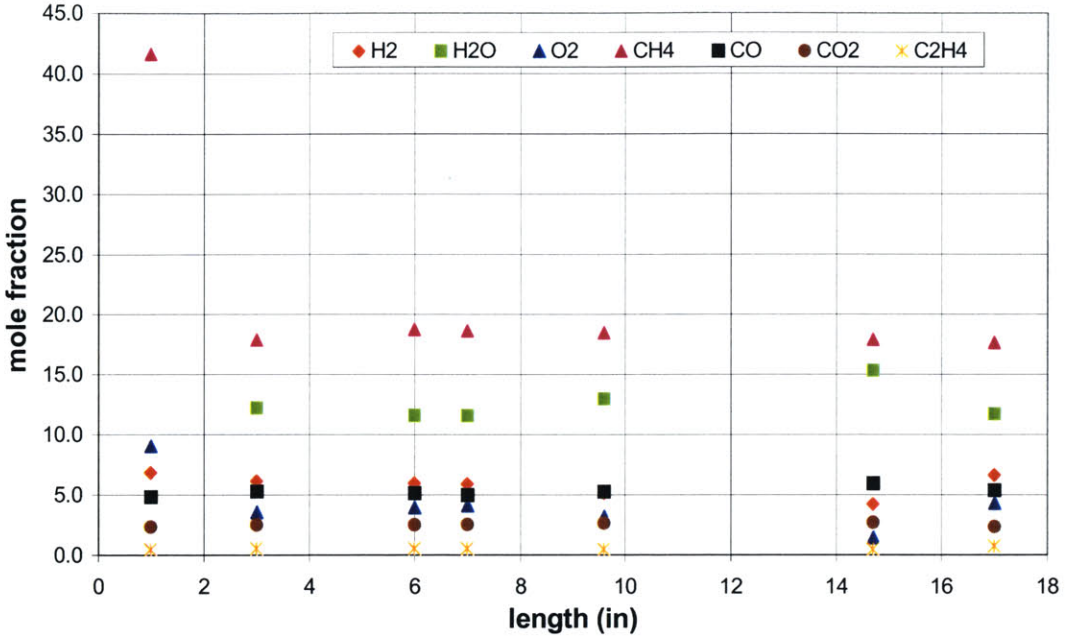

Figure 2.17 Molar Composition of the Gas Mixture along the Plasmatron for Methane Partial Oxidation with O/C = 1.06, 23% O_2 Enrichment in Air and a 700-W Power Supply (Wet Basis)

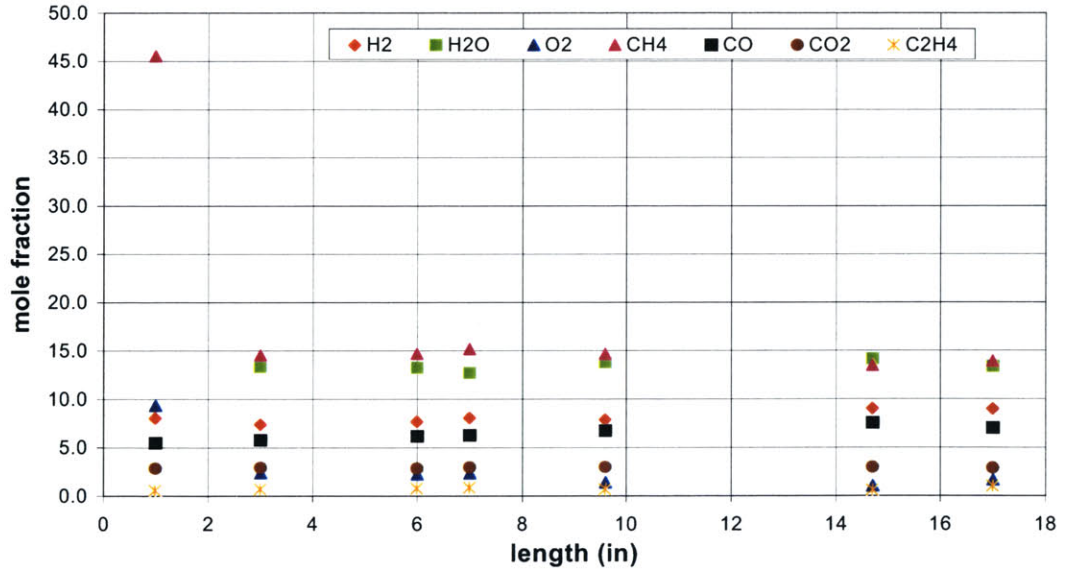

Figure 2.18 Molar Composition of the Gas Mixture along the Plasmatron for Methane Partial Oxidation with O/C = 1.11, 23% O_2 Enrichment in Air and a 700-W Power Supply (Wet Basis)

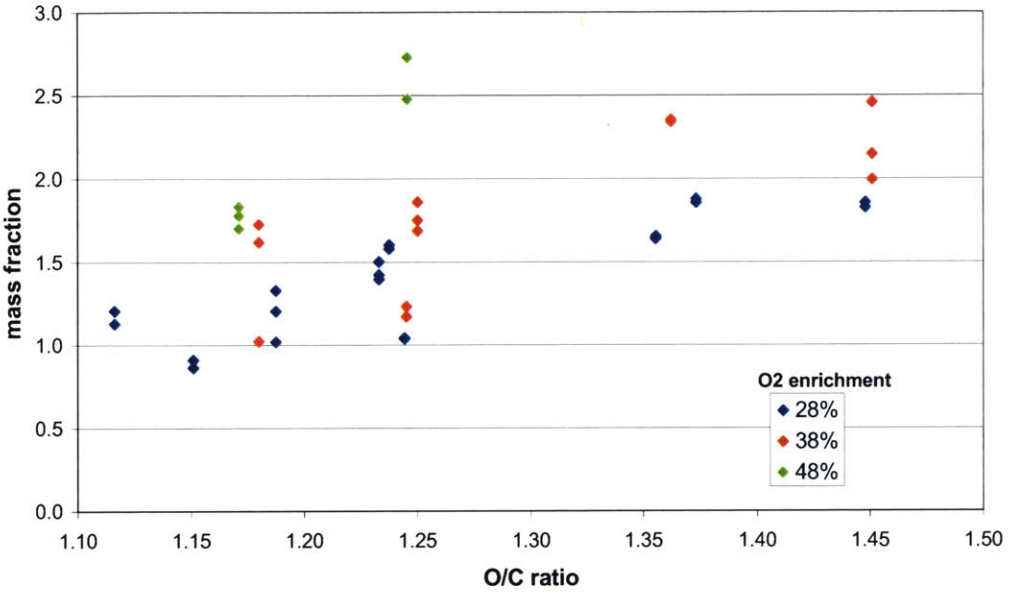

Figure 2.19 Experimental Hydrogen Production Measured at the Exhaust of the Discharge Region as a Function of O/C ratio for Different O_2 Air Enrichment of Methane Partial Oxidation (Mass Fraction)

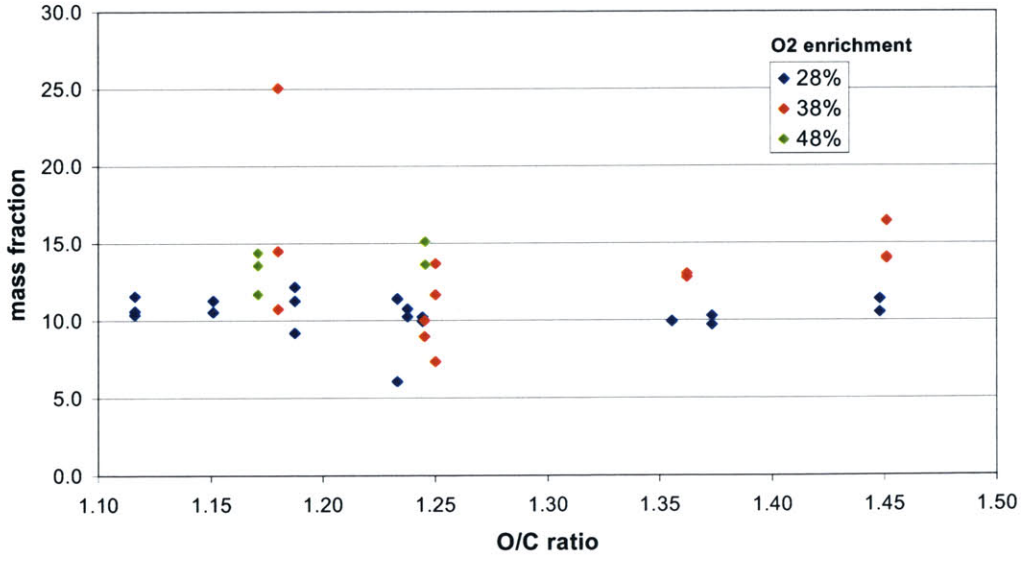

Figure 2.20 Experimental Water Production Measured at the Exhaust of the Discharge Region as a Function of O/C ratio for Different O_2 Air Enrichment of Methane Partial Oxidation (Mass Fraction)

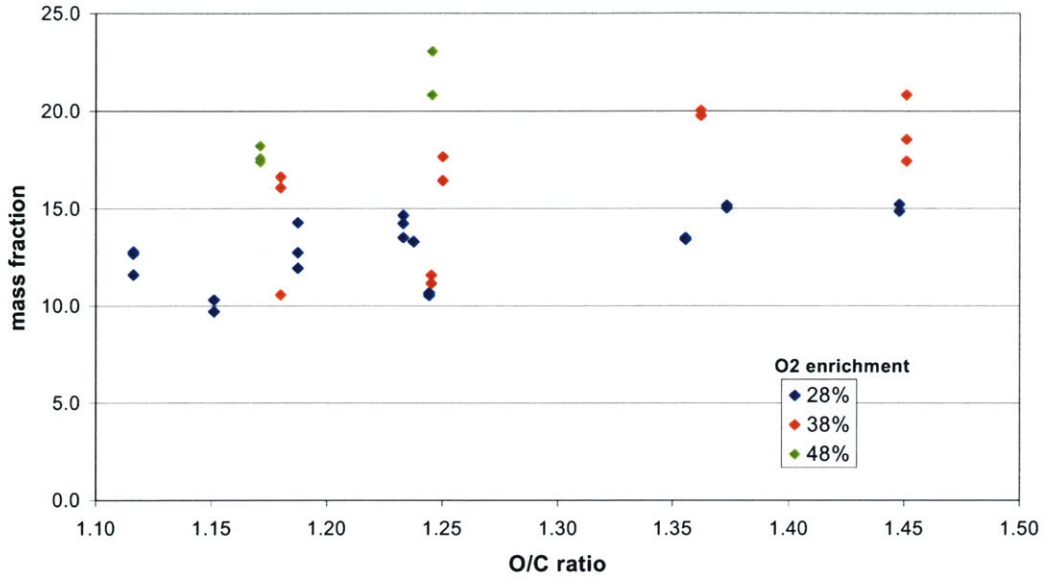

Figure 2.21 Experimental CO Production Measured at the Exhaust of the Discharge Region as a Function of O/C ratio for Different O_2 Air Enrichment of Methane Partial Oxidation (Mass Fraction)

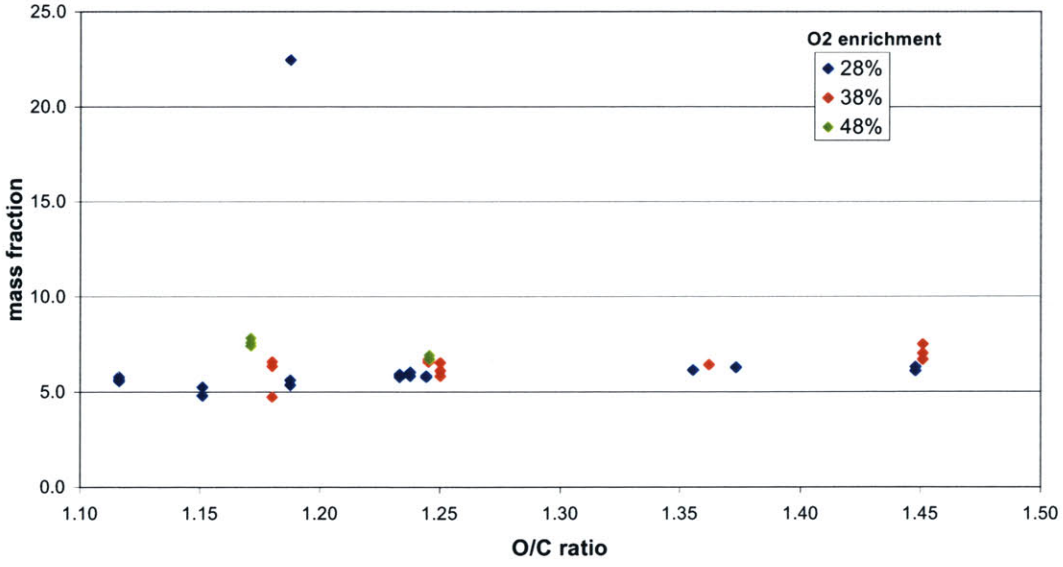

Figure 2.22 Experimental CO_2 Production Measured at the Exhaust of the Discharge Region as a Function of O/C ratio for Different O_2 Air Enrichment of Methane Partial Oxidation (Mass Fraction)

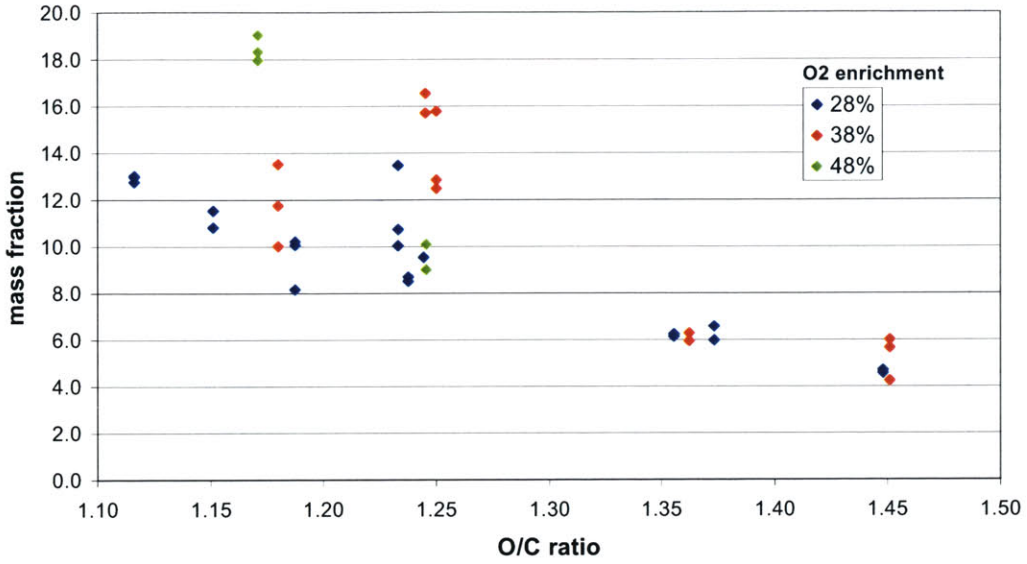

Figure 2.23 Experimental Methane Composition Measured at the Exhaust of the Discharge Region as a Function of O/C ratio for Different O_2 Air Enrichment of Methane Partial Oxidation (Mass Fraction)

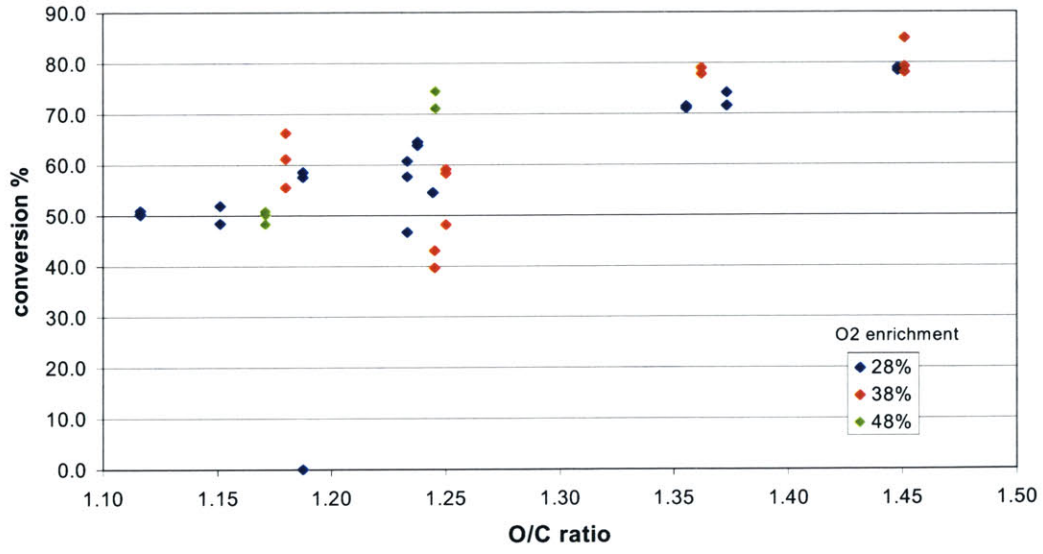

Figure 2.24 Experimental Methane Conversion at the Exhaust of the Discharge Region as a Function of O/C ratio for Different O_2 Air Enrichment of Methane Partial Oxidation

Working on a mole fraction basis, the mayor species concentrations at the discharge exhaust are:

- Hydrogen: 6% - 7%
- Water: 10% - 15%
- Carbon monoxide: 4% - 6%
- Carbon dioxide: 3% - 4%
- Methane: 15% -20%
- Other hydrocarbons: ~ 1%

When converted to a mass fraction basis, those result:

- Hydrogen: 1.0% - 2.5%
- Water: 10% - 15%
- Carbon monoxide: 10% - 20%
- Carbon dioxide: 5% - 7%
- Methane: 4% -10%
- Other hydrocarbons: ~ 1%

Chapter 3
MODELING APROACH

The approach required to develop a model for the plasmatron has two main elements. On one hand, the chemical processes that take place in the reactor are an important factor in our study. On the other hand, the mixing processes are a mayor focus. These latter involve the fluid mechanics of the system, while the thermodynamics are present in both sections: chemistry and mixing.

3.1 Chemical modeling

To investigate the chemical behavior of the plasma reformer, we need to define the species and reactions involved in the process. Chemistry may be considered to occur in two different ways: reaction may be sufficiently rapid to achieve complete conversion (which corresponds to the equilibrium state for combustion systems), or it may be time-dependent and therefore happen progressively, following a series of mechanisms that define the real phenomena taking place, generating a specific rate of conversion.

3.1.1 Equilibrium simulations

Equilibrium of a chemical reaction is a state in which the forward and reverse reactions of the system occur at equal rates so that the concentration of the reactants and products does not change with time. In our combustion process at constant pressure, equilibrium occurs when a group of reactants evolve into the respective products that maintain the enthalpy balance of the system equal to zero.

The results for equilibrium simulations correspond to the ideal solutions, the maximum possible yield of partial oxidation products. In fact, two kinds of equilibrium can be considered: one in which the products are exclusively H_2 and CO, and one in which the spe-

cies in equilibrium can be any of the ones involved in the chemical mechanism of the global reaction. CHEMKIN includes an application called EQUIL that is capable to estimate the equilibrium state involving any set of species and any thermodynamic conditions

We used EQUIL to find the equilibrium results for different initial temperatures for a given methane combustion process: we consider them the best possible solution to aim for. We determined the equilibrium product concentration and temperature for an initial mixture of gaseous methane and air at O/C ratio equal 1, pressure of 1 atm and different initial temperatures. The process was at constant pressure and enthalpy. Two different sets of products were tried: Partial Oxidation of methane, which assumed that methane was converted into hydrogen and carbon monoxide only, and Complete Oxidation, where the combustion products allowed were carbon monoxide, hydrogen, water and carbon dioxide. The goal was to estimate the dependence of the equilibrium species concentration on initial temperature, assuming that this initial temperature was achieved by ohmic heating of the gas mixture within the arc. Table 3.1 includes the results obtained when using EQUIL.

TABLE 3.1 Equilibrium Temperature and Molar Composition for Methane Oxidation with O/C =1 and Different Initial Temperatures for Limited Species

	O/C = 1 **Partial Oxidation Products**			**O/C = 1** **Complete Oxidation Products**				
Initial T (K)	T (K)	x CO	x H_2	T (K)	x CO	x H_2	x CO_2	x H_2O
2000	2150	0.205	0.409	2177	0.205	0.409	$1.4x10^{-6}$	$1.5x10^{-6}$
3000	3197	0.205	0.409	3267	0.205	0.409	$1.4x10^{-7}$	$2.2x10^{-6}$
4000	4241	0.205	0.409	4371	0.205	0.409	$5.0x10^{-8}$	$9.1x10^{-7}$
5000	5278	0.205	0.409	5409	0.205	0.409	$3.0x10^{-8}$	$6.0x10^{-7}$

At temperatures over 2,000 K, the equilibrium composition does not change significantly with initial temperature. Equilibrium composition primarily depends on the species involved in the problem. CO and hydrogen are always the two principal products even when allowing methane combustion to evolve into CO_2 and water. However, equilibrium temperatures (which correspond to the adiabatic temperatures) change modestly. Equilib-

rium temperature is higher for all complete-combustion-allowed cases. Experiments with the plasmatron present exhaust temperatures of the order of 1,000 K - 2,000 K, much lower than what equilibrium calculations show. Initial temperature of the plasmatron inlet however is 300 K. For initial temperature equal to 300 K, equilibrium composition is the same (40% of H_2 and 20% of CO), but equilibrium temperature is 550 K for the Partial Oxidation case and 930 K for the Complete Oxidation case.

When choosing to run EQUIL including all mechanism species as possible products of the reaction, it was found that temperature dropped significantly, to lower values than those of the initial temperature (for initial temperatures above 3,000 K). The principal endothermic reaction that takes place under this conditions is the dissociation of hydrogen into its radical H. H had been disregarded in the previous table. Table 3.3 shows the comparison between the amount of hydrogen in molecular form and in elemental form.

TABLE 3.2 Equilibrium Temperature and Molar Composition for Methane Oxidation with O/C =1 and Different Initial Temperatures for All Mechanism Species

	O/C = 1 **Partial Oxidation Products + H**			**O/C = 1** **Complete Combustion Products + H**		
Initial T (K)	T (K)	x H	x H_2	T (K)	x H	x H_2
2000	2159	$2.5x10^{-3}$	0.407	2134	$2.8x10^{-3}$	0.407
3000	2868	$5.6x10^{-2}$	0.365	2838	$6.2x10^{-2}$	0.365
4000	3245	0.167	0.301	3209	0.170	0.289
5000	3511	0.260	0.213	3473	0.262	0.212

Summing-up, we concluded that at high initial temperature, the equilibrium composition for partial oxidation of methane with air corresponds to 40% molar of hydrogen and 20% molar of carbon monoxide, and that the dissociation of H_2 must be taken into account. Also we found 2% H_2O and 1% CO at equilibrium when H was included in the simulation.

3.1.2 Kinetic models: mechanisms

A kinetic chemistry model requires a group of reactions individually defined. Each reaction is described by its production rate, which is proportional to the temperature-dependent kinetic rate constant k. The most common characterization for the kinetic rate constant follows the Arrhenius scheme, which is given by the product of a pre-exponential A, the temperature to the power β (or temperature exponent) and the exponential term, which includes the activation energy E.

$$k_i = A_i \times T^{\beta} \times \exp\left(\frac{E_i}{R \times T}\right) \tag{3.1}$$

In Equation 3.1, T refers to the gas temperature and R to the ideal gas constant.

In many cases the elementary kinetics are not precisely known, and the experimental measurements result in a rate of reaction proportional to a kinetic constant and the concentration of species raised to a power different than the stoichiometric coefficients.

The quasi-elementary reactions and their associated rate coefficients expressions form the global reaction of interest and define the performance of the kinetic system along time. In some instances, a third body efficiency is also included with the reaction characterization. Third bodies are species whose presence in the mixture may enhance the rate of production.

Prior to starting the simulation of the system, we researched into the different currently available methane mechanisms. Three well-developed and validated mechanism for methane combustion were found (see details in Appendix B):

1. Leeds mechanism,
2. GRI mechanism,
3. Warnatz mechanism (developed together with Sandia Laboratories).

The mechanism developed at the University of Leeds in the United Kingdom is the Leeds methane oxidation mechanism version 1.5 (published in March 2001). It contains 34 spe-

cies and 164 equations. It is a compilation of reactions that have been tested and measured for temperatures that reach up to 6,000 K. Several publications of its authors in the Journal of Chemical Kinetics validate it. A positive aspect of this mechanism is that the latest version is available from the World Wide Web at [Hughes, 2001].

The mechanism from the GRI (Gas Research Institute) is probably the most used of the three [Smith, 2000]. It has been extensively tested for many different conditions and even though there are periodically new updates, the findings indicate that there are no notable disagreements with the predecessors. This mechanism comprises 325 elementary reactions and includes 53 different species. Although it has been optimized for a temperature range between 1,000 K and 2,500 K, the data should be valid for up to 5,000 K. The pressure range is from 10 torr to 10 atm and the equivalence ratio (phi) can go from 0.1 to 5 for premixed systems (plasmatron conditions are 1 atm and phi for partial oxidation equals 4). It is an interesting mechanism since it includes soot and NOx formation. Mainly for this reason, it becomes our primary reference for the chemical simulation.

We found two versions of the same methane combustion mechanism developed by Warnatz. The first one, with 34 species and 164 equations, does not include nitrogen chemistry. The second one, considers NOx formation within the methane oxidation mechanism. That results in 299 equations and 52 species in total. We concentrated our interested in the last one [Warnatz, 1997], one of the first ones to be developed for methane combustion.

The differences between the mechanisms are primarily in specific reaction rates, that is to say, the elementary chemical reactions involved in the process are in most cases the same ones, but some of the kinetics rate constants vary from one model to the other one.

One first step consisted of the comparison between the three mechanisms for simple rich combustion simulations. Simulations using the PLUG application of CHEMKIN were performed in order to compare the outputs of each methane oxidation mechanism for different specified cases. We run only partial oxidation reactions, since this is the focus of

this thesis, however, we examined more than one O/C ratio. We also varied the initial temperature in the reactor.

No significant differences were observed between the three mechanisms for the particular cases tested. Temperature profile and species composition did not differ by more than 5% in most of the them. In Figures 3.1, 3.2 and 3.3 we show the simulation output for each one of the mechanisms (Leeds, GRI and Warnatz, respectively) using a methane-air mixture with O/C ratio equal 1 and an initial temperature of 1,500 K. Compared to the experi-

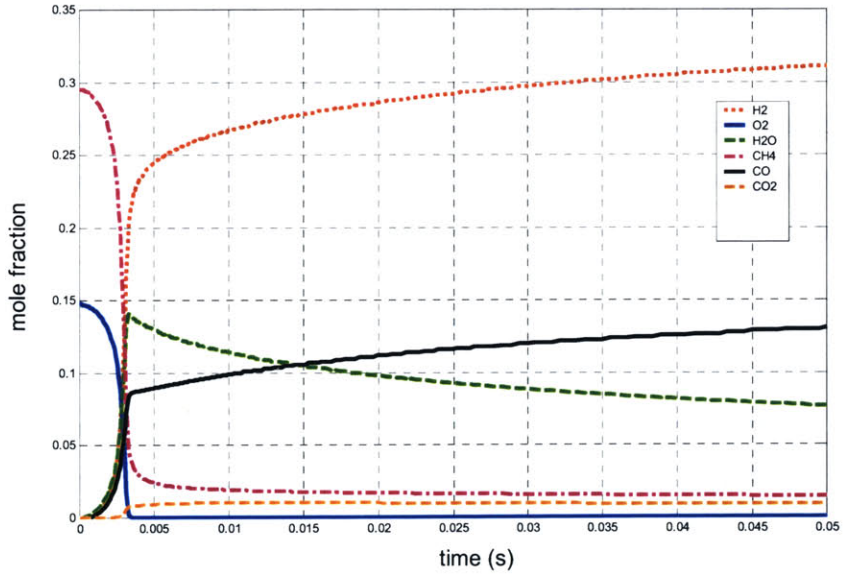

Figure 3.1 Molar Composition along Time in a PLUG reactor for Methane Partial Oxidation with Air at O/C=1 and T=1,500K using the Leeds Mechanism

mental data, all three mechanisms are suitable to model the plasmatron partial oxidation process, since species concentration and evolution are similar in all the cases.

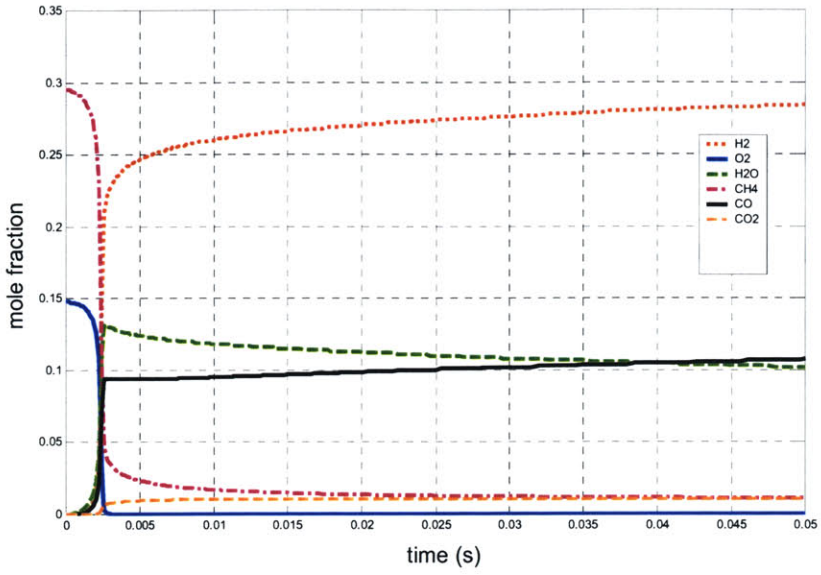

Figure 3.2 Molar Composition along Time in a PLUG reactor for Methane Partial Oxidation with Air at O/C=1 and T=1,500K using the GRI Mechanism

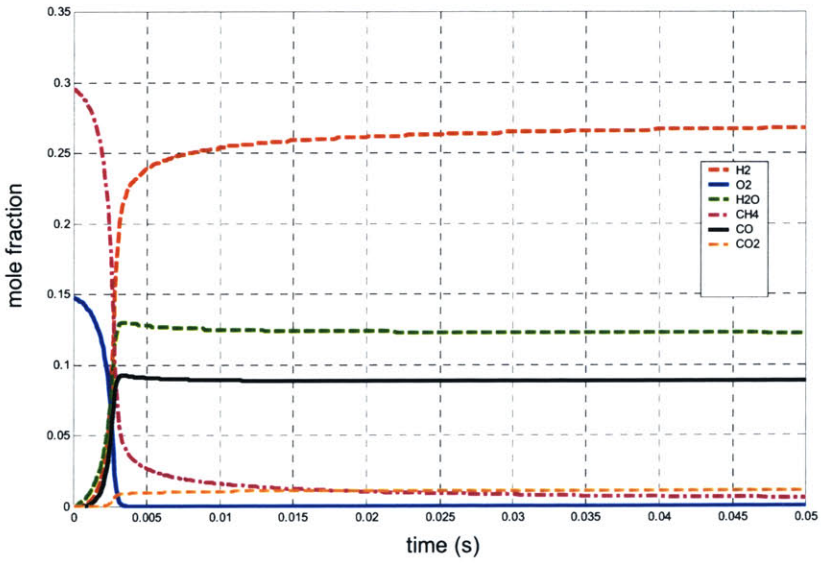

Figure 3.3 Molar Composition along Time in a PLUG reactor for Methane Partial Oxidation with Air at O/C=1 and T=1,500K using the Warnatz Mechanism

3.2 Mixing process

The most complicated and least defined aspect of the plasmatron performance is the evolution of the mixing process. Although some Computational Fluid Dynamics (CFD) calculations have been carried out, the solution to this question is still an enigma.

3.2.1 Mixing parameters: epsilon and kappa

At large scales, the mean kinetic energy of the flow is transferred to turbulent kinetic energy κ or kappa:

$$\kappa = const \times u^2 \tag{3.2}$$

Here u is the root mean square of velocity fluctuations of the flow, thus kappa is a kinetic energy per unit mass.

This turbulent kinetic energy is then transferred from eddies of large scales to eddies in microscales, where it will be dissipated by viscous motion. This is how the mixing action is physically explained. Then, the mixing process in a reactor may be characterized by the mixing frequency τmix, which is usually modeled by the reciprocal of the turbulence time scale [Komiyama, 1975] or also known as mixing rate intensity β:

$$\frac{1}{\tau mix} = \beta = \frac{u}{L} \tag{3.3}$$

where L is the size of the integral scale. The integral scale is the length scale that establishes the time scale of mixing. Turbulence theory states that the mixing intensity is determined by the integral scale and the energy dissipation rate. Hence now, we define the energy dissipation rate ε (epsilon) as the reciprocal time scale multiplied by the kinetic energy per unit mass:

$$\varepsilon = \frac{u}{L} \times u^2 \tag{3.4}$$

Assuming that the integral scale is directly related to the geometry of the reactor, and knowing that ε is the total power input P divided by the total mass M in the reactor, we can derive the expression:

$$\beta = C \times \left(\frac{P}{M \times D^2} \right)^{\frac{1}{3}} \tag{3.5}$$

considering D as the characteristic diameter, and C as a constant that depends on the flow configuration, for example the amount of swirl. This equation may be useful to estimate τmix directly from measurements. Here, the power is evaluated from the energy of the flow through the various orifices to the reactor; the mass M is easily calculated as the average density ρ times the volume V of the reactor; and the constant C is assumed to be close to one. This last assumption is reasonable, since our flow configuration does not change (the plasma reformer design was not varied during the study).

The volume of the reactor[1] is equal to 2.2×10^{-6} m^3 and the average density of the mixture inside the discharge region is close to 1.1 kg/m^3. The analysis of the power input into the reactor is presented in Table 3.3 next.

TABLE 3.3 Turbulent Kinetic Energy from the Input Air and Fuel Stream Jets

	Atomizer jet	**Wall air jet**	**Swirl air jet**
No. of orifices	1	2	6
Inlet diameter (mm)	2.5	2.5	2.5
Mass Flow Rate (g/s)	0.84	1.94	1.94
Density (kg/m^3)	0.65	1.2	1.2
Velocity (m/s)	155	160	53
kappa (m^2/s^2)	3.25×10^4	1.27×10^4	1.41×10^3

1. This considers only the discharge region of the plasmatron.

The atomizer jet kinetic energy becomes the primary source for the turbulent kinetic energy which is dissipated in the turbulent mixing process. The air swirl provides for more efficient kinetic energy transfer from the mean to the turbulent flow.

From these numbers, one can estimate the average $\kappa = 7.40 \times 10^3$ m^2/s^2 as well as the average $\varepsilon = 6.15 \times 10^7$ m^2/s^3 for the system. Those will later help us determine τmix.

On the other hand, τmix can be computed from CFD calculations that find the values of kappa and epsilon. From the same expressions above, one can observe that the following equation is valid:

$$\tau mix = C \times \frac{\kappa}{\varepsilon} \tag{3.6}$$

Proportionality is through the constant C, that is chosen to be one in our calculations.

CFD calculations using FLUENT 6.0 software were performed at the PSFC [Bromberg, 2002] in order to provide the system τmix. For different flow configurations, but maintaining the same plasmatron design, the estimated values for kappa and epsilon resulted in average of the order of $\kappa = 200$ m^2/s^2 and $\varepsilon = 2 \times 10^6$ m^2/s^3. These numbers are both one order below the estimated numbers with Equations 3.2 and 3.4. However, when we use Equation 3.6 to find τmix, we obtain in the CFD case and the theoretic case respectively that $\tau mix = 1.0 \times 10^{-4}$ s and $\tau mix = 1.2 \times 10^{-4}$ s. Thus we conclude that the mixing time is of order tens of microseconds.

Figures 3.4 and 3.5 show the results that were obtained for one of the various configurations that were tested. The average calculated for epsilon and kappa is the mean from all the tested configurations.

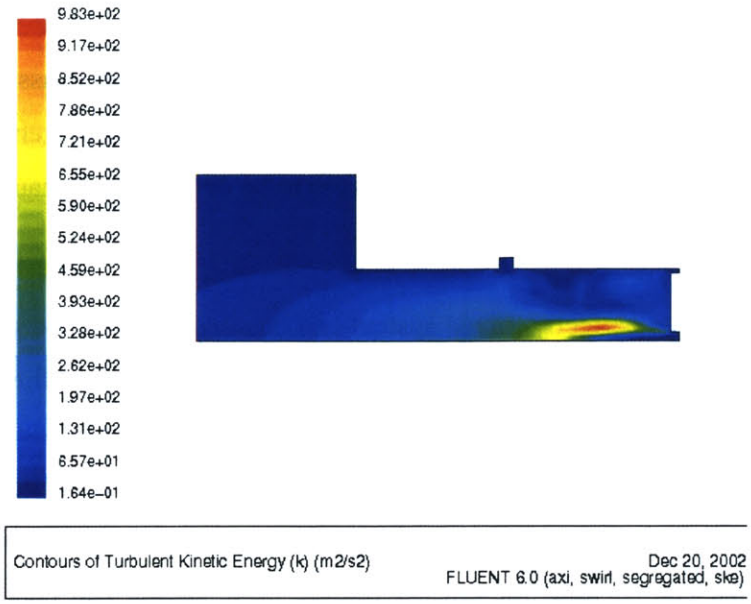

Figure 3.4 Turbulent Kinetic Energy in the Plasmatron Reactor Zone for Swirl Velocity 50 m/s and Total Mass Flow Rate of 5.9 g/s

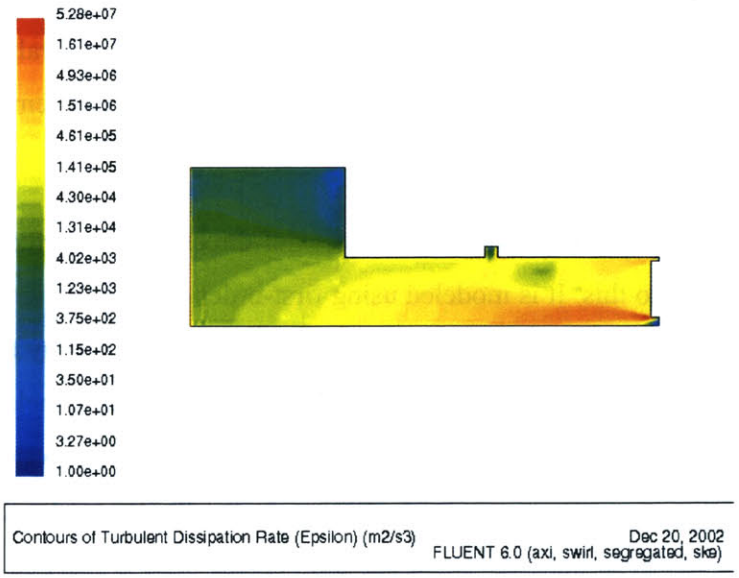

Figure 3.5 Turbulent Dissipation Rate in the Plasmatron Reactor Zone for Swirl Velocity 50 m/s and Total Mass Flow Rate of 5.9 g/s

3.2.2 Perfectly mixed

The ideal case for a reactor system is a perfectly-stirred reactor. It is assumed to be spatially uniform due to high diffusion rates, the particles instantaneously generate a homogeneous mixture. In fact, there is no mixing process to be considered, because the mixing is immediate.

Also, a homogeneous perfectly mixed system can be simulated using a one-dimensional uniform reactor model (plug flow reactor). A plug flow reactor models the non-dispersive, one-dimensional flow of a chemically reacting, ideal-gas mixture in a conduit of essentially arbitrary geometry. CHEMKIN includes in its software package an application called PLUG [Reaction Design, 2002]. This is a general model for the steady-state tube flow reactor that can be used for process design, optimization and control. It involves transport phenomena, kinetics and thermodynamics. CHEMKIN assumes the thermodynamic properties to be thermally perfect, only function of temperature and given in terms of polynomial fits to the heat capacity molar in standard state. The pertinent information includes the species name, the elemental composition of the species, and the temperature ranges over which the polynomial fits to the thermodynamic data are valid. The fits consist of seven coefficients for each of two temperature ranges. The temperature ranges cover a margin between 300 K and 5,000 K.

A plug flow reactor assumes no mixing in the axial direction but perfect mixing in the directions transverse to this. It is modeled using first-order ordinary differential equations (ODE'S) that include general relations for conservation of mass, energy and momentum. DASSL [Petzold, 1982] is a solver for systems of ODE'S that uses a backward differentiation formula (BDF) method. The methods are variable step-size and variable order. The system of equations is written in an implicit form. In the PLUG model, DASSL will be used to integrate fictitious transient equations until steady state is reached. Steady state is assumed to be achieved when there is no significant change (tolerance specified by user) in the site fractions over the course of one time step.

The plug flow reactor can be isothermal, adiabatic or may have a specified overall heat-transfer coefficient to calculate the heat exchange with the environment. Both last features will be used for the plasma reformer simulation study.

3.2.3 Partially mixed

In comparison to the perfectly stirred idea, we find that, most of the time, reactors deviate significantly from an ideally mixed situation. Indeed, there is a certain time involved in the diffusion process. The turbulent mixing rate is basically not fast enough compared to the chemical kinetics, they are often in the same time order, and the degree of mixing has a mayor impact on the reactor behavior. A gaseous air-fuel case cannot be treated as uniformly mixed.

We used the PASR application of CHEMKIN to model this reactor concept [Reaction Design, 2003]. Inside the PASR, the mean thermo-chemical properties are assumed to be spatially homogeneous, but imperfectly mixed at the molecular level, i.e., the reactive fluids are not completely diffused into each other. The mixing process in the PASR is characterized by the mixing frequency, which is modeled by the reciprocal of the turbulence time scale. The PASR does not resolve fluid dynamic details, therefore the mixing frequency parameter must be prescribed as a user input. The composition and temperature in the PASR are described by a probability density function (PDF). Velocity fluctuations are ignored and thus the PDF is over scalars only. The mean thermo-chemical properties inside the reactor are assumed to be spatially homogeneous. These average statistics are the sum of the properties of independent elements of the reactive mixture weighted by the PDF of the time they have been inside the reactor.

The mean reactor residence time and the chemical reaction time are the other two characteristic times of the reactor. The average residence time of the reactor is defined as:

$$\tau res = \frac{V \times \bar{\rho}}{\dot{m}} \tag{3.7}$$

the reactor volume V times the average density ρ, divided by the total mass flow rate m through the reactor. τres is a necessary input for the software.

On the other hand, the chemical reaction time $\tau chem$ is internally computed from the set of reactions that describe the kinetic mechanism. Finally, the previously mentioned mixing time is considered to be proportional to the turbulent eddy turnover time as shown in Equation 3.6. τmix is proportional to the ratio of turbulent kinetic energy κ and inversely proportional to its dissipation rate ε, which represents the time scale of the energy-containing eddies that explain the mixing action. κ and ε are parameters that can be estimated from the fluid dynamics analysis of the system, as previously explained in Section 3.2.1, and from their value one can calculate and input τmix in the PASR software.

The results from the PASR approach a perfectly stirred reactor limit when the ratios $\tau mix/\tau res$ and $\tau mix/\tau chem$ are significantly smaller than one, or in other words, when the characteristic mixing time is so small compared to the other characteristic times than mixing can be considered to be instantaneous.

PASR provides three different types of a DVODE package to solve the ODE'S problem. A non-stiff Adams method, an implicit Adams method or the backwards differentiation formulas (BDF) may be chosen to integrate the equations. Another solver called DDASPK package is available, although it has not been used because the DVODE is proved to be faster and more tolerant. DVODE does not check for the consistency of the first time derivatives, thus it is not as robust but it performs better in our quasi-stiff case. In particular, the BDF type is the one which provides faster and more appropriate solutions.

Stochastic Mixing Models (SMM): Modified Curl's model and Interaction by Exchange with the Mean model

The stochastic mixing model represents the composition of the fluid at any position in a reactor as an ensemble of fluid elements which are identified in terms of their individual thermodynamic states. The state of each element may be assumed to be uniform through-

out its volume at any instant of time. However, this given state may vary with time as a result of mixing and reaction within the element.

A group of N equal mass fluid elements represents the incoming fluid composition. A fraction of these elements, Na/N represents the flow through the fuel atomizer, the remaining N - Na represent the pure combustion air. Each element is assigned a number index, and is allowed to mixed completely, separate, and then react according to the appropriate chemical rate equations.

Mixing interactions are computed sequentially. The frequency at which elements collide or mix, the mixing time, needs to be determined. At each mixing iteration a group of n elements is chosen at random from the entire ensemble of N. Those chosen elements mix by pairs, yielding two new elements of exactly same thermodynamic properties and composition. At any time, the mean composition and other mean properties can be evaluated by taking an average over the N fluid elements. Between mixings, each element will individually experience chemistry appropriate to its own conditions. The Monte Carlo integration is usually used to solve the master equations, which include mass conservation, energy conservation and chemical kinetics differential equations.

One can choose between two different mixing models within the PASR: the modified Curl's mixing model and the Linear-Mean-Square-Estimation (LMSE) or Interaction-by-Exchange-with-the-Mean (IEM) model. In order to distinguish between the two different methods, an unmixedness parameter is defined. The unmixedness or segregation variable is a parameter used to quantify the unmixed nature of the system, and its formula is:

$$unmixedness = \frac{1}{1 + Cmix \times \frac{\tau res}{\tau mix}} \tag{3.8}$$

where the constant C*mix* is equal to 1/3 for the modified Curl's model and dependent on flow configurations for the IEM model.

[Reaction Design, 2003] states that the modified Curl's model predicts wider spread particle temperatures comparing to results obtained by the IEM model.

Specification of the PASR inputs and outputs

The PASR application uses a collection of keywords to specify the necessary inputs that define the system. We will only comment on the main required ones.

PRES: reactor pressure in atm.

FLRT: inlet total mass flow rate in g/s.

TAU: residence time of the gas in the reactor in s.

FORT: stream 1 (FUEL) to stream 2 (OXID) molar flow rate ratio (dimensionless).

TFUE: gas temperature of stream 1 in K.

FUEL: stream 1 mass or mole fraction for the given species (dimensionless).

TOX: gas temperature of stream 2 in K.

OXID: stream 2 mass or mole fraction for the given species (dimensionless).

MIX/CHEM/EQUI: flag indicating whether it is a mixing only problem with no chemical reaction (MIX), a chemical kinetics reacting problem (CHEM) or an equilibrium problem (EQUI).

WELL/CURL/IEM: flag indicating whether it is used a well mixed model (WELL), the modified Curl's model (CURL) or the interaction-by-exchange-with-the-mean model (IEM).

MIXT: the characteristic mixing time in the reactor in s.

CMIX: the controlling parameter for the modified Curl's and the IEM models.

DT: the time step size of the Monte Carlo integration in s.

NPAR: the number of statistical events or particles used by the Monte Carlo process to form the stochastic ensemble.

BDF/ADAM/NOJC: flag indicating DVODE method used to integrate the equations (stand for Backward Differentiation Formulas, implicit Adams, Non Jacobian).

We are constrained by those input parameters. The several drawbacks that arise are listed:

1. There are only two inlet streams that feed the reactor. They are by default called oxidizer (OXID) and fuel (FUEL), although they are not required to be constituted but such type of substances.
2. The inlet streams can only be represented by homogenous mixtures of different species. Neither temperature nor concentration can be introduced using a probability distribution function (PDF).
3. The number of elements is extremely dependent on the time step size chosen for the Monte Carlo integration. The smaller the integral time, the larger the number of particles must be. This directly affects the model performance, since the number of particles varies the output of the simulation, and the Monte Carlo time step cannot be kept constant because different reaction conditions require limited computation depending on the stiffness of the system of equations.

   One could try to run simulations in order to find a solution that is independent of the number of particles (increasing gradually the number of particles until constant values are obtained). However, this is very time consuming and was not done at this time.

The outputs provided by the software can be grouped in three different classes:

1. Average thermodynamic properties of the mixture at the exhaust, such as: temperature, pressure, density.
2. Average species composition at the exhaust of the reactor, for each of the species present in the mechanism.
3. The standard deviation of the thermodynamic properties and the species compositions. The standard deviation is the square root of the sample variance σ^2, which is the average over the number of samples n of the square of the variance of a variable y:

$$\sigma^2 = \frac{1}{n} \times \sum_{1}^{n} \langle y_i - \bar{y} \rangle^2 \tag{3.9}$$

All those outputs are variant along the simulated real time, and the user can set how often they have to be reported. There are advantages and disadvantages regarding the outputs of the model:

1. The software provides the reactor composition in a mass fraction basis.
2. We are given the standard deviation of compositions, density and temperature of the system, not along time, but among the total number of elements in the reactor at that time.
3. Although numbered, we cannot follow each individual element independently. Investigating which particles interact with each other and how they evolve is not featured in the PASR.
4. The particular thermodynamic properties and species composition of each individual element, which can be develop into a PDF profile, can only be obtained at the end of the simulation, that is to say, one model run provides one unique PDF of the outlet stream at one single end time.

As an example of computation time, using a Celeron Pentium III processor, with CPU of 1.6 GHz and 256 MB of RAM, a one residence time (1 ms) simulation run takes between 6 h and 12 h to be completed, depending on the chosen DT and NPAR.

Chapter 4
PERFECTLY MIXED MODEL

Using the PLUG application of CHEMKIN, a series of calculations have been run to learn about the behavior of the plasmatron electric discharge and the combustion process that takes place inside the reactor. Determining how the reaction is initiated and how diverse operating conditions have a general impact on the plasmatron performance are the main goals of this chapter, since the perfectly mixed model cannot be directly linked to a real system.

4.1 Chemical effects of the discharge

One of the main interests of the plasmatron model is finding the effect of the mass and temperature of the plasma generated by the electric discharge. We have studied in Chapter 2 the arc behavior from the movies and pictures of its aspect and shape. In addition, we have learned about the energy input that transformed into thermal energy represents an important temperature boost. We decided to explore two possible outcomes produced by the current travelling through the arc:

- Temperature increase
- Radicals generation

By ranging these parameters we tried to determine their influence on the ignition time and the subsequent combustion process.

4.1.1 Temperature effect

Several simulations for methane partial oxidation with air have been carried out using the PLUG application of CHEMKIN that predicts the evolution of all species involved in a chemical scheme with time. We used the GRI mechanism for such calculations. The reac-

tants considered were methane and air as a mixture of 79% nitrogen and 21% oxygen. Reaction was assumed to occur at atmospheric pressure. Initial conditions for the O/C ratio of the inlet mass were kept constant and equal to 1.

To check the variability of the system performance depending on initial temperature, we swept a range of values from standard temperature 300 K to 2,000 K. The aim was to initiate combustion within the reactor. Therefore, we used two residence times: the residence time of the flow inside the whole plasmatron and the residence time of the flow in the discharge zone. The latter had been previously calculated, and it was found to be 3 ms. The former is approximately 100 ms at 200 l/min and 500 ms for the lowest flow rate, considering the plasmatron reactor to be 30 cm long.

In general, the temperature profile presents a peak at the ignition point, and a subsequent drop towards a steady value between the initial and the peak temperatures (see Figures 4.2 and 4.4). Temperature is thought to decrease after the maximum because of endothermic cracking of CH_4, C_2H_6 and C_2H_4 to C_2H_2 and H_2.

Based on the longest residence time (500 ms), a minimum temperature of 1,100 K was necessary for the reaction to start inside the fuel reformer, and a higher temperature was required (1,500 K) for ignition to occur inside the discharge zone (3 ms). The ignition delay was found to decay exponentially with temperature as shown in Figure 4.5. For initial temperatures above 1,500 K, the steady value happens to be over 1,700 K, which causes water concentration to decrease to half its initial value. Methane undergoes steam reforming. The steam reforming process is the reaction of water with any hydrocarbon, methane and its co-products ethylene and ethane in this case, to produce hydrogen and carbon monoxide, that in effect, experience concentration increase at those conditions.

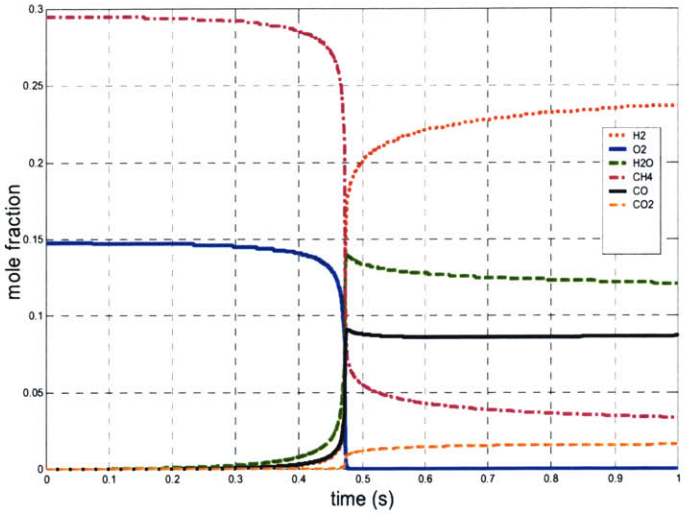

Figure 4.1 Molar Concentration of Species along Time and along the Plug Flow Reactor for 1,100K Initial Temperature and O/C=1

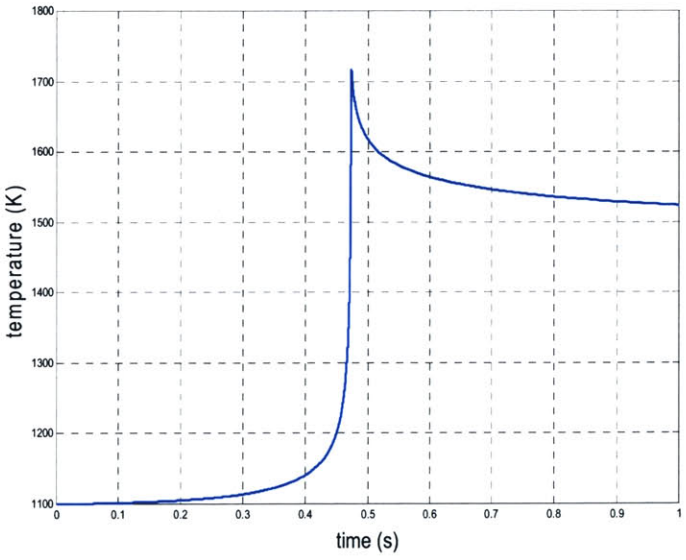

Figure 4.2 Temperature Profile inside the Plug Flow Reactor along Time for 1,100K Initial Temperature and O/C=1

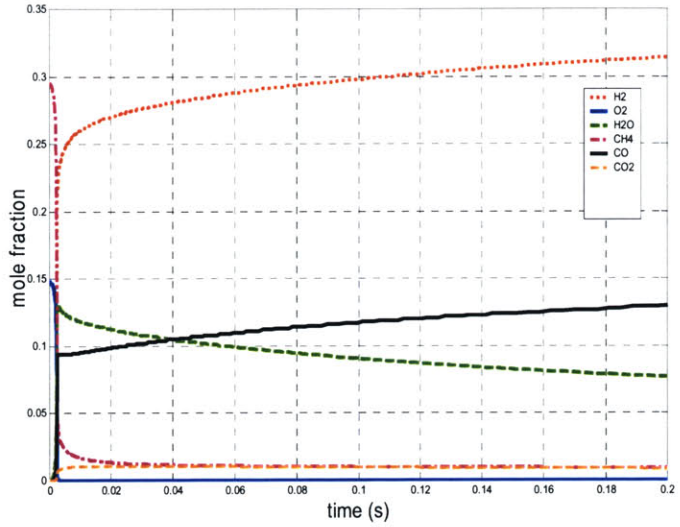

Figure 4.3 Molar Concentration of Species along Time and along the Plug Flow Reactor for 1,500K Initial Temperature and O/C=1 (Steam Reforming)

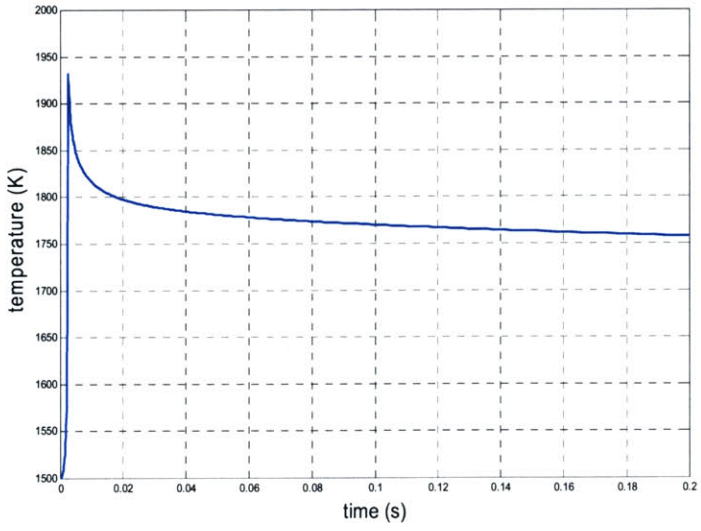

Figure 4.4 Temperature Profile inside the Plug Flow Reactor along Time for 1,500K Initial Temperature and O/C=1 (Steam Reforming)

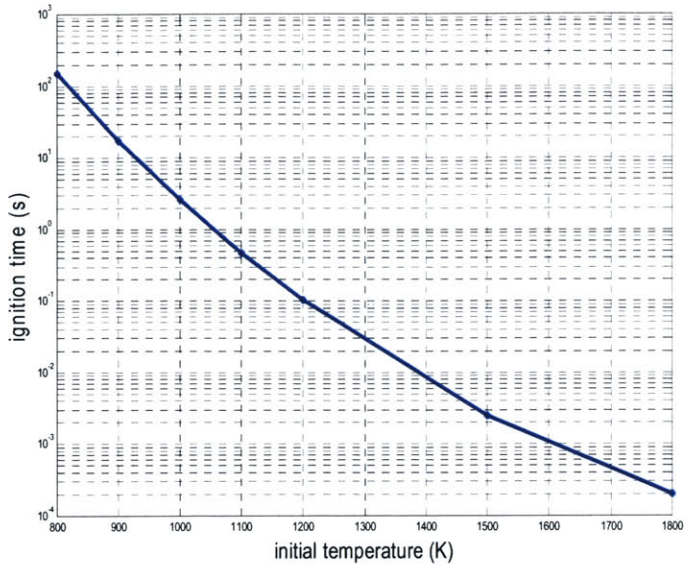

Figure 4.5 Ignition Time as a Function of Initial Temperature in the Plug Flow Reactor for O/C=1

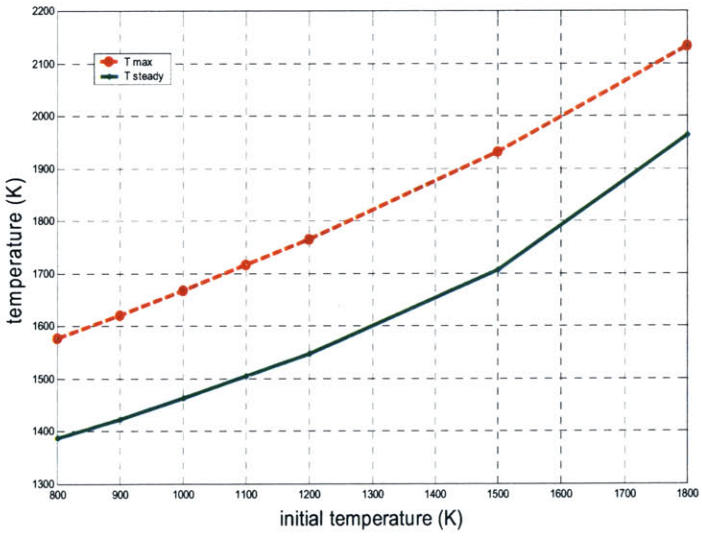

Figure 4.6 Temperature Peak and Steady State Temperature as a Function of Initial Temperature in the Plug Flow Reactor for O/C=1

4.1.2 Radicals presence

The next step consisted of testing the response to seeding the gas flow with radicals (such as OH) or assuming that part of the reactants are partially dissociated into O or H in the plasma zone. It is known that free O radicals, obtained from dissociation of oxygen, are able to start the H_2-O_2 branching mechanism that is responsible for the fuel-air mixture ignition. On the other hand, we can also obtain H radicals from the pyrolysis of methane, which corresponds to the endothermic elemental reaction: $CH_4 + M = CH_3 + H + M$, where M is any other species present in the system. OH is an alternative combustion initiation precursor. A possible route for OH generation is through aldehyde formation from methyl (CH_3). All those mechanisms are more likely to happen at high temperatures.

Ignition delay of combustion was studied for different concentrations of radicals at different initial temperatures. We tested 1%, 10% and 20% dissociation of oxygen into O (which correspond to 0.3%, 2.8% and 5.8% mole fraction of O), and 1%, 10% and 20% dissociation of methane into H and CH_3 (which correspond to 0.3%, 2.7% and 5.6% mole fraction for H and for CH_3), individually and simultaneously combined. Also, we tried seeding with OH radical in fractions of 0.3% and 3% molar. Table 4.1 shows the results obtained.

To check whether the tested concentrations correspond to reasonable concentrations of radicals in the plasmatron flow, we estimated the necessary amount of energy to convert 10% of the O_2 gas in the reactor into its radicals O. Considering that each O radical needs approximately 10eV to be created (960 kJ/mol), 1 kW would be necessary to dissociate 10% of the oxygen into O for a flow rate of 1g/s through the plasmatron. This amount of energy is not available. The plasmatron power supply delivers less than 900 W and we estimated in Chapter 2 that the energy loss is 75%, which represents a maximum power of 225 W though the arc. Therefore, it is not reasonable that we find such large fraction of radicals in the electric discharge plasma region, but it would be possible to have lower concentrations. In fact, we believe that part of the energy input from the electric discharge is converted into thermal energy (moderate temperature increase of the order of 5,000 K)

TABLE 4.1 Reaction Ignition Time (s) due to Radicals Presence

Species concentration	Ignition time (s)	
	T_i = 500 K	T_i = 1,000 K
No radicals	>1,000	0.31
x O = 0.3%	195	0.23
x H = 0.3%	240	0.29
x OH = 0.3%	290	0.25
x O = x H = 0.3%	140	0.23
x O = x OH = 0.3%	125	0.21
x O = 2.8%	10	$5x10^{-3}$
x H = 2.7%	2	$3x10^{-3}$
x OH = 3%	$3x10^{-5}$	$4x10^{-6}$
x O = x H = 3%	$4x10^{-6}$	$4x10^{-7}$
x O = 5.8%	$1x10^{-5}$	$1x10^{-6}$
x H = 5.6%	$2x10^{-5}$	$3x10^{-6}$

and part is used as chemical energy to break up the bonds of molecules and create a source of primary radicals. We calculated in Section 2.1.2 that 0.6 J are necessary to heat and dissociate the discharge mass. If the total amount of oxygen molecules present in the discharge were dissociated, the resulting concentration of O in the reactor would be lower than 0.01%. In conclusion, although we are not able to quantify how much power of the available 225 W is used for gas dissociation, radicals composition below 1% seems more reasonable than above 1%.

Ignition or delay time is calculated as the inflection point of the temperature rise curve. At low initial temperatures (500 K), when ignition does not occur fast enough to imitate combustion inside the reactor, radicals in concentration higher than 1% do significantly reduce delay time. However, it is not possible to have so high concentrations under the plasmatron conditions. For concentrations lower than 1%, the presence of radicals does not have a strong effect at high initial temperatures (1,000 K). Even though ignition time is reduced in all cases, the difference is not significant because combustion cannot start within the reactor. We need initial temperatures above 1,000 K to trigger the reaction within the resi-

dence time of the reactor, and at those temperatures the effect of radicals at 1% concentration is found to be negligible.

The O radical is the species that has a stronger effect on the combustion process at concentrations below 1%. OH causes the maximum reduction on ignition time at 3% molar fraction. Excess radical presence has another particular effect in the mixture. When concentrations of 1% molar are introduced, temperature in the reactor is increased around 100 K. At 5% molar fraction, temperature increases in approximately 500 K. Finally, if concentrations are raised up to 10%, an increment in temperature results in more than 1,000 K. This increment in temperature, probably driven by recombination of the elements, enhances ignition, rather than the radicals on their own.

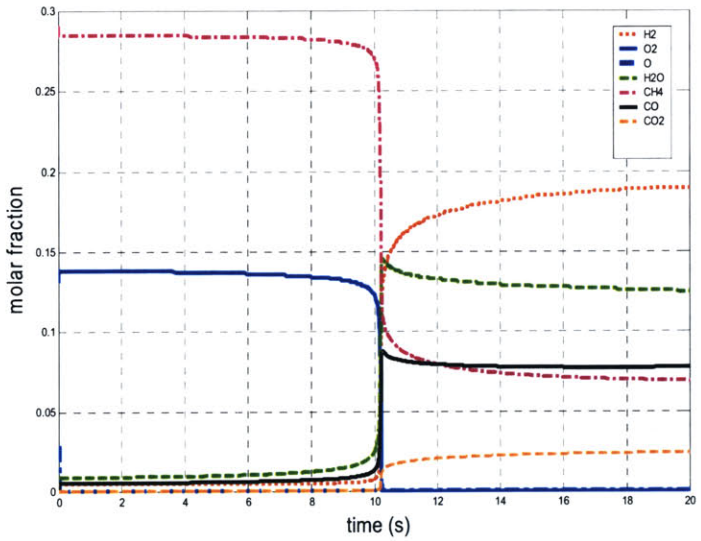

Figure 4.7 Molar Concentration of Species along Time and along the Plug Flow Reactor for 500K Initial Temperature, O/C=1 and 10% of Initial Oxygen Dissociated into Radicals O (3% molar fraction)

Figure 4.7 demonstrates how initial 3% molar fraction O radicals are immediately recombined into molecular oxygen O_2. It can be appreciated how oxygen concentration rises and O concentration drops to zero right at the start of the simulation. Methane also experi-

ments a rapid small decrease in concentration, which is due to pyrolysis into methyl and hydrogen gas caused by the radicals themselves and the rise in temperature driven by their recombination. This temperature increment is shown in Figure 4.8. Initial temperature rises from 500 K to 800 K at the first interval of integration time.

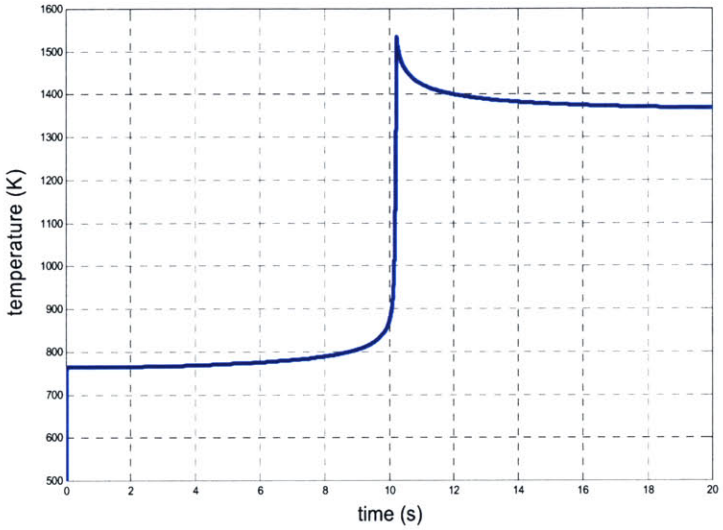

Figure 4.8 Temperature along Time and along the Plug Flow Reactor for 500K Initial Temperature, O/C=1 and 10% of Initial Oxygen Dissociated into Radicals O (3% molar fraction)

4.2 Sensitivity analysis: adiabatic plug flow model

In a plug flow reactor (PFR) there is one single homogeneous stream that moves along the reactor with no axial mixing (exclusively perfect radial mixing). It represents a system based analysis since we actually follow the particles as they advance. The lack of transverse gradients implies that mass-transfer limitations are absent, enhancing the reactor performance. The total energy of the flowing gas may change due to heat flux from the gas to the inner tube wall, and from the outer tube wall to the surroundings. However, an adiabatic model assumes the wall is perfectly isolated and no heat flux is exchanged with the exterior ($Q = 0$).

4.2.1 Premixed one-stage process

Calculations have been run using the PLUG model. By varying parameters such as the O/C ratio, we can compare the actual experimental results with the plug flow reactor model simulations. We had seen that temperature affects the ignition time and how quickly steady state is achieved. However, the exhaust composition tends to be constant for those cases in which ignition is contained within the discharge zone. At initial temperature higher than 1,500 K the molar concentration of species at the plasmatron exit is: 30% of H_2, 12% of CO, 8% of H_2O, 1% of CO_2 and 1% of CH_4. In Figure 4.9, we studied the variation of hydrogen yield and syngas composition as a function of O/C ratio. We found a maximum around O/C=1.2 for hydrogen production. This is caused by a trade-off between residence time and ignition time. As O/C ratio increases, the delay time drops (Figure 4.10) and the temperature in the reactor increases (Figure 4.11).

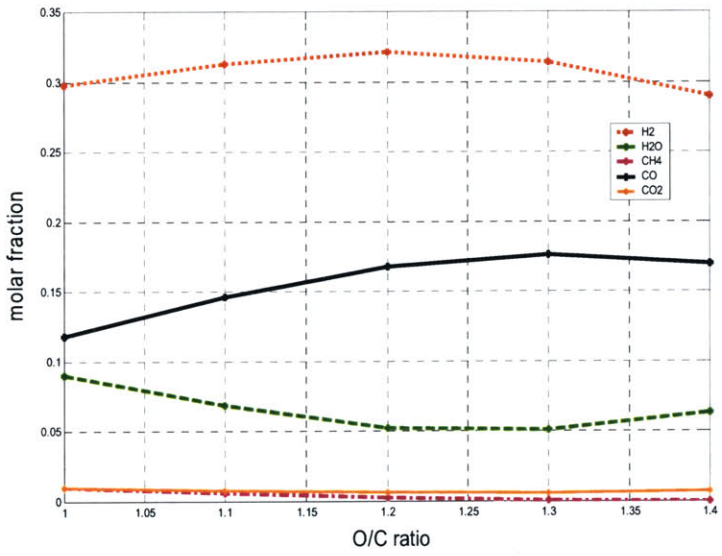

Figure 4.9 Molar Composition of the Syngas at the Plasmatron Exit (4g/s and 30cm long) as a Function of O/C Ratio using an Adiabatic Plug Flow Reactor Model (Tinitial=1,500K)

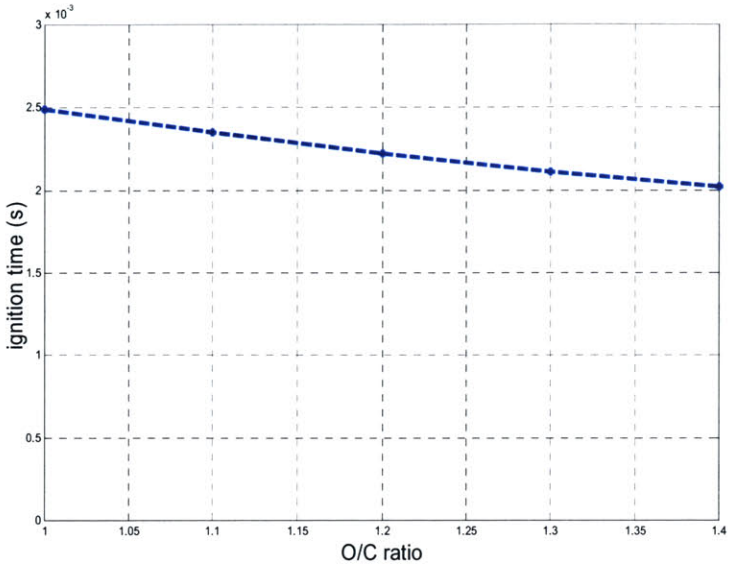

Figure 4.10 Ignition Delay Time at the Plasmatron as a Function of O/C Ratio (Tinitial=1,500K) using an Adiabatic PFR Model

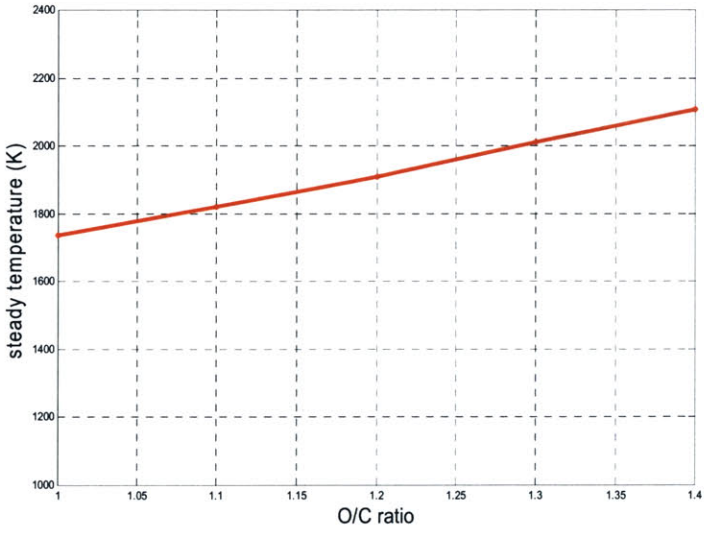

Figure 4.11 Steady Temperature in the Plasmatron as a Function of O/C Ratio (Tinitial=1,500K) using an Adiabatic PFR Model

Higher temperature reduces the residence time in the plasmatron. Therefore, while shorter delay time enhances hydrogen yield, shorter residence time diminishes hydrogen production at the exit. At O/C ratios higher than 1.4, the combustion process is increasingly oxidizing and thus hydrogen concentration at exhaust is significantly reduced.

4.2.2 Oxygen enrichment

Adding pure oxygen to the air stream produces oxygen enrichment in the flow, i.e., the volume fraction of oxygen in air is higher than 21%. Concentrations of 20%, 30% and 40% in air were tested. It was found that hydrogen and carbon monoxide concentrations increase with the amount of oxygen in air.

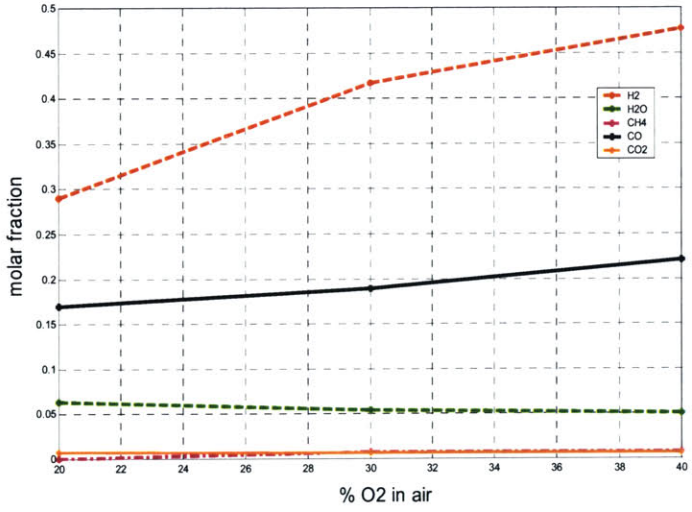

Figure 4.12 Molar Composition of the Syngas at the Plasmatron Exit (4g/s and 30cm long) as a Function of O_2 Enrichment using an Adiabatic Plug Flow Reactor Model (T=1,500K; O/C=1)

Figure 4.12 shows a trend of the syngas composition to reach equilibrium concentrations. Molar fractions higher than 40% in hydrogen (equilibrium composition for methane partial oxidation in air) are achieved because of the decrease in nitrogen concentrations[1]. The

1. Equilibrium H_2 molar fraction for methane in O_2 enriched air is 48% for 30% O_2 and 53% for 40% O_2.

partial oxidation products increase because of higher oxygen enrichment. This is because while O/C is maintained constant and equal to one, oxygen concentration increases which helps methane rich combustion and improves its conversion into syngas.

4.2.3 Two-stage process: pre-combustion

A partial modification to the plasmatron was also modeled. Oxidation of methane is designed to happen in two stages, assuming a global O/C for partial combustion equal to 1.2, 1.4 and 1.6[1]:

1. First, a certain fraction of the initial methane is pre-combusted, using complete combustion stoichiometry. We use air as oxidizer and also air enriched with 30% and 40% of oxygen. We let the mixture reach equilibrium.
2. Then, the methane and air at ambient temperature that were not precombusted, are added to the previous gas mixture, that is already hot. We calculate the initial temperature of the whole system as a simple thermal energy exchange at constant pressure between the two masses (see Equation 2.2).

The results obtained are summarized in Tables 4.2, 4.3 and 4.4. The higher fraction of methane pre-combusted, the higher the global temperature becomes. This helps methane conversion into hydrogen, although the second stage does not release as much energy since there is not as much oxygen left. For O/C=1.2, the maximum methane conversion we obtain is of the order of 80% and H_2 composition is lower than 30%, which indicates no improvement relative to the one-stage reactor. O_2 enrichment helps hydrogen production when the O/C ratio and the pre-combusted fraction are maintained. For higher global O/C ratios methane conversion rises, but it does not produce more H_2, because reaction stoichiometry moves away from partial oxidation. In order to get 90% or more of methane conversion, we need to work either with a global 40% of oxygen enrichment or set the O/C equal to 1.6, which is not beneficial for H_2. Hydrogen concentrations are under 25% for all the simulations.

1. For lower O/C ratios the problem is that not enough oxygen is present in order to realize a complete oxidation at the pre-combustion stage.

TABLE 4.2 PLUG Molar Results and Initial Temperature at the Second Stage for Partial Oxidation of Methane in a Two Stage Reactor using O/C =1.2

%O_2 in air	%precombusted	CH4 conversion	x H_2	x H_2O	T_i (K)
20	10	0.004	0.001	0.052	830
20	20	0.552	0.110	0.149	1350
20	30	0.698	0.138	0.162	1880
30	10	0.023	0.004	0.068	870
30	20	0.758	0.195	0.186	1440
30	30	0.880	0.214	0.205	1990
40	10	0.094	0.015	0.103	880
40	20	0.840	0.256	0.211	1460
40	30	0.945	0.275	0.211	2040

TABLE 4.3 PLUG Molar Results and Initial Temperature at the Second Stage for Partial Oxidation of Methane in a Two Stage Reactor using O/C =1.4

%O_2 in air	%precombusted	CH4 conversion	x H_2	x H_2O	T_i (K)
20	10	0.000	0.001	0.045	770
20	20	0.637	0.107	0.155	1240
20	30	0.750	0.125	0.165	1700
30	10	0.015	0.003	0.059	810
30	20	0.085	0.191	0.195	1330
30	30	0.935	0.198	0.212	1840
40	10	0.049	0.007	0.081	830
40	20	0.917	0.248	0.230	1350
40	30	0.986	0.256	0.238	1880

Figures 4.13 to 4.15 show that for higher fraction pre-combusted, hydrogen production benefits. This is because the more methane is totally combusted, the higher is the initial temperature in the second step, and hence the delay time decreases. On the other hand, the figures also show that when the O/C ratio is increased, hydrogen concentration is not improved. Although oxygen enrichment is advantageous for hydrogen production, the two-stage combustion reactor is not and the one-stage structure provides higher hydrogen concentration. The two-stage reactor is positive for methane conversion only.

TABLE 4.4 PLUG Molar Results and Initial Temperature at the Second Stage for Partial Oxidation of Methane in a Two Stage Reactor using O/C =1.6

%O_2 in air	%precombusted	CH4 conversion	x H_2	x H_2O	T_i (K)
20	10	0.005	0.001	0.040	720
20	20	0.659	0.090	0.161	1140
20	30	0.814	0.116	0.169	1560
30	10	0.012	0.003	0.052	770
30	20	0.929	0.184	0.202	1230
30	30	0.978	0.183	0.215	1700
40	10	0.193	0.025	0.199	780
40	20	0.992	0.162	0.269	1260
40	30	0.994	0.230	0.214	1720

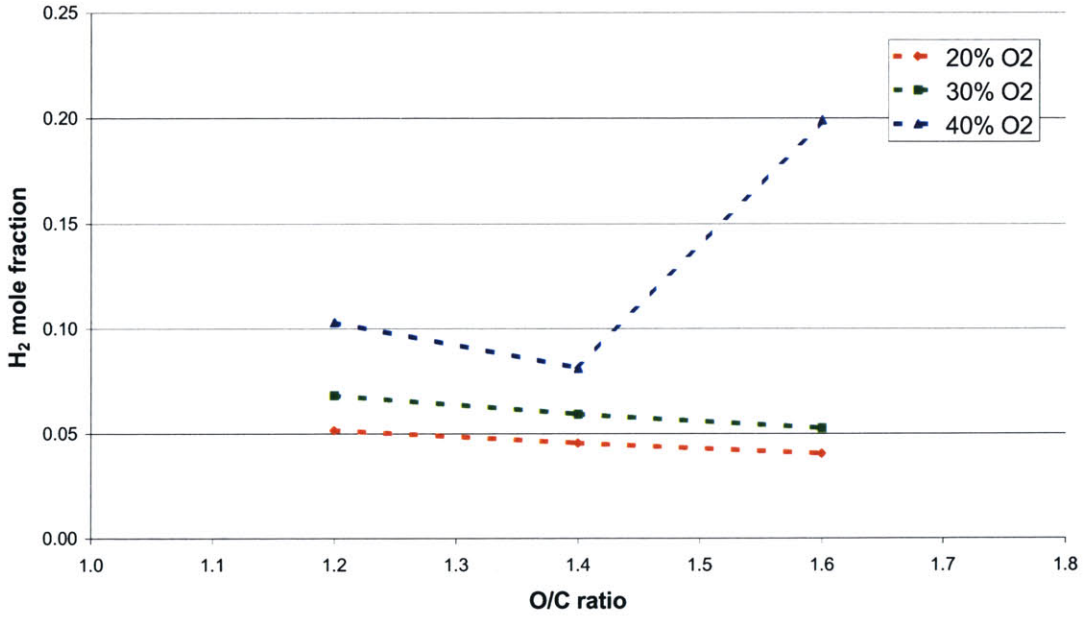

Figure 4.13 Hydrogen Molar Fraction at the Plasmatron Exit as a Function of Global O/C ratio for Different Air Oxygen Enrichment, using a Two-stage Combustion Model with 10% CH_4 Precombusted

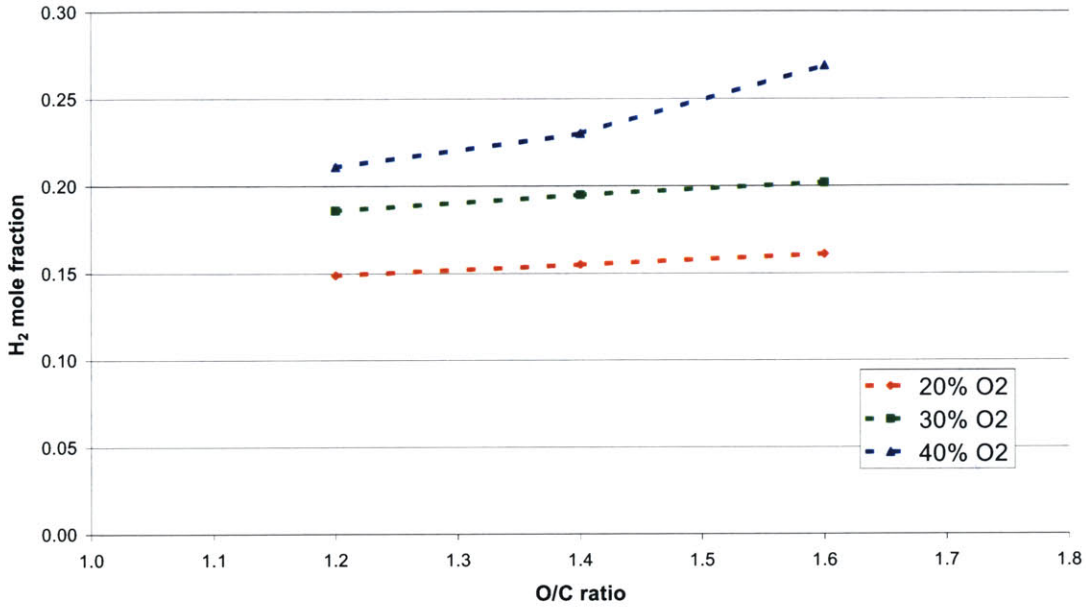

Figure 4.14 Hydrogen Molar Fraction at the Plasmatron Exit as a Function of Global O/C ratio for Different Air Oxygen Enrichment, using a Two-stage Combustion Model with 20% CH_4 Precombusted

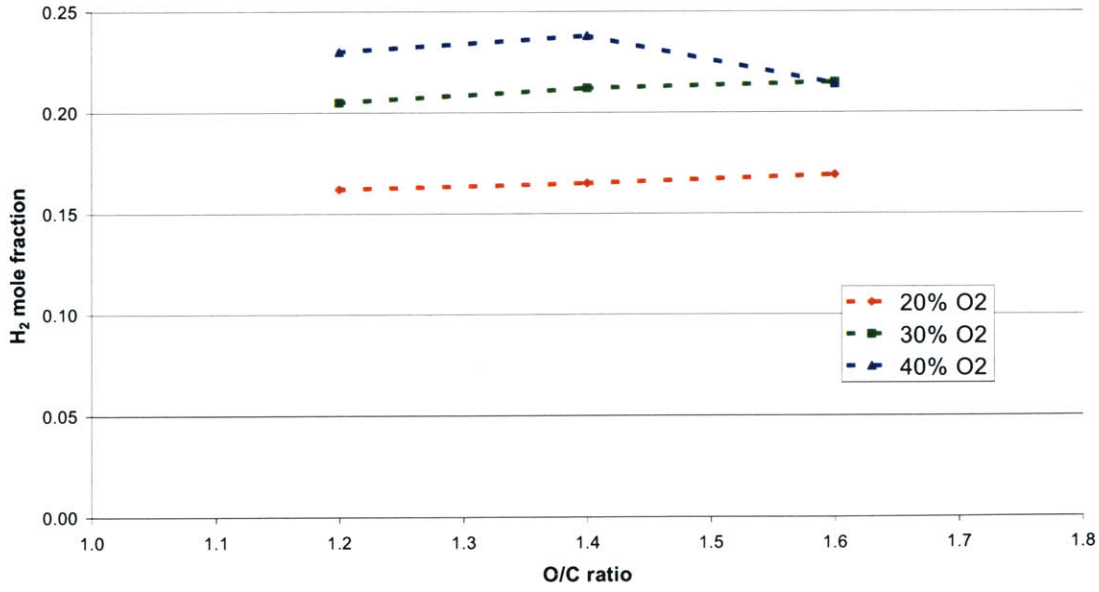

Figure 4.15 Hydrogen Molar Fraction at the Plasmatron Exit as a Function of Global O/C ratio for Different Air Oxygen Enrichment, using a Two-stage Combustion Model with 30% CH_4 Precombusted

4.3 Non-adiabatic plug flow model

In most cases, the reactor cannot be completely thermally insulated. Then, we have to account for heat losses. Knowing that the material of the plasmatron is steel, we estimated a value for the overall heat transfer coefficient of the system, U.

$$\frac{1}{U} = \frac{1}{h_1} + \frac{w}{\lambda} + \frac{1}{h_2} \tag{4.1}$$

We picked an appropriate value for the thermal conductivity λ of steel: 21 W/mK. From the geometry of the reactor we evaluated the exposed surface area A, and the wall thickness w. The convection heat transfer coefficients h_i of the gas mixture represented in this case less than 10% of the heat transfer coefficient λ/w for steel, thus they were finally neglected, obtaining a value for U=1050 W/m^{2}K.

The model will evaluate the heat loss rate (heat transfer rate through the wall) using:

$$\dot{Q} = U \times A \times (T_{wall} - T_{amb}) \tag{4.2}$$

The temperature of the wall T_{wall} is assumed to be the same as the gas mixture temperature. The exterior temperature is set equal to the ambient temperature T_{amb}=298 K.

We performed the same simulations varying initial temperature (from 300 K to 2,000 K) and O/C (from 1 to 1.4) for the adiabatic reactor, with this new setup. It was found that much higher temperatures are needed to reach the same conversion than with the adiabatic reactor. Due to heat loss, 1,500 K at O/C=1 is not enough to get ignition within the discharge zone. At that temperature the heat loss is so important that the heat released by the chemical reaction is not enough to overcome it and the temperature in the reactor drops drastically, quenching the reaction propagation. Initial temperatures of 1,800 K and higher are necessary to assure combustion. Figure 4.16 represents the combustion heat release per unit time in the reactor and the heat exchange per unit time with the exterior for a plug

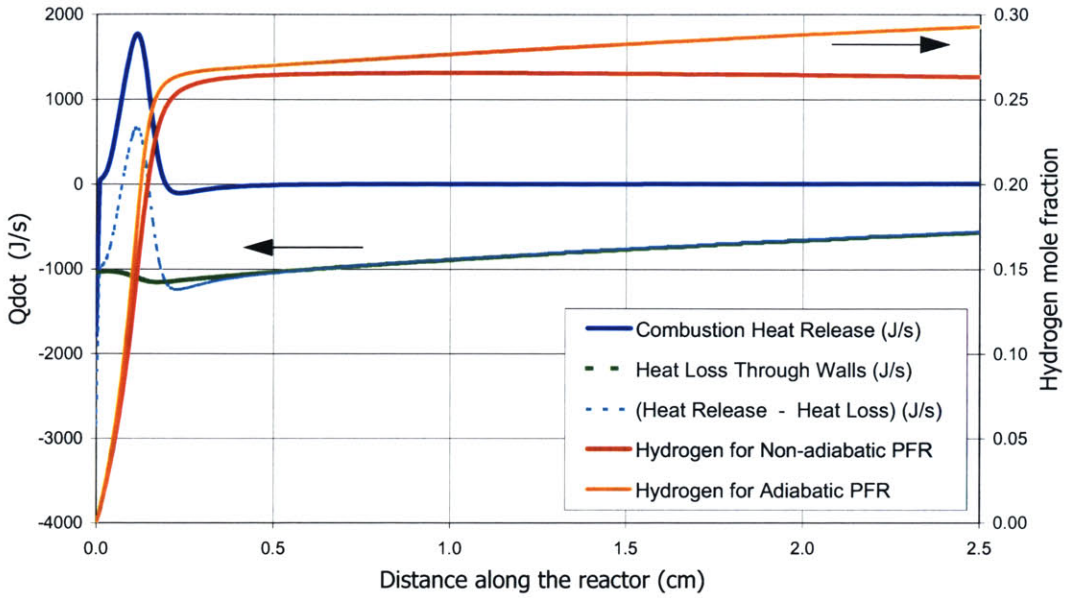

Figure 4.16 Heat of Combustion and Heat Loss through the Walls along a Non-Adiabatic PFR with U=1050 W/m^{2}K, Initial Temperature=2,000K and O/C=1. Comparison between Hydrogen Composition along the Reactor with Equal Operating Conditions for an Adiabatic and a Non-Adiabatic System

flow reactor with initial temperature equal to 2,000 K and O/C=1. At this conditions, the heat of combustion is sufficient to start the oxidation process and maintain it.

Trends in hydrogen molar fraction at exhaust for adiabatic and non-adiabatic systems for different O/C ratio and initial temperature are similar. However, the non-adiabatic reactor yields in all cases about 20% less H_2 at the plasmatron exit (30 cm) than the adiabatic reactor (see example in Figure 4.16 for the discharge zone). Therefore, working with an insulated reactor rather than a non-insulated reactor implies better system performance in terms of hydrogen production.

4.4 NOx generation: ammonia and hydrogen cyanide presence

Nitrogen related reactions have been proved to be an important factor in the performance of the methane oxidation mechanism [Glassman, 1996]. Primarily, nitrogen presence has an effect on the heat capacity of the system. At low temperature (below 1,000 K) it is an

inert gas which operates as a temperature moderator since it may absorb energy without undergoing any chemical reactions. However, high temperature processes with air are usually accompanied by the formation of nitrogen oxides (NOx). Therefore, if indeed high temperatures are achieved in the plasmatron reactor, we might expect nitrogen to react with oxygen and form NOx. For C-H-N-O systems with O/C=1, the highest equilibrium concentration of NO occurs at temperatures above 4,500 K[1] [Suris, 1985]. For the same system at lower temperatures (500 K - 2,000 K), the equilibrium formation of oxides of nitrogen is replaced by the formation of ammonia and hydrogen cyanide.

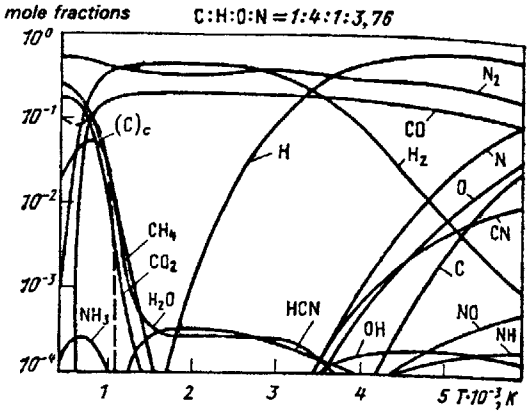

Figure 4.17 Equilibrium Composition of Products of Conversion of Methane with Air for O/C=1 [Suris, 1985]

Kinetic experiments for methane partial oxidation using the PLUG application of CHEMKIN have proved that nitrogen is partly dissociated and converted into ammonia and hydrogen cyanide for initial temperatures in the reactor from 1,500 K to 2,000 K. While ammonia is produced at low temperature and increases with time (1,500 K), hydrogen cyanide reaches a peak and steadily drops. The concentration of those species is below the order of ppm.

1. At 4,500 K the entire oxygen is in atomic state.

For higher temperatures (2,000 K), hydrogen cyanide is also the most important product derived from nitrogen, now in much higher concentration, of order hundreds of ppm. It is followed by ammonia and NO, although both decrease in time (see Figures 4.18 and 4.19).

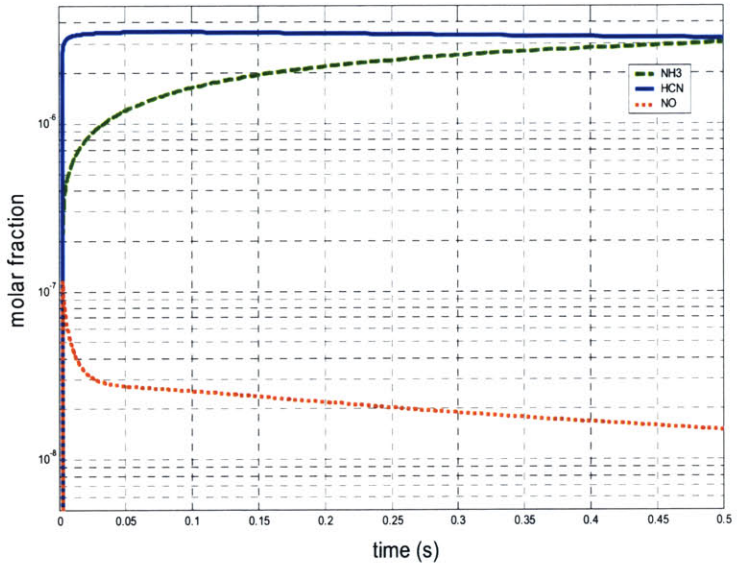

Figure 4.18 Molar Fraction along Time of Nitrogen-Based Species in a PFR for methane combustion with O/C=1 and Tinitial=1,500K. Simulation using PLUG

We cannot measure ammonia or hydrogen cyanide in the experimental results, because they are immediately oxidized to NOx once in contact with oxygen in the atmosphere. However, measurements for NOx were pursued and the plasmatron running with O/C close to 1 and a 900-W power supplied yielded about 300 ppm of nitrogen oxides.

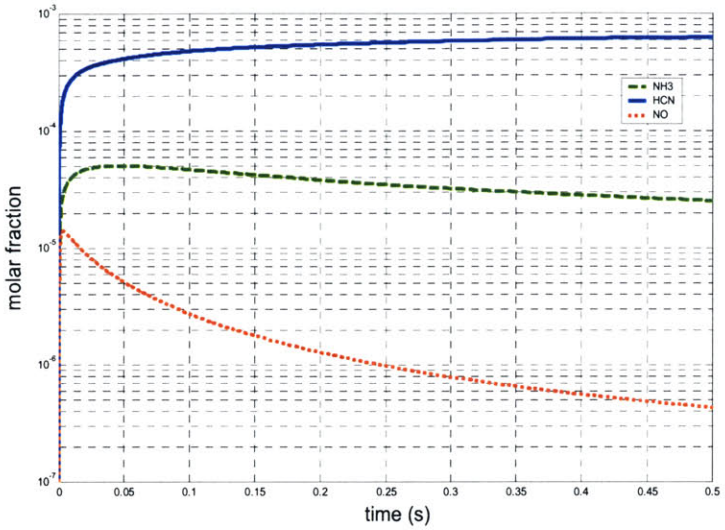

Figure 4.19 Molar Fraction along Time of Nitrogen-Based Species in a PFR for methane combustion with O/C=1 and Tinitial=2,000K. Simulation using PLUG

Chapter 5

PARTIALLY STIRRED REACTOR MODEL: PASR

The PASR is an application of CHEMKIN that allows us to model the plasmatron as a partially stirred reactor in which the combustion process is limited by the mixing frequency of the gaseous elements that enter and fill the reactor. With the PASR, the turbulence mixing process between turbulent eddies (or lumps of fluid that behave coherently until they lose their identity through diffusion) is modeled by dividing the flow into a large number of elements. An element is defined by its mass, species composition and thermodynamic properties. All elements interact randomly with each other simulating the mixing process while chemistry evolves separately in each element. The basics of the PASR have been explained in Chapter 3. In this chapter we used the PASR tool to analyze the behavior of a methane partial oxidation system in which combustion is initiated by energy supplied in form of heat to a limited number of elements. We studied the effect of different amounts of energy delivered and the behavior of the system when different fractions of the elements receive this energy supply.

5.1 Methane results with PASR

In Section 3.2.3 we defined the inputs necessary to specify the characteristics of a partially stirred reactor. The two principal parameters that describe the PASR are the characteristic times: the mixing time and the residence time. For a plasmatron device working with a flow of 3 g/s of air-fuel mixture the residence time in the discharge zone is estimated to be 1 ms. The mixing time, on the other hand, was evaluated in Section 3.2.1 and found to be 0.1 ms.

Based on these values, a series of simulations for methane partial oxidation were carried out. A high temperature and fraction of elements at that high temperature were the variables that allowed us to model the effects of the arc in the discharge zone and to study the combustion initiation and propagation process in the plasmatron.

As previously discussed, our discharge model assumes ohmic heating of gas mixture within the average arc volume equal to $9x10^{-9}$ m^3, which represents less than 1% of the total discharge region. The temperature achieved by the air-fuel mixture was estimated to be around 5,000 K. Therefore, our first calculations tried to simulate the methane oxidation for an O/C=1, residence time (tres)=1 ms and mixing time (tmix)=0.1 ms, with 1% of the molar flow through the reactor at 5,000 K and the rest of the flow at ambient temperature (300 K). One percent of the flow at high temperature, however, proved insufficient to achieve significant methane conversion into syngas (less than 5%). Combustion was initiated in the hot elements but the energy propagation by mixing with other elements rapidly quenched the chemistry; this number of hot elements was too small compared to the total.

To first analyze the system response to an O/C ratio change, we set 10% of the molar flow at high temperature (4,000 K) and the same characteristic times as before. Results are shown in Figure 5.1. Temperature and gas composition at the exhaust of the discharge region are plotted as a function of O/C ratio. The trends show that the more oxygen is present in the flow, the higher the methane conversion is, yielding higher concentration of oxygenated products such as CO, H_2O and CO_2. Hydrogen production stays practically unvariable..

Varying the mixing time to a smaller value, tmix=1 μs, and maintaining the other variables constant, we observe the same tendencies for all species composition except for water, which presents a minimum close to partial oxidation stoichiometry (O/C=1). Under this conditions, mixing is so fast that the PASR behaves closer to a perfectly mixed reactor. The trends are similar to those obtained by the PLUG simulation in Section 4.2.1 (see Figure 4.9 in molar fraction). In the PLUG case, temperature was homogeneous and it is set to

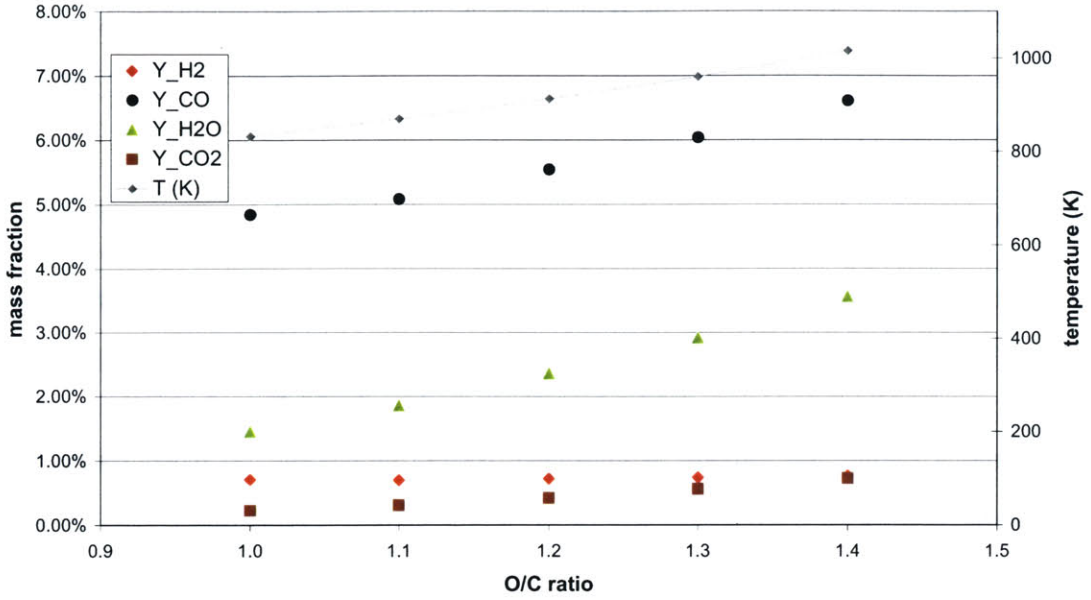

Figure 5.1 PASR Exhaust Composition (Mass Fraction) for Methane Partial Oxidation using Different O/C, tmix=0.1ms and tres=1ms, and setting 10% of the Molar Flow at 4,000K

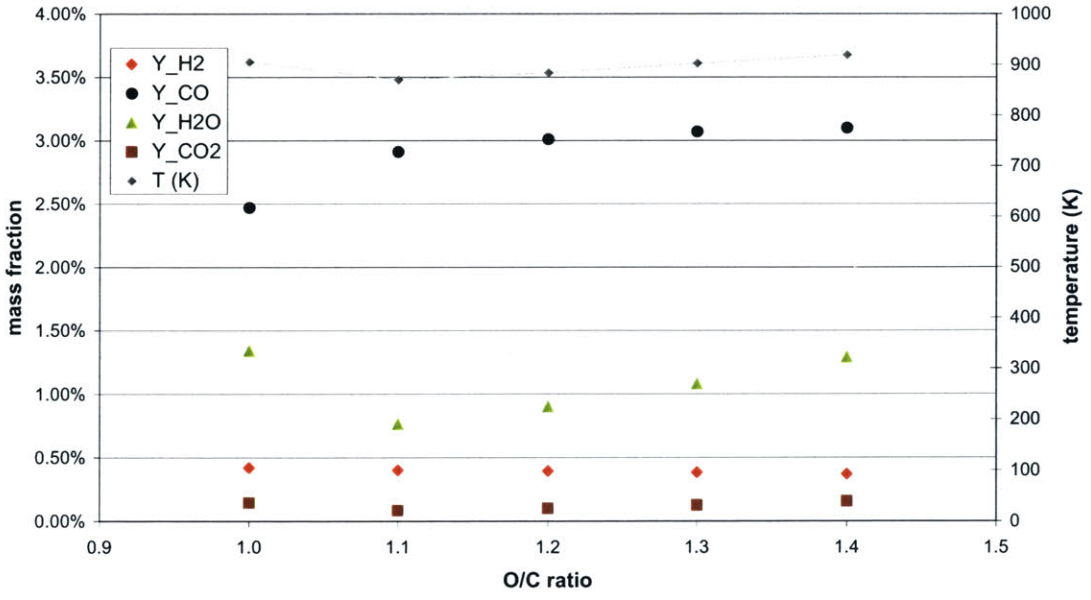

Figure 5.2 PASR Exhaust Composition (Mass Fraction) for Methane Partial Oxidation using Different O/C, tmix=1μs and tres=1ms, and setting 10% of the Molar Flow at 4,000K

1,500 K for the whole system, while in the PASR reactor, only 10% of the flow is initially at 4,000 K. However, dependence with O/C ratio is the same for both reactor types, which proves that combustion can be propagated through the whole PASR system if the mixing conditions are appropriate.

5.1.1 Effect of mixing time to residence time ratio

For a fraction of hot elements equal to 10% of the molar flow into the plasmatron, we studied the effect on syngas production for different mixing times, the same residence time and varying the temperature of the hot elements from 2,000 K to 5,000 K. Figures 5.3, 5.4 and 5.5 show the fraction of hydrogen, carbon monoxide and water (principal products) at the exhaust of the discharge region (tres=1 ms).

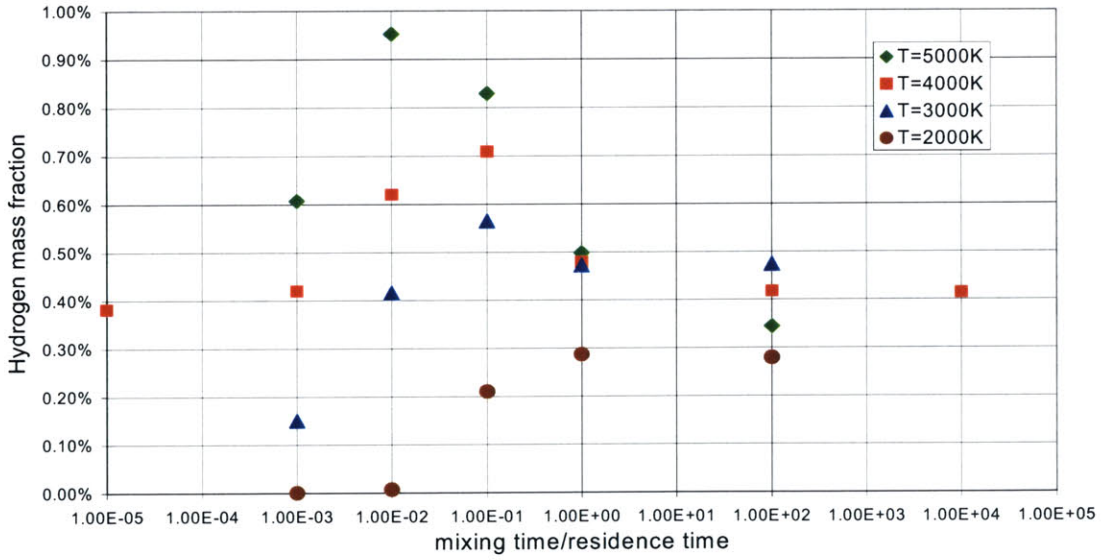

Figure 5.3 PASR H_2 Exhaust Composition (Mass Fraction) for Methane Partial Oxidation using tres=1ms, O/C=1 and Different tmix, setting 10% of the Molar Flow at Different Initial Temperatures

Focusing on hydrogen production, we observe how higher initial temperature for the hot elements yields higher amounts of H_2. In fact, for tmix=0.01 ms and T=5,000 K for 10%

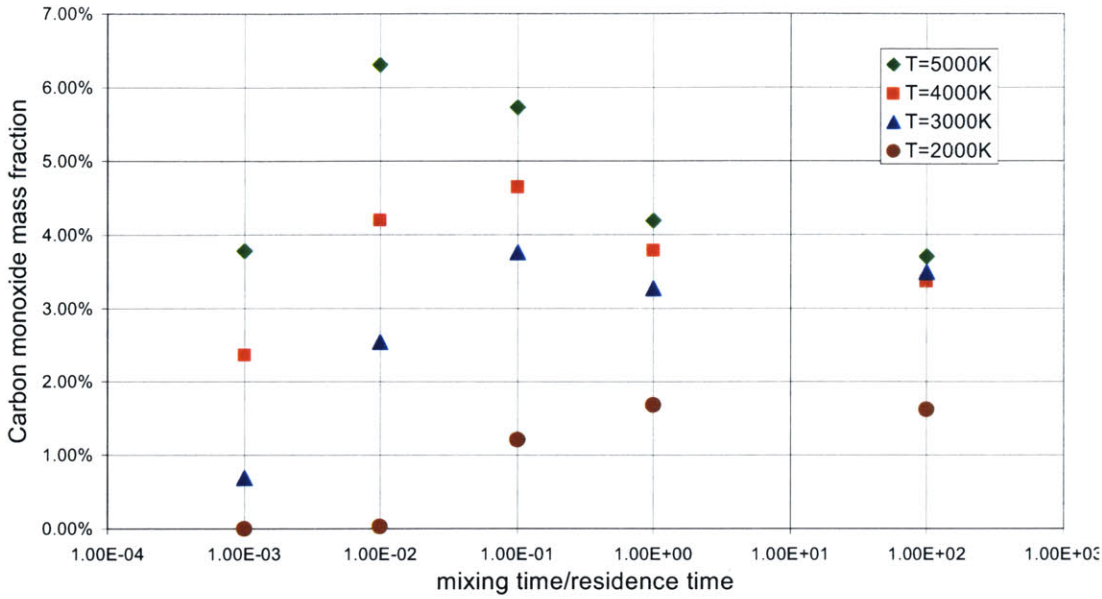

Figure 5.4 PASR CO Exhaust Composition (Mass Fraction) for Methane Partial Oxidation using tres=1ms, O/C=1 and Different tmix, setting 10% of the Molar Flow at Different Initial Temperatures

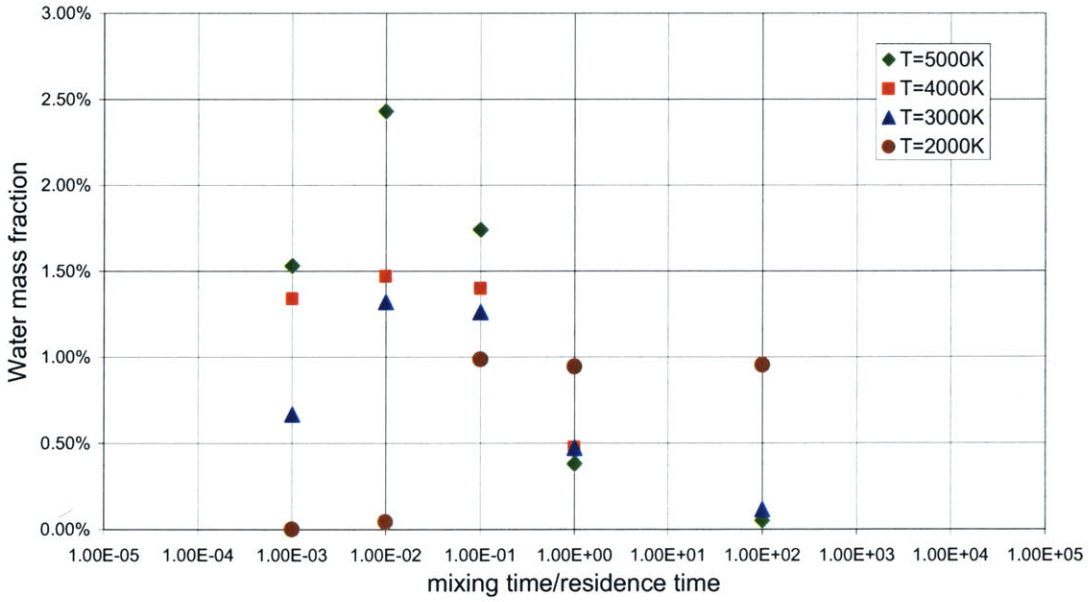

Figure 5.5 PASR H_2O Exhaust Composition (Mass Fraction) for Methane Partial Oxidation using tres=1ms, O/C=1 and Different tmix, setting 10% of the Molar Flow at Different Initial Temperatures

of the elements, the PASR simulation produces as much hydrogen as the experiments performed with the plasmatron.

If we look at other trends in the graph, we see a maximum or optimal mixing/residence time ratio for hydrogen generation for each initial temperature of the hot elements. This maximum moves towards lower mixing times as temperature rises, that is to say, the higher the initial temperature of hot elements, the shorter is the mixing time necessary to reach the hydrogen peak. This phenomenon is explained by quenching. When the mixing process is fast (lower tmix), the hot elements mix more often and transfer their energy to more elements. Thus, if they have low temperature (2,000 K) and mix rapidly, they lose the ignition potential quicker and fewer non-hot elements can benefit from energy transfer to initiate combustion and produce H_2. At high temperature (5,000 K), more energy is available and therefore more mixes are possible before hot elements are quenched, allowing short mixing times to enhance methane conversion. For low mixing rates (tmix>tres) and high temperature (5,000 K), combustion kinetics occur faster than mixing and thus the temperature of the hot elements decreases[1] before they are able to initiate combustion in other elements.

Carbon monoxide results follow the same trend as hydrogen. The quenching theory can be applied to CO production, as well as the fact that higher temperature generates higher amounts of the syngas species. However, water composition at exhaust of the discharge region for different mixing times presents a peculiarity. At long mixing times (poor mixing for tmix>tres), high temperature (4,000 K-5,000 K) does not produce higher concentration of water than low temperature (2,000 K).

1. Adiabatic temperature for methane partial oxidation is lower than initial temperature when T_i>3,000 K.

5.1.2 Different energy supply

To explain why 1% of the molar flow into the plasmatron at high temperature (4,000 K) was not sufficient to propagate combustion to the whole reactor, we explored the influence of different fractions of hot elements at different initial temperatures.

We have plotted H_2, H_2O and CO production in Figures 5.6, 5.7 and 5.8. PASR conditions are tmix=0,1 ms and tres=1 ms. For 1% of the flow at hot temperature, none of the initial temperatures tried was enough to generate more than 10% of the experimental production of hydrogen (equal to 1% mass fraction).

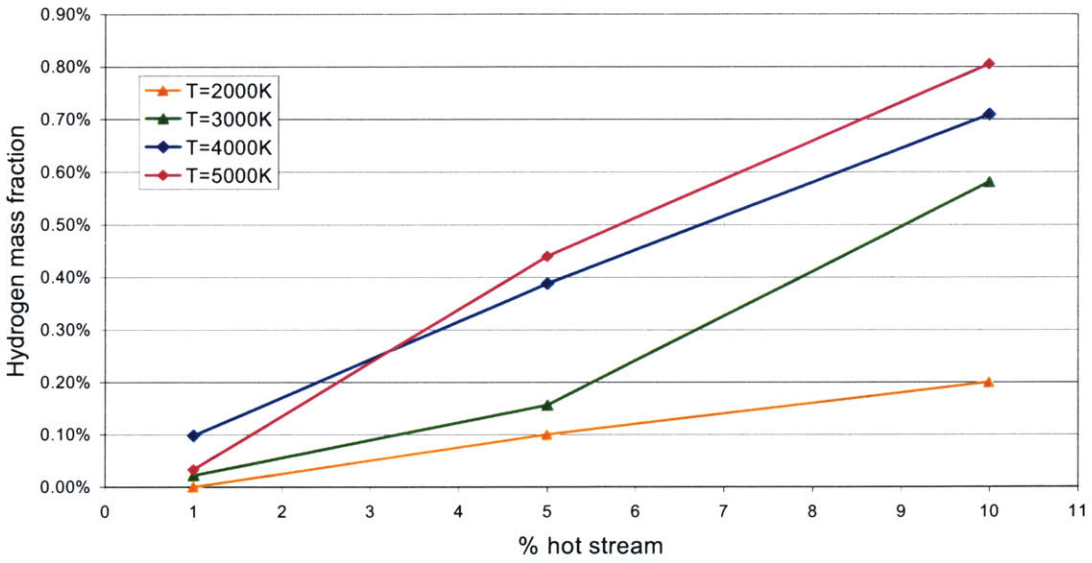

Figure 5.6 PASR H_2 Exhaust Composition (Mass Fraction) for Methane Partial Oxidation using tmix=0.1ms, tres=1ms, O/C=1 and setting Different Fractions of the Molar Flow at Different Initial Temperatures

For all the species, each temperature produced a straight line from the origin (corresponding to zero production for zero hot elements) to a point at 10% of hot stream. Again, when temperature increases, the composition of the species increased, although not significantly. For 2,000 K, concentrations for all product species were considerably lower. This

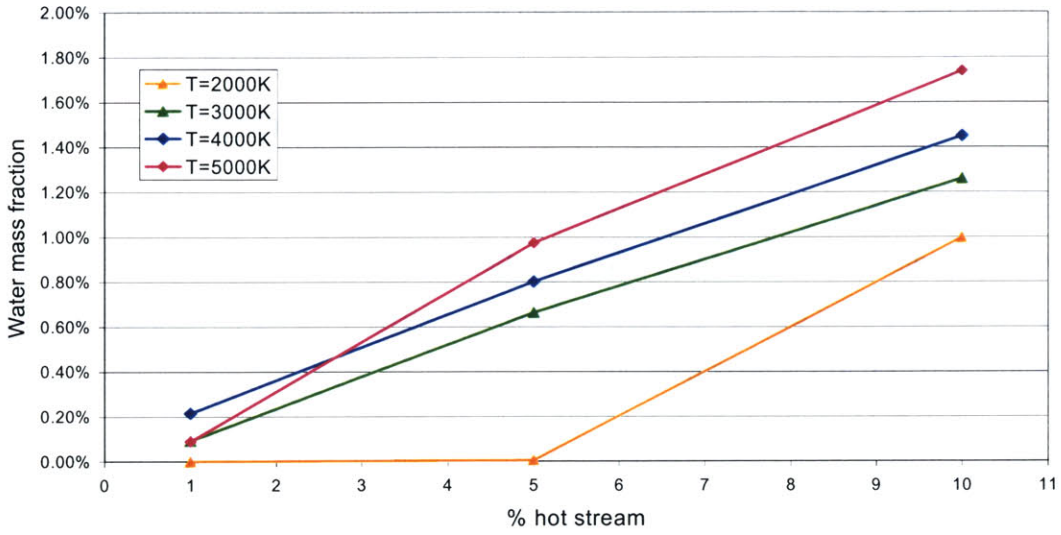

Figure 5.7 PASR H_2O Exhaust Composition (Mass Fraction) for Methane Partial Oxidation using tmix=0.1ms, tres=1ms, O/C=1 and setting Different Fractions of the Molar Flow at Different Initial Temperatures

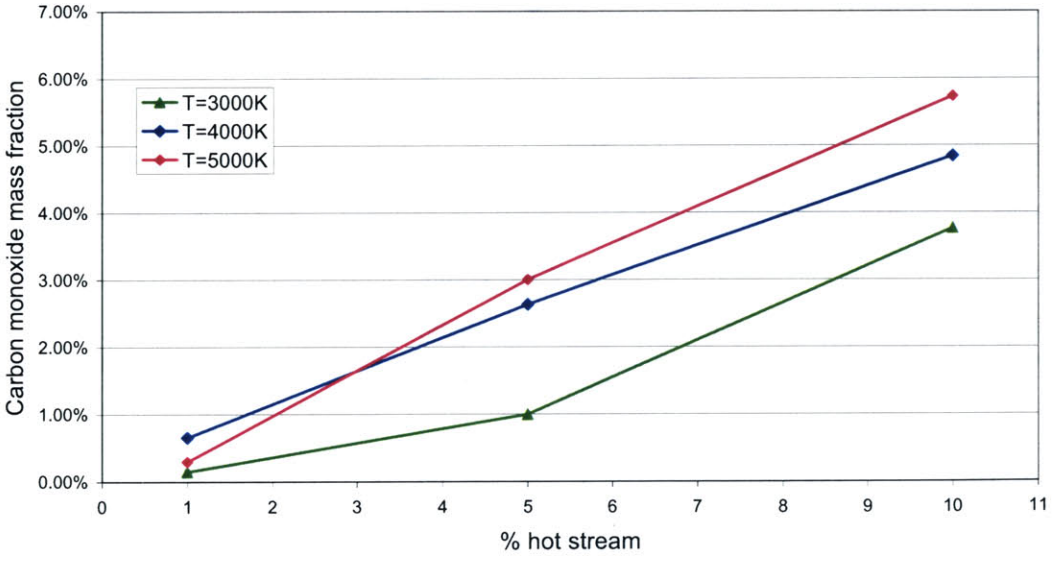

Figure 5.8 PASR CO Exhaust Composition (Mass Fraction) for Methane Partial Oxidation using tmix=0.1ms, tres=1ms, O/C=1 and setting Different Fractions of the Molar Flow at Different Initial Temperatures

scheme shows us that, in general, more elements at moderate temperature (3,000 K) can produce as much or more syngas than fewer elements at a higher temperature (5,000 K).

The previous statement represents an issue for our model, since we know that the arc volume is smaller than 1% of the total reactor volume and the temperature reached in the discharge is estimated to be between 3,000 and 13,000 K; while the simulation calculations proved that higher fractions of hot stream with lower energy would be more advantageous to methane conversion. A question is thus posed: is the arc heating the same mass for the total discharge duration or is it affecting more mass than the one in the arc volume, and thus heating it up to lower temperatures than the calculated ones? [Thiele, 2002] did a 2-D study of a spark ignition system in which shows how the hot temperature region is not only limited to the mass within the arc, but that there is also a radial heat transfer by convection to the surrounding areas that could explain higher fractions of hot elements at temperatures lower than the arc, but still high enough to initiate combustion. This convection process can affect lengths up to 4 times larger than the arc diameter, which would represent that the real arc volume would be 16 times bigger than the estimated by visualization. In that case, the fraction of hot elements at high temperature would be about a 2% of the flow. Nevertheless, the physical model developed for the plasmatron discharge is based on assumptions and further experiments should be carried out to validate them.

5.1.3 Temperature analysis

The discrepancy between the experimental energy supply for the plasmatron to produce syngas from methane and the amount of energy necessary in the PASR simulations to reach a similar level of methane conversion has yet to be adequately explained. In Figure 5.9 we plotted the power required (or delivered through the discharge) for the gas mixture under the arc to reach a certain temperature for both experimental and simulation cases. The experimental study of the discharge in Chapter 2, based on two assumptions, showed us that the plasmatron power supply was able to heat the arc up to temperatures between about 3,000 K (for the arc duration time assumption) and 13,000 K (for the residence time

assumption). The power requirement to heat the mass within the arc between the tested values 1,000 K and 5,000 K lies in both cases under 500 W. When we look at the power required for the PASR simulation to heat 1% of the flow through the plasmatron, we are in that range, but we obtain less than 10% of the methane conversion that the experimental results show for the same amount of power. We need to heat up 5% of the flow to 5,000 K to produce the amount of hydrogen that the experiments produce, and this requires 3 kW, which is much higher than the available power. This energy discrepancy could be explained by the assumed simulation system mixture uniformity. In the experiments, the

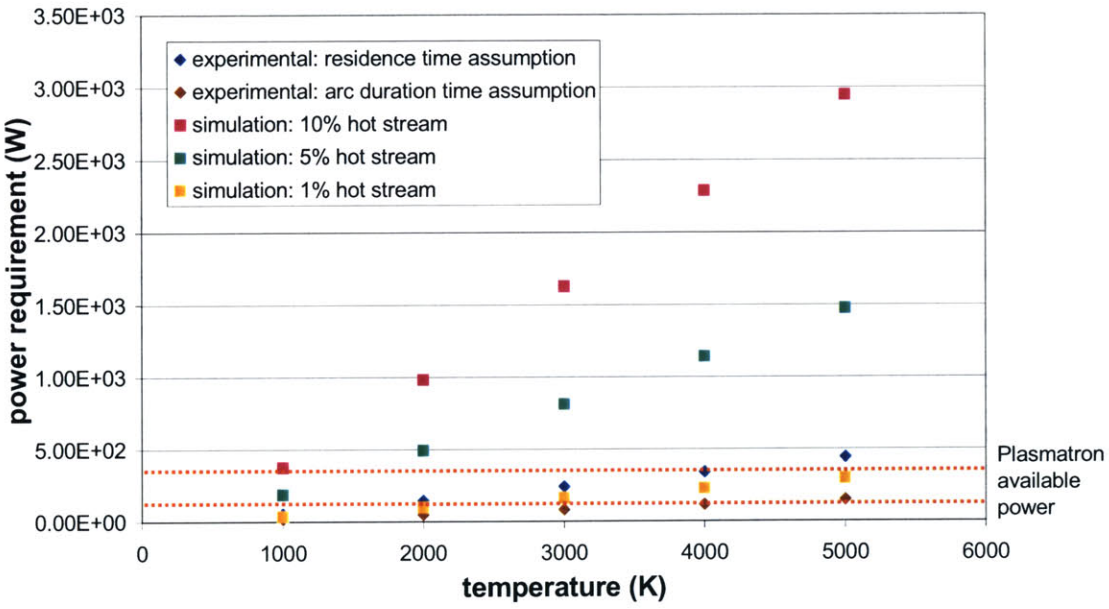

Figure 5.9 Power Required to Heat the Arc Volume (Experimentally Measured and Simulations Calculated) to Different Temperatures

heterogeneity of the gas within the reactor facilitates combustion of zones in which oxygen concentration is higher even though temperature is lower, releasing extra energy from the exothermic combustion reaction. However, the PASR simulation assumes all elements initially have the same relative air/fuel ratio, in other words, the two reactor streams (hot and cold one) are homogeneous and have the same composition. If the element distribu-

tion is uniform, there are elements in which methane is not converted and the energy released by its conversion is not made available to the system. The chemical energy latent in the fuel flow could become the additional energy above the experimental electrical discharge energy necessary to reach simulation levels for syngas production. We were not able with the available PASR model to simulate non-uniformity in mixture composition.

5.1.4 Alternative model for energy supply

Simulations in which we used an inert gas at high temperature as a source of thermal energy into the system instead of increasing the gas mixture temperature directly were also performed. The fractions of hot elements tested were: 1%, 5% and 10% of the molar flow. The hot stream was in this case pure argon and the cold stream (at ambient temperature) was a methane-air mixture with O/C=1. For tres=1 ms and tmix=0.1 ms methane conversion was in all simulation cases below 10% of the experimental conversion. Therefore, it was concluded that the energy must be directly delivered to the gas mixture for the plasmatron to produce syngas. If the energy is delivered to the system and it can only be transferred by mixing, the process is not efficient enough. As commented previously, we are losing the chemical energy released by the gas mixture when instantaneously burns at high temperature.

5.2 Comparison with experimental results

Species concentration at the exhaust of the discharge zone for the simulation calculations and the plasmatron experiments are compared in Table 5.1 for methane partial oxidation at O/C=1. The PASR model was set with tmix=0.1 ms and tres=1 ms as the closest estimated values to the experimental system.

One can observe that the simulation case that matches the hot stream input thermal energy to the electrical power supplied to the discharge in the experiments (300 W) yields lower concentrations for all the syngas species. Using the PASR model, we need to increase the power to almost ten times the experimental power to achieve hydrogen and CO composi-

TABLE 5.1 Mass Fractions of Plasmatron Products at Exhaust of the Discharge Region and Power Supplied to the Discharge for PASR Simulations and Experiments (Methane Partial Oxidation with O/C=1)

	Power (W)	Y_H_2	Y_CO	Y_H_2O	Y_CO_2
Experimental	300	0.60	5.0	7.0	4.0
10% at 5,000 K	3,000	0.80	5.7	1.8	0.3
5% at 5,000 K	1,500	0.45	3.0	1.0	0.2
1% at 5,000 K	300	0.03	0.3	0.1	0.05

tions of the same order than the plasmatron production. Even in that case, water and CO_2 concentrations do not match. The explanation for the power discrepancy was commented in Section 5.1.3. Methane latent heat could provide the energy difference through heterogeneous combustion. The difference in concentration for the complete oxidation products when simulation and experiments meet regarding syngas production could also be due to mixture non-uniformity effects.

Clearly, the PASR model must be further developed so that it better matches the experimental situation. We already commented in Chapter 3 on the limitations of the software. We believe that capability for using a probability distribution profile for variables such as temperature or composition entering the reactor could help reproduce the expected heterogeneity of the real system. However, such a feature is not yet available. Therefore, the software improvements necessary to model the plasmatron more completely are proposed as future work following this thesis.

Chapter 6
CONCLUSIONS

From the results obtained with the homogeneous reactor model we concluded that:

- The temperature rise of the gas mixture within the arc is a direct effect of the power supplied to the discharge and it is necessary for the initiation of the combustion process. Combustion is then propagated by mixing of this hot reacted gas mass with the surroundings. A discharge model that assumes ohmic heating of the gas mixture has been developed and used to estimate temperatures between about 3,000 K and 13,000 K for the mass within the visible arc region. The power supply to the system suffers energy losses of 75%.
- Radicals generated by the discharge are not the primary ignition trigger of the process. Radical presence helps combustion initiation at temperatures under 1,000 K. However, at the temperatures reached at the arc, above 3,000 K, the radicals formed do not provide any significant benefit.
- The plug flow reactor model has proved the presence of water and carbon dioxide as a coproduct of the syngas. We also found cyanide and ammonia at the exhaust of the plasmatron in concentrations that may contribute a few ppm of NOx production by oxidation in later stages.
- Alternative models to the plasmatron setting were also tested. A two-stage reactor model was found effective to increase methane conversion when combined with O_2 enrichment of the air stream. A non-adiabatic reactor with realistic heat losses caused a 20% reduction in hydrogen production at the exhaust of the plasmatron.

From the results obtained with the partially stirred reactor model we concluded that:

- There is an optimum mixing time for each residence time of the plasmatron reactor that depends on the temperature reached at the arc; it is of order of the residence time for 2,000 K and of order 1/100 of the residence time for 5,000 K. There is a quenching effect that moves this maximum towards

lower mixing rates for lower arc gas temperatures (2,000 K). The optimum for higher arc gas temperatures (5,000 K) is of the order of the estimated mixing time for the real plasmatron (0.1 ms) and produces similar methane conversion into syngas than the experiments.

- The more elements of the PASR at intermediate temperature (3,000 K) simulating the arc, the higher methane conversion we obtain. Fewer hot elements at high temperature (5,000 K) provide equal or less syngas production for the same power delivery.
- An alternative energy model studied the input through a non-reacting system such as argon. This non-reacting energy supply was not as effective as equivalent temperature fuel-air mixture.
- Experimental hydrogen and carbon monoxide production was matched with the PASR model but required 2-3 kW higher electrical power supply. This power discrepancy is thought to be due to the assumed homogeneity of the PASR model. Non uniformities in relative fuel-air ratio are believed to contribute the additional thermal energy needed to effectively initiate much more complete chemical reaction within the plasmatron.
- The PASR does not adequately simulate the fuel-air and temperature non uniformities in the experimental plasmatron in the current format. Several modifications that involve the number of streams entering the reactor, heterogeneity of these streams and capability to create a temperature probability distribution profile for these streams could help improve the simulation results.

REFERENCES

[Tully, 2002] Tully, E. J., *Lean-Burn Characteristics of a Gasoline Engine Enriched with Hydrogen from a Plasmatron Fuel Reformer,* MIT M.S. Thesis in Mechanical Engineering, June 2002.

[Topinka, 2003] Topinka, J., *Knock Behavior of a Lean-Burn, Hydrogen-Enhanced Engine Concept,* MIT M.S. Thesis in Mechanical Engineering, September 2003.

[Bromberg, 2000] Bromberg, L., Rabinovich, A., Cohn, D., Heywood, J., "Emissions Reductions Using Hydrogen from Plasmatron Fuel Converters", Diesel Engine Emissions Reduction Workshop, 2000.

[Curran, 2002] Curran, H. J., Gaffuri, P., Pitz, W. J., Westbrook, C. K., "A Comprehensive Modeling Study of iso-Octane Oxidation", *Combustion and Flame*, vol. 129, pp. 253-280, 2003.

[Curran, 1998] Curran, H. J., Gaffuri, P., Pitz, W. J., Westbrook, C. K., "A Comprehensive Modeling Study of n-Heptane Oxidation", *Combustion and Flame*, vol. 114, pp. 149-177, 1998.

[Edwards, 1985] Edwards, C. F., Stewart, H. E., Oppenheim, A. K., "A Photographic Study of Plasma Ignition Systems", SAE International Congress and Exposition, 1985.

[Heywood, 1988] Heywood, J. B., Internal Combustion Engine Fundamentals, McGraw-Hill, Inc., New York, 1988.

[Pischinger, 1989] Pischinger, S., *Effects of Spark Plug Design Parameters on Ignition and Flame Development in a SI Engine,* MIT Ph. D. Thesis in Mechanical Engineering, January 1989.

[Suris, 1985] Suris, A. L., Handbook of Thermodynamic High Temperature Process Data, Hemisphere Publishing Corporation, Moscow, 1985.

[Bromberg, 1999] Bromberg, L., Rabinovich, A., Cohn, D., "Plasma Catalytic Reforming of Methane", *Int. J. of Vehicle Design,* 1999.

[Hughes, 2001] Hughes, K. J., Turanyi, T., Pilling, M. J., Leeds methane oxidation mechanism, http://www.chem.leeds.ac.uk/Combustion/Combustion.html.

[Smith, 2000] Smith, G. P., Golden, D. M., Frenklach, M., Moriarty, N. W., Eiteneer, B., Goldenberg, M., Bowman, C. T., Harnson, R. K., Song, S., Gardiner, W. C., Vitali, V., GRI mechanism 3.0, http://www.me.berkeley.edu/gri_mech/.

[Warnatz, 1997] Warnatz, J., Klaus, P., Mechanism C_2/NO, http://www.ca.sandia.gov/tdf/3rdWorkshop/ch4mech.html.

[Mallampalli, 1996] Mallampali, H. P., Fletcher, T. H., Chen, J. Y., "Evaluation of CH_4/NO_x Global Mechanisms Used for Modeling Lean Premixed Turbulent Combustion of Natural Gas", Fall Meeting of the Western States Section of the Combustion Institute, October 1996.

[Komiyama, 1975] Komiyama, K., *The effects of Fuel Injector Characteristics on Fuel-Air Mixing in a Burner*, MIT Ph. D. Thesis in Mechanical Engineering, January 1975.

[Bromberg, 2002] Bromberg, L., CFD Calculations for the Plasmatron, PSFC Internal Report, 2002.

[Petzold, 1982] Petzold, L. R., A Description of DASSL, Sandia National Laboratories Report, 1982.

[Reaction Design, 2002] Reaction Design, PLUG Application User Manual, CHEMKIN Collection 3.7, 2002.

[Reaction Design, 2003] Reaction Design, PASR Application User Manual, CHEMKIN Collection 3.7.1, 2003.

[Glassman, 1996] Glassman, I., Combustion, Academic Press, Inc., California, 1996.

[Flagan, 1973] Flagan, R. C., Appleton, P., A Stochastic Model of Turbulent Mixing with Chemical Reaction: Nitric Oxide Formation in a Plug-Flow Burner, MIT Fluid Mechanics Laboratory, December 1973.

[Brown, 1996] Brown, J., *An stochastic Mixing Model for Predicting Emissions in a Direct Injection Diesel Engine*, MIT Ph. D. Thesis in Ocean Engineering, September 1996.

[Thiele, 2002] Thiele, M., Selle, S., Riedel, U., Warnatz, J., Schiessl, R., Maas, U., "A Detailed Two-Dimensional Numerical Study of Spark Ignition Including Ionization", SAE 2002 World Congress, March 2002.

[Sher, 1986] Sher, E., Keck, J. C., "Spark Ignition of Combustible Gas Mixtures", *Combustion and Flame*, vol. 66, pp. 17-25, 1986.

[O'Brien, 1996] O'Brien, C. J., Hochgreb, S., Bromberg, L., Rabinovich, A., Cohn, D., "Hydrogen Production via Plasma Reformers", 31st Intersociety Energy Conversion Engineering Conference, August 1996.

[Benilov, 2003] Benilov, M. S., Naidis, G. V., "Simulation of Hydrogen-rich Gas Production by Plasma Reforming of Hydrocarbon Fuels", ISPC-683, 2003.

[Berger, 1999] Berger, R. J., Marin, G. B., "Investigation of gas phase reactions occurring at conditions typical for partial oxidation of methane to synthesis gas", *Industrial and Engineering Chemistry Research*, vol. 38, no. 7, pp. 2582-2592, 1999.

[Goralski, 2000] Goralski Jr., C. T., O'Connor, R. P., Schimdt, L. D., "Modeling Homogeneous and Heterogeneous Chemistry in the Production of Syngas from Methane", *Chemical Engineering Science*, vol. 55, pp. 1357-1370, 2000.

[Eliasson, 1991] Eliasson, B., Kogelschatz, U., "Nonequilibrium Volume Plasma Chemical Processing", *IEEE Transactions on Plasma Science,* vol. 19, no.6, December 1991.

Appendix A
ADDITIONAL EXPERIMENTAL RESULTS

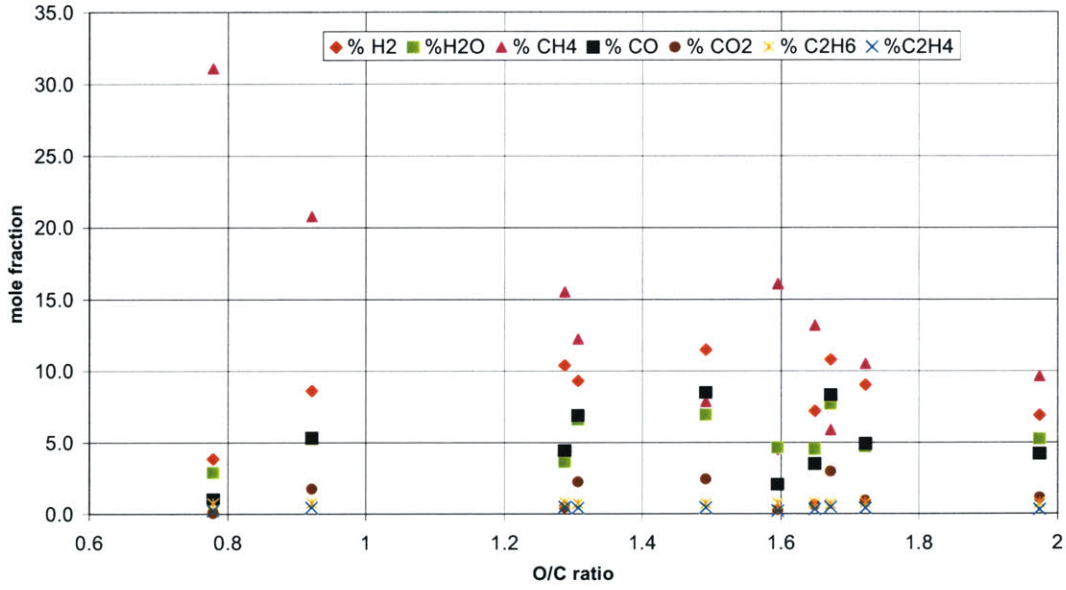

Figure 6.1 Experimental Measured Composition at the Exhaust of the Discharge Region as a Function of O/C ratios for Different Power Inputs (see next figure)

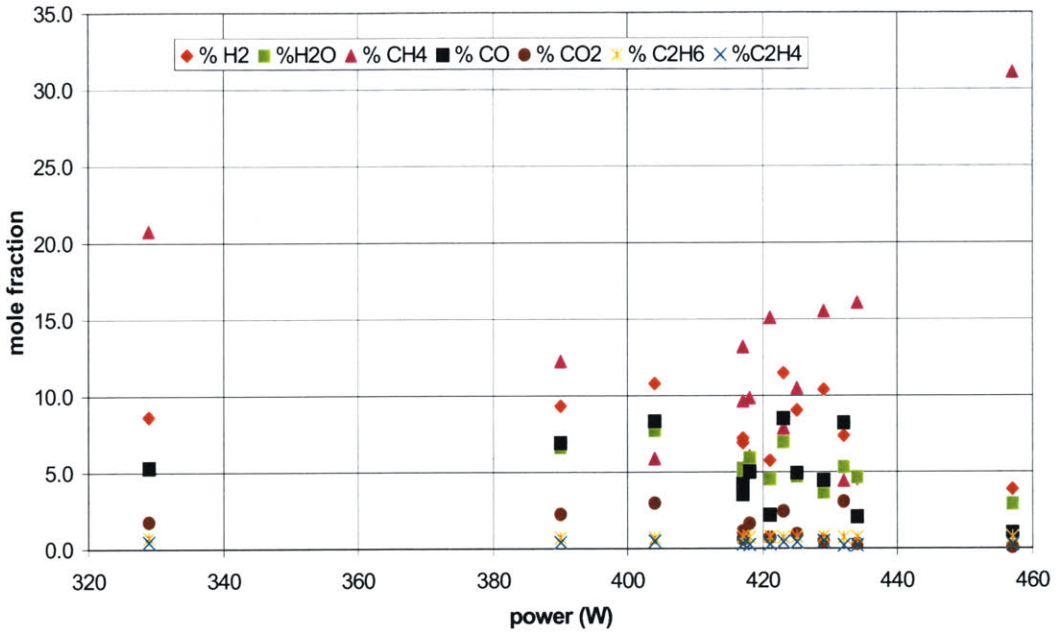

Figure 6.2 Experimental Measured Composition at the Exhaust of the Discharge Region as a Function of Power Inputs for Different O/C ratios (see previous figure)

Appendix B
KINETIC MECHANISMS

The format for the mechanisms here shown corresponds to the format compiled by the CHEMKIN interpreter software.

B.1 Leeds mechanism

CHEMKIN INTERPRETER OUTPUT: CHEMKIN-II Version 3.1 Feb. 1993
DOUBLE PRECISION

ELEMENTS CONSIDERED	ATOMIC WEIGHT
1. C	12.0112
2. H	1.00797
3. O	15.9994
4. N	14.0067

SPECIES CONSIDERED	C P H H A A R S E E	G MOLEC WEIGHT	TEMPERATURE LOW	TEMPERATURE HIGH	ELEMENT COUNT C	H	O	N
1. H2	G 0	2.01594	300.0	5000.0	0	2	0	0
2. O2	G 0	31.99880	300.0	5000.0	0	0	2	0
3. O	G 0	15.99940	300.0	5000.0	0	0	1	0
4. OH	G 0	17.00737	300.0	5000.0	0	1	1	0
5. H2O	G 0	18.01534	300.0	5000.0	0	2	1	0
6. H	G 0	1.00797	300.0	5000.0	0	1	0	0
7. HO2	G 0	33.00677	300.0	5000.0	0	1	2	0
8. H2O2	G 0	34.01474	300.0	5000.0	0	2	2	0
9. CH4	G 0	16.04303	300.0	5000.0	1	4	0	0

```
10. CO          G 0  28.01055  300.0 5000.0  1  0  1  0
11. CO2         G 0  44.00995  300.0 5000.0  1  0  2  0
12. CH2O        G 0  30.02649  300.0 5000.0  1  2  1  0
13. CHO         G 0  29.01852  300.0 5000.0  1  1  1  0
14. CH2OH       G 0  31.03446  250.0 4000.0  1  3  1  0
15. CH3OH       G 0  32.04243  300.0 5000.0  1  4  1  0
16. CH3         G 0  15.03506  300.0 5000.0  1  3  0  0
17. CH3O        G 0  31.03446  300.0 3000.0  1  3  1  0
18. CH          G 0  13.01912  300.0 5000.0  1  1  0  0
19. CH2         G 0  14.02709  250.0 4000.0  1  2  0  0
20. CH2(S)      G 0  14.02709  300.0 4000.0  1  2  0  0
21. C2H2        G 0  26.03824  300.0 5000.0  2  2  0  0
22. C2H3        G 0  27.04621  300.0 5000.0  2  3  0  0
23. C2H4        G 0  28.05418  300.0 5000.0  2  4  0  0
24. C2H5        G 0  29.06215  300.0 5000.0  2  5  0  0
25. C2H6        G 0  30.07012  300.0 4000.0  2  6  0  0
26. CH3O2       G 0  47.03386  300.0 5000.0  1  3  2  0
27. CH3O2H      G 0  48.04183  298.1 5000.0  1  4  2  0
28. C2H         G 0  25.03027  300.0 5000.0  2  1  0  0
29. HCCO        G 0  41.02967  300.0 4000.0  2  1  1  0
30. CH2CO       G 0  42.03764  300.0 5000.0  2  2  1  0
31. CH2CHO      G 0  43.04561  300.0 5000.0  2  3  1  0
32. CH3CO       G 0  43.04561  300.0 5000.0  2  3  1  0
33. CH3CHO      G 0  44.05358  300.0 5000.0  2  4  1  0
34. N2          G 0  28.01340  300.0 5000.0  0  0  0  2
```

REACTIONS CONSIDERED	(k = A T**b exp(-E/RT)) A	b	E
1. O2+H=OH+O	8.70E+13	.0	60300.0
2. H2+O=OH+H	5.06E+04	2.7	26300.0
3. H2+OH=H2O+H	1.00E+08	1.6	13800.0
4. OH+OH=H2O+O	1.50E+09	1.1	420.0
5. H+H+M=H2+M	1.80E+18	-1.0	.0
H2 Enhanced by	1.000E+00		
H2O Enhanced by	6.500E+00		
O2 Enhanced by	4.000E-01		
N2 Enhanced by	4.000E-01		
CO Enhanced by	7.500E-01		
CO2 Enhanced by	1.500E+00		
CH4 Enhanced by	3.000E+00		
6. O+O+M=O2+M	2.90E+17	-1.0	.0

```
     H2          Enhanced by   1.000E+00
     H2O         Enhanced by   6.500E+00
     O2          Enhanced by   4.000E-01
     N2          Enhanced by   4.000E-01
     CO          Enhanced by   7.500E-01
     CO2         Enhanced by   1.500E+00
     CH4         Enhanced by   3.000E+00
 7. H+OH+M=H2O+M                    2.20E+22  -2.0       .0
     H2          Enhanced by   1.000E+00
     H2O         Enhanced by   6.500E+00
     O2          Enhanced by   4.000E-01
     N2          Enhanced by   4.000E-01
     CO          Enhanced by   7.500E-01
     CO2         Enhanced by   1.500E+00
     CH4         Enhanced by   3.000E+00
 8. H+O2+M=HO2+M                  2.30E+18   -.8       .0
     H2          Enhanced by   1.000E+00
     H2O         Enhanced by   6.500E+00
     O2          Enhanced by   4.000E-01
     N2          Enhanced by   4.000E-01
     CO          Enhanced by   7.500E-01
     CO2         Enhanced by   1.500E+00
     CH4         Enhanced by   3.000E+00
 9. HO2+H=OH+OH                   1.50E+14    .0    4200.0
10. HO2+H=H2+O2                   2.50E+13    .0    2900.0
11. HO2+H=H2O+O                   3.00E+13    .0    7200.0
12. HO2+O=OH+O2                   1.80E+13    .0   -1700.0
13. HO2+OH=H2O+O2                   6.00E+13    .0       .0
14. HO2+HO2=H2O2+O2                   2.50E+11    .0   -5200.0
15. OH+OH+M=H2O2+M                    3.25E+22  -2.0       .0
     H2          Enhanced by   1.000E+00
     H2O         Enhanced by   6.500E+00
     O2          Enhanced by   4.000E-01
     N2          Enhanced by   4.000E-01
     CO          Enhanced by   7.500E-01
     CO2         Enhanced by   1.500E+00
     CH4         Enhanced by   3.000E+00
16. H2O2+H=H2+HO2                 1.70E+12    .0   15700.0
17. H2O2+H=H2O+OH                   1.00E+13    .0   15000.0
18. H2O2+O=OH+HO2                   2.80E+13    .0   26800.0
19. H2O2+OH=H2O+HO2                   5.40E+12    .0    4200.0
20. CO+OH=CO2+H                   4.76E+07   1.2     290.0
21. CO+HO2=CO2+OH                   1.50E+14    .0   98700.0
```

```
22. CO+O+M=CO2+M                    7.10E+13    .0  -19000.0
      H2          Enhanced by   1.000E+00
      H2O         Enhanced by   6.500E+00
      O2          Enhanced by   4.000E-01
      N2          Enhanced by   4.000E-01
      CO          Enhanced by   7.500E-01
      CO2         Enhanced by   1.500E+00
      CH4         Enhanced by   3.000E+00
23. CO+O2=CO2+O                   2.50E+12    .0  200000.0
24. CH+O=CO+H                     4.00E+13    .0       .0
25. CH+O2=CHO+O                   3.00E+13    .0       .0
26. CH+CO2=CHO+CO                 3.40E+12    .0    2900.0
27. CH+OH=CHO+H                   3.00E+13    .0       .0
28. CH+H2O=CH2O+H                 4.56E+12    .0   -3200.0
29. CH+H2O=CH2+OH                 1.14E+12    .0   -3200.0
30. CHO+M=CO+H+M                  7.10E+14    .0   70300.0
      H2          Enhanced by   1.000E+00
      H2O         Enhanced by   6.500E+00
      O2          Enhanced by   4.000E-01
      N2          Enhanced by   4.000E-01
      CO          Enhanced by   7.500E-01
      CO2         Enhanced by   1.500E+00
      CH4         Enhanced by   3.000E+00
31. CHO+H=CO+H2                   9.00E+13    .0       .0
32. CHO+O=CO+OH                   3.00E+13    .0       .0
33. CHO+O=CO2+H                   3.00E+13    .0       .0
34. CHO+OH=CO+H2O                 1.00E+14    .0       .0
35. CHO+O2=CO+HO2                 3.00E+12    .0       .0
36. CHO+CHO=CH2O+CO               3.00E+13    .0       .0
37. CH2+H=CH+H2                   6.00E+12    .0   -7500.0
38. CH2+O=>CO+H+H                 8.40E+12    .0       .0
39. CH2+CH2=C2H2+H2               1.20E+13    .0    3400.0
40. CH2+CH2=C2H2+H+H              1.10E+14    .0    3400.0
41. CH2+CH3=C2H4+H                4.20E+13    .0       .0
42. CH2+O2=CO+OH+H                1.30E+13    .0    6200.0
43. CH2+O2=CO2+H2                 1.20E+13    .0    6200.0
44. CH2(S)+M=CH2+M                1.20E+13    .0       .0
      H2          Enhanced by   1.000E+00
      H2O         Enhanced by   6.500E+00
      O2          Enhanced by   4.000E-01
      N2          Enhanced by   4.000E-01
      CO          Enhanced by   7.500E-01
      CO2         Enhanced by   1.500E+00
```

```
    CH4          Enhanced by   3.000E+00
45. CH2(S)+O2=CO+OH+H                    3.10E+13    .0       .0
46. CH2(S)+H2=CH3+H                      7.20E+13    .0       .0
47. CH2(S)+H2O=>CH3+OH                   7.90E+13    .0       .0
48. CH2(S)+CH3=C2H4+H                    1.60E+13    .0   -2380.0
49. CH2O+M=CHO+H+M                       5.00E+16    .0  320000.0
    H2           Enhanced by   1.000E+00
    H2O          Enhanced by   6.500E+00
    O2           Enhanced by   4.000E-01
    N2           Enhanced by   4.000E-01
    CO           Enhanced by   7.500E-01
    CO2          Enhanced by   1.500E+00
    CH4          Enhanced by   3.000E+00
50. CH2O+H=CHO+H2                        2.30E+10    1.1   13700.0
51. CH2O+O=CHO+OH                        4.15E+11    .6    11600.0
52. CH2O+OH=CHO+H2O                      3.40E+09    1.2   -1900.0
53. CH2O+HO2=CHO+H2O2                    3.00E+12    .0    54700.0
54. CH2O+CH3=CHO+CH4                     1.00E+11    .0    25500.0
55. CH2O+O2=CHO+HO2                      6.00E+13    .0   170700.0
56. CH3+M=CH2+H+M                        1.00E+16    .0   379000.0
    H2           Enhanced by   1.000E+00
    H2O          Enhanced by   6.500E+00
    O2           Enhanced by   4.000E-01
    N2           Enhanced by   4.000E-01
    CO           Enhanced by   7.500E-01
    CO2          Enhanced by   1.500E+00
    CH4          Enhanced by   3.000E+00
57. CH3+O=CH2O+H                         8.43E+13    .0       .0
58. CH3+H=CH4                            1.93E+36   -7.0    38000.0
59. CH3+OH=>CH3O+H                       2.26E+14    .0    64800.0
60. CH3O+H=>CH3+OH                       4.75E+16   -.1    88000.0
61. CH3+O2=>CH2O+OH                      3.30E+11    .0    37400.0
62. CH3+HO2=CH3O+OH                      1.80E+13    .0       .0
63. CH3+HO2=CH4+O2                       3.60E+12    .0       .0
64. CH3+CH3=>C2H4+H2                     1.00E+16    .0   134000.0
65. CH3+CH3=C2H6                         1.69E+53  -12.0    81240.0
66. CH3+M=CH+H2+M                        6.90E+14    .0   345030.0
    H2           Enhanced by   1.000E+00
    H2O          Enhanced by   6.500E+00
    O2           Enhanced by   4.000E-01
    N2           Enhanced by   4.000E-01
    CO           Enhanced by   7.500E-01
    CO2          Enhanced by   1.500E+00
```

```
    CH4          Enhanced by   3.000E+00
67. CH3+OH=>CH2(S)+H2O                    2.30E+13   .0      .0
68. CH3O+M=CH2O+H+M                       5.00E+13   .0  105000.0
    H2           Enhanced by   1.000E+00
    H2O          Enhanced by   6.500E+00
    O2           Enhanced by   4.000E-01
    N2           Enhanced by   4.000E-01
    CO           Enhanced by   7.500E-01
    CO2          Enhanced by   1.500E+00
    CH4          Enhanced by   3.000E+00
69. CH3O+H=CH2O+H2                        1.80E+13   .0      .0
70. CH3O+O2=CH2O+HO2                      4.00E+10   .0   8900.0
71. CH2O+CH3O=>CH3OH+CHO                  6.00E+11   .0  13800.0
72. CH3OH+CHO=>CH2O+CH3O                  6.50E+09   .0  57200.0
73. CH3O+O=O2+CH3                         1.10E+13   .0      .0
74. CH3O+O=OH+CH2O                        1.40E+12   .0      .0
75. CH2OH+M=CH2O+H+M                      5.00E+13   .0  105000.0
    H2           Enhanced by   1.000E+00
    H2O          Enhanced by   6.500E+00
    O2           Enhanced by   4.000E-01
    N2           Enhanced by   4.000E-01
    CO           Enhanced by   7.500E-01
    CO2          Enhanced by   1.500E+00
    CH4          Enhanced by   3.000E+00
76. CH2OH+H=CH2O+H2                       3.00E+13   .0      .0
77. CH2OH+O2=CH2O+HO2                     1.00E+13   .0   30000.0
78. CH3O2+M=>CH3+O2+M                     7.24E+16   .0  111100.0
    H2           Enhanced by   1.000E+00
    H2O          Enhanced by   6.500E+00
    O2           Enhanced by   4.000E-01
    N2           Enhanced by   4.000E-01
    CO           Enhanced by   7.500E-01
    CO2          Enhanced by   1.500E+00
    CH4          Enhanced by   3.000E+00
79. CH3+O2+M=>CH3O2+M                     1.41E+16   .0   -4600.0
    H2           Enhanced by   1.000E+00
    H2O          Enhanced by   6.500E+00
    O2           Enhanced by   4.000E-01
    N2           Enhanced by   4.000E-01
    CO           Enhanced by   7.500E-01
    CO2          Enhanced by   1.500E+00
    CH4          Enhanced by   3.000E+00
80. CH3O2+CH2O=>CH3O2H+CHO                1.30E+11   .0  37700.0
```

```
81. CH3O2H+CHO=>CH3O2+CH2O                    2.50E+10   .0   42300.0
82. CH3O2+CH3=>CH3O+CH3O                      3.80E+12   .0   -5000.0
83. CH3O+CH3O=>CH3O2+CH3                      2.00E+10   .0       .0
84. CH3O2+HO2=>CH3O2H+O2                      4.60E+10   .0  -10900.0
85. CH3O2H+O2=>CH3O2+HO2                      3.00E+12   .0  163300.0
86. CH3O2+CH3O2=>CH2O+CH3OH+O2                1.80E+12   .0       .0
87. CH2O+CH3OH+O2=>CH3O2+CH3O2                0.00E+00   .0       .0
88. CH3O2+CH3O2=>CH3O+CH3O+O2                 3.70E+12   .0    9200.0
89. CH3O+CH3O+O2=>CH3O2+CH3O2                 0.00E+00   .0       .0
90. CH4+H=H2+CH3                              1.30E+04   3.0   33600.0
91. CH4+O=OH+CH3                              6.92E+08   1.6   35500.0
92. CH4+OH=H2O+CH3                            1.60E+07   1.8   11600.0
93. CH4+HO2=H2O2+CH3                          1.10E+13   .0   103100.0
94. CH4+CH=C2H4+H                             3.00E+13   .0    -1700.0
95. CH4+CH2=CH3+CH3                           1.30E+13   .0    39900.0
96. CH3OH=CH3+OH                              9.51E+29  -4.3   404100.0
97. CH3OH+H=CH2OH+H2                          4.00E+13   .0    25500.0
98. CH3OH+O=CH2OH+OH                          1.00E+13   .0    19600.0
99. CH3OH+OH=CH2OH+H2O                        1.00E+13   .0     7100.0
100. CH3OH+HO2=>CH2OH+H2O2                    6.20E+12   .0    81100.0
101. CH2OH+H2O2=>HO2+CH3OH                    1.00E+07   1.7   47900.0
102. CH3OH+CH3=CH4+CH2OH                      9.00E+12   .0    41100.0
103. CH3O+CH3OH=>CH2OH+CH3OH                  2.00E+11   .0    29300.0
104. CH2OH+CH3OH=>CH3O+CH3OH                  2.20E+04   1.7   45400.0
105. CH3OH+CH2O=>CH3O+CH3O                    1.53E+12   .0   333200.0
106. CH3O+CH3O=>CH3OH+CH2O                    3.00E+13   .0       .0
107. CH3O2H=CH3O+OH                           4.00E+15   .0   180500.0
108. OH+CH3O2H=H2O+CH3O2                      2.60E+12   .0       .0
109. C2H+O=CO+CH                              1.00E+13   .0       .0
110. C2H+O2=HCCO+O                            3.00E+12   .0       .0
111. HCCO+H=CH2+CO                            1.50E+14   .0       .0
112. HCCO+O=>CO+CO+H                          9.60E+13   .0       .0
113. HCCO+CH2=C2H3+CO                         3.00E+13   .0       .0
114. C2H2+M=C2H+H+M                           3.60E+16   .0   446000.0
     H2          Enhanced by   1.000E+00
     H2O         Enhanced by   6.500E+00
     O2          Enhanced by   4.000E-01
     N2          Enhanced by   4.000E-01
     CO          Enhanced by   7.500E-01
     CO2         Enhanced by   1.500E+00
     CH4         Enhanced by   3.000E+00
115. C2H2+O2=HCCO+OH                          2.00E+08   1.5   126000.0
116. C2H2+H=C2H+H2                            6.02E+13   .0   116400.0
```

```
117. C2H2+O=CH2+CO                      2.17E+06  2.1    6570.0
118. C2H2+O=HCCO+H                      5.06E+06  2.1    6570.0
119. C2H2+OH=H2O+C2H                    6.00E+13   .0   54200.0
120. CH2CO+M=CH2+CO+M                   1.00E+16   .0  248000.0
     H2          Enhanced by  1.000E+00
     H2O         Enhanced by  6.500E+00
     O2          Enhanced by  4.000E-01
     N2          Enhanced by  4.000E-01
     CO          Enhanced by  7.500E-01
     CO2         Enhanced by  1.500E+00
     CH4         Enhanced by  3.000E+00
121. CH2CO+H=CH3+CO                     3.60E+13   .0   14100.0
122. CH2CO+O=CHO+CHO                    2.30E+12   .0    5700.0
123. CH2CO+OH=CH2O+CHO                  1.00E+13   .0       .0
124. C2H3=C2H2+H                     4.73E+40  -8.8  194500.0
125. C2H3+OH=C2H2+H2O                   5.00E+13   .0       .0
126. C2H3+H=C2H2+H2                     1.20E+13   .0       .0
127. C2H3+O=C2H2+OH                     1.00E+13   .0       .0
128. C2H3+O=CH3+CO                      1.00E+13   .0       .0
129. C2H3+O=CHO+CH2                     1.00E+13   .0       .0
130. C2H3+O2=CH2O+CHO                   3.00E+12  -.1   -3324.0
131. C2H3+O2=CH2CHO+O                   2.46E+15  -.8   13120.0
132. CH3CO=CH3+CO                    2.32E+26  -5.0   75120.0
133. CH3CO+H=CH2CO+H2                   2.00E+13   .0       .0
134. CH2CHO+H=CH2CO+H2                  2.00E+13   .0       .0
135. C2H4+M=C2H2+H2+M                   7.50E+17   .0  332000.0
     H2          Enhanced by  1.000E+00
     H2O         Enhanced by  6.500E+00
     O2          Enhanced by  4.000E-01
     N2          Enhanced by  4.000E-01
     CO          Enhanced by  7.500E-01
     CO2         Enhanced by  1.500E+00
     CH4         Enhanced by  3.000E+00
136. C2H4+M=C2H3+H+M                    8.50E+17   .0  404000.0
     H2          Enhanced by  1.000E+00
     H2O         Enhanced by  6.500E+00
     O2          Enhanced by  4.000E-01
     N2          Enhanced by  4.000E-01
     CO          Enhanced by  7.500E-01
     CO2         Enhanced by  1.500E+00
     CH4         Enhanced by  3.000E+00
137. C2H4+H=C2H3+H2                     5.40E+14   .0   62900.0
138. C2H4+O=CH2CHO+H                    1.02E+06  2.1       .0
```

```
139. C2H4+O=CHO+CH3                    2.42E+06  2.1      .0
140. C2H4+OH=C2H3+H2O                  2.20E+13   .0    24900.0
141. CH3CHO+M=CH3+CHO+M                7.00E+15   .0   342800.0
     H2          Enhanced by  1.000E+00
     H2O         Enhanced by  6.500E+00
     O2          Enhanced by  4.000E-01
     N2          Enhanced by  4.000E-01
     CO          Enhanced by  7.500E-01
     CO2         Enhanced by  1.500E+00
     CH4         Enhanced by  3.000E+00
142. CH3CHO+H=CH3CO+H2                 2.10E+09  1.2    10100.0
143. CH3CHO+H=CH2CHO+H2                2.00E+09  1.2    10100.0
144. CH3CHO+O=CH3CO+OH                 5.00E+12   .0     7600.0
145. CH3CHO+O=CH2CHO+OH                8.00E+11   .0     7600.0
146. CH3CHO+O2=CH3CO+HO2               4.00E+13   .0   164300.0
147. CH3CHO+OH=CH3CO+H2O               2.30E+10   .7    -4700.0
148. CH3CHO+HO2=CH3CO+H2O2             3.00E+12   .0    50000.0
149. CH3CHO+CH2=CH3CO+CH3              2.50E+12   .0    15900.0
150. CH3CHO+CH3=CH3CO+CH4              2.00E-06  5.6    10300.0
151. C2H5=C2H4+H                   1.02E+43  -9.1   224150.0
152. C2H5+H=CH3+CH3                3.00E+13   .0       .0
153. C2H5+O=CH3CHO+H               5.00E+13   .0       .0
154. C2H5+O=CH2O+CH3               1.00E+13   .0       .0
155. C2H5+O2=C2H4+HO2              1.10E+10   .0    -6300.0
156. C2H5+CH3=C2H4+CH4             1.14E+12   .0       .0
157. C2H5+C2H5=C2H4+C2H6           1.40E+12   .0       .0
158. C2H6+H=C2H5+H2                1.40E+09  1.5    31100.0
159. C2H6+O=C2H5+OH                1.00E+09  1.5    24400.0
160. C2H6+OH=C2H5+H2O              7.20E+06  2.0     3600.0
161. C2H6+HO2=C2H5+H2O2            1.70E+13   .0    85900.0
162. C2H6+O2=C2H5+HO2              6.00E+13   .0   217000.0
163. C2H6+CH2=C2H5+CH3             2.20E+13   .0    36300.0
164. C2H6+CH3=C2H5+CH4             1.50E-07  6.0    25400.0
```

NOTE: E units Joules/mole, A units mole-cm-sec-K

B.2 GRI mechanism

```
CHEMKIN INTERPRETER OUTPUT: CHEMKIN-II Version 3.1 Feb. 1993
                  DOUBLE PRECISION
```

ELEMENTS CONSIDERED	ATOMIC WEIGHT
1. C	12.0112
2. H	1.00797
3. O	15.9994
4. N	14.0067

SPECIES CONSIDERED	PHASE	GAS/ELEC	MOLEC WEIGHT	TEMPERATURE LOW	TEMPERATURE HIGH	ELEMENT COUNT C	H	O	N
1. H2	G	0	2.01594	200.0	3500.0	0	2	0	0
2. H	G	0	1.00797	200.0	3500.0	0	1	0	0
3. O	G	0	15.99940	200.0	3500.0	1	0	0	0
4. O2	G	0	31.99880	200.0	3500.0	2	0	0	0
5. OH	G	0	17.00737	200.0	3500.0	1	1	0	0
6. H2O	G	0	18.01534	200.0	3500.0	1	2	0	0
7. HO2	G	0	33.00677	200.0	3500.0	2	1	0	0
8. H2O2	G	0	34.01474	200.0	3500.0	2	2	0	0
9. C	G	0	12.01115	200.0	3500.0	0	0	1	0
10. CH	G	0	13.01912	200.0	3500.0	0	1	1	0
11. CH2	G	0	14.02709	200.0	3500.0	0	2	1	0
12. CH2(S)	G	0	14.02709	200.0	3500.0	0	2	1	0
13. CH3	G	0	15.03506	200.0	3500.0	0	3	1	0
14. CH4	G	0	16.04303	200.0	3500.0	0	4	1	0
15. CO	G	0	28.01055	200.0	3500.0	1	0	1	0
16. CO2	G	0	44.00995	200.0	3500.0	2	0	1	0
17. HCO	G	0	29.01852	200.0	3500.0	1	1	1	0
18. CH2O	G	0	30.02649	200.0	3500.0	1	2	1	0
19. CH2OH	G	0	31.03446	200.0	3500.0	1	3	1	0
20. CH3O	G	0	31.03446	300.0	3000.0	1	3	1	0
21. CH3OH	G	0	32.04243	200.0	3500.0	1	4	1	0
22. C2H	G	0	25.03027	200.0	3500.0	0	1	2	0
23. C2H2	G	0	26.03824	200.0	3500.0	0	2	2	0
24. C2H3	G	0	27.04621	200.0	3500.0	0	3	2	0
25. C2H4	G	0	28.05418	200.0	3500.0	0	4	2	0
26. C2H5	G	0	29.06215	200.0	3500.0	0	5	2	0

```
27. C2H6          G 0  30.07012  200.0 3500.0  0  6  2  0  0
28. HCCO          G 0  41.02967  300.0 4000.0  1  1  2  0  0
29. CH2CO         G 0  42.03764  200.0 3500.0  1  2  2  0  0
30. HCCOH         G 0  42.03764  300.0 5000.0  1  2  2  0  0
31. N           G 0  14.00670  200.0 6000.0  0  0  0  1  0
32. NH          G 0  15.01467  200.0 6000.0  0  1  0  1  0
33. NH2         G 0  16.02264  200.0 6000.0  0  2  0  1  0
34. NH3         G 0  17.03061  200.0 6000.0  0  3  0  1  0
35. NNH         G 0  29.02137  200.0 6000.0  0  1  0  2  0
36. NO          G 0  30.00610  200.0 6000.0  1  0  0  1  0
37. NO2         G 0  46.00550  200.0 6000.0  2  0  0  1  0
38. N2O         G 0  44.01280  200.0 6000.0  1  0  0  2  0
39. HNO         G 0  31.01407  200.0 6000.0  1  1  0  1  0
40. CN          G 0  26.01785  200.0 6000.0  0  0  1  1  0
41. HCN         G 0  27.02582  200.0 6000.0  0  1  1  1  0
42. H2CN        G 0  28.03379  300.0 4000.0  0  2  1  1  0
43. HCNN        G 0  41.03252  300.0 5000.0  0  1  1  2  0
44. HCNO        G 0  43.02522  300.0 5000.0  1  1  1  1  0
45. HOCN        G 0  43.02522  300.0 5000.0  1  1  1  1  0
46. HNCO        G 0  43.02522  300.0 5000.0  1  1  1  1  0
47. NCO         G 0  42.01725  200.0 6000.0  1  0  1  1  0
48. N2          G 0  28.01340  300.0 5000.0  0  0  0  2  0
49. AR          G 0  39.94800  300.0 5000.0  0  0  0  0  1
50. C3H7        G 0  43.08924  300.0 5000.0  0  7  3  0  0
51. C3H8        G 0  44.09721  300.0 5000.0  0  8  3  0  0
52. CH2CHO        G 0  43.04561  300.0 5000.0  1  3  2  0  0
53. CH3CHO        G 0  44.05358  200.0 6000.0  1  4  2  0  0
-------------------------------------------------------------------------------

                                                (k = A T**b exp(-E/RT))
  REACTIONS CONSIDERED                            A       b       E

 1. 2O+M<=>O2+M                          1.20E+17  -1.0       .0
     H2          Enhanced by   2.400E+00
     H2O         Enhanced by   1.540E+01
     CH4         Enhanced by   2.000E+00
     CO          Enhanced by   1.750E+00
     CO2         Enhanced by   3.600E+00
     C2H6        Enhanced by   3.000E+00
     AR          Enhanced by   8.300E-01
 2. O+H+M<=>OH+M                          5.00E+17  -1.0       .0
     H2          Enhanced by   2.000E+00
     H2O         Enhanced by   6.000E+00
```

```
     CH4          Enhanced by   2.000E+00
     CO           Enhanced by   1.500E+00
     CO2          Enhanced by   2.000E+00
     C2H6         Enhanced by   3.000E+00
     AR           Enhanced by   7.000E-01
 3. O+H2<=>H+OH                          3.87E+04   2.7    6260.0
 4. O+HO2<=>OH+O2                        2.00E+13    .0       .0
 5. O+H2O2<=>OH+HO2                      9.63E+06   2.0    4000.0
 6. O+CH<=>H+CO                          5.70E+13    .0       .0
 7. O+CH2<=>H+HCO                        8.00E+13    .0       .0
 8. O+CH2(S)<=>H2+CO                     1.50E+13    .0       .0
 9. O+CH2(S)<=>H+HCO                     1.50E+13    .0       .0
10. O+CH3<=>H+CH2O                       5.06E+13    .0       .0
11. O+CH4<=>OH+CH3                       1.02E+09   1.5    8600.0
12. O+CO(+M)<=>CO2(+M)                   1.80E+10    .0    2385.0
   Low pressure limit:  .60200E+15  .00000E+00  .30000E+04
     H2           Enhanced by   2.000E+00
     O2           Enhanced by   6.000E+00
     H2O          Enhanced by   6.000E+00
     CH4          Enhanced by   2.000E+00
     CO           Enhanced by   1.500E+00
     CO2          Enhanced by   3.500E+00
     C2H6         Enhanced by   3.000E+00
     AR           Enhanced by   5.000E-01
13. O+HCO<=>OH+CO                        3.00E+13    .0       .0
14. O+HCO<=>H+CO2                        3.00E+13    .0       .0
15. O+CH2O<=>OH+HCO                      3.90E+13    .0    3540.0
16. O+CH2OH<=>OH+CH2O                    1.00E+13    .0       .0
17. O+CH3O<=>OH+CH2O                     1.00E+13    .0       .0
18. O+CH3OH<=>OH+CH2OH                   3.88E+05   2.5    3100.0
19. O+CH3OH<=>OH+CH3O                    1.30E+05   2.5    5000.0
20. O+C2H<=>CH+CO                        5.00E+13    .0       .0
21. O+C2H2<=>H+HCCO                      1.35E+07   2.0    1900.0
22. O+C2H2<=>OH+C2H                      4.60E+19  -1.4   28950.0
23. O+C2H2<=>CO+CH2                      6.94E+06   2.0    1900.0
24. O+C2H3<=>H+CH2CO                     3.00E+13    .0       .0
25. O+C2H4<=>CH3+HCO                     1.25E+07   1.8     220.0
26. O+C2H5<=>CH3+CH2O                    2.24E+13    .0       .0
27. O+C2H6<=>OH+C2H5                     8.98E+07   1.9    5690.0
28. O+HCCO<=>H+2CO                       1.00E+14    .0       .0
29. O+CH2CO<=>OH+HCCO                    1.00E+13    .0    8000.0
30. O+CH2CO<=>CH2+CO2                    1.75E+12    .0    1350.0
31. O2+CO<=>O+CO2                        2.50E+12    .0   47800.0
```

```
32. O2+CH2O<=>HO2+HCO                    1.00E+14   .0   40000.0
33. H+O2+M<=>HO2+M                       2.80E+18  -.9       .0
    O2          Enhanced by   0.000E+00
    H2O         Enhanced by   0.000E+00
    CO          Enhanced by   7.500E-01
    CO2         Enhanced by   1.500E+00
    C2H6        Enhanced by   1.500E+00
    N2          Enhanced by   0.000E+00
    AR          Enhanced by   0.000E+00
34. H+2O2<=>HO2+O2                       2.08E+19  -1.2       .0
35. H+O2+H2O<=>HO2+H2O                   1.13E+19  -.8        .0
36. H+O2+N2<=>HO2+N2                     2.60E+19  -1.2       .0
37. H+O2+AR<=>HO2+AR                     7.00E+17  -.8        .0
38. H+O2<=>O+OH                          2.65E+16  -.7    17041.0
39. 2H+M<=>H2+M                          1.00E+18  -1.0       .0
    H2          Enhanced by   0.000E+00
    H2O         Enhanced by   0.000E+00
    CH4         Enhanced by   2.000E+00
    CO2         Enhanced by   0.000E+00
    C2H6        Enhanced by   3.000E+00
    AR          Enhanced by   6.300E-01
40. 2H+H2<=>2H2                          9.00E+16  -.6        .0
41. 2H+H2O<=>H2+H2O                      6.00E+19  -1.3       .0
42. 2H+CO2<=>H2+CO2                      5.50E+20  -2.0       .0
43. H+OH+M<=>H2O+M                       2.20E+22  -2.0       .0
    H2          Enhanced by   7.300E-01
    H2O         Enhanced by   3.650E+00
    CH4         Enhanced by   2.000E+00
    C2H6        Enhanced by   3.000E+00
    AR          Enhanced by   3.800E-01
44. H+HO2<=>O+H2O                        3.97E+12    .0    671.0
45. H+HO2<=>O2+H2                        4.48E+13    .0   1068.0
46. H+HO2<=>2OH                          8.40E+13    .0    635.0
47. H+H2O2<=>HO2+H2                      1.21E+07   2.0   5200.0
48. H+H2O2<=>OH+H2O                      1.00E+13    .0   3600.0
49. H+CH<=>C+H2                          1.65E+14    .0      .0
50. H+CH2(+M)<=>CH3(+M)                  6.00E+14    .0      .0
  Low pressure limit:  .10400E+27 -.27600E+01  .16000E+04
  TROE centering:      .56200E+00  .91000E+02  .58360E+04  .85520E+04
    H2          Enhanced by   2.000E+00
    H2O         Enhanced by   6.000E+00
    CH4         Enhanced by   2.000E+00
    CO          Enhanced by   1.500E+00
```

```
    CO2          Enhanced by   2.000E+00
    C2H6         Enhanced by   3.000E+00
    AR           Enhanced by   7.000E-01
51. H+CH2(S)<=>CH+H2                      3.00E+13   .0      .0
52. H+CH3(+M)<=>CH4(+M)                   1.39E+16   -.5     536.0
  Low pressure limit:  .26200E+34 -.47600E+01  .24400E+04
  TROE centering:      .78300E+00  .74000E+02  .29410E+04  .69640E+04
    H2           Enhanced by   2.000E+00
    H2O          Enhanced by   6.000E+00
    CH4          Enhanced by   3.000E+00
    CO           Enhanced by   1.500E+00
    CO2          Enhanced by   2.000E+00
    C2H6         Enhanced by   3.000E+00
    AR           Enhanced by   7.000E-01
53. H+CH4<=>CH3+H2                        6.60E+08   1.6   10840.0
54. H+HCO(+M)<=>CH2O(+M)                  1.09E+12   .5    -260.0
  Low pressure limit:  .24700E+25 -.25700E+01  .42500E+03
  TROE centering:      .78240E+00  .27100E+03  .27550E+04  .65700E+04
    H2           Enhanced by   2.000E+00
    H2O          Enhanced by   6.000E+00
    CH4          Enhanced by   2.000E+00
    CO           Enhanced by   1.500E+00
    CO2          Enhanced by   2.000E+00
    C2H6         Enhanced by   3.000E+00
    AR           Enhanced by   7.000E-01
55. H+HCO<=>H2+CO                         7.34E+13   .0      .0
56. H+CH2O(+M)<=>CH2OH(+M)                5.40E+11   .5    3600.0
  Low pressure limit:  .12700E+33 -.48200E+01  .65300E+04
  TROE centering:      .71870E+00  .10300E+03  .12910E+04  .41600E+04
    H2           Enhanced by   2.000E+00
    H2O          Enhanced by   6.000E+00
    CH4          Enhanced by   2.000E+00
    CO           Enhanced by   1.500E+00
    CO2          Enhanced by   2.000E+00
    C2H6         Enhanced by   3.000E+00
57. H+CH2O(+M)<=>CH3O(+M)                 5.40E+11   .5    2600.0
  Low pressure limit:  .22000E+31 -.48000E+01  .55600E+04
  TROE centering:      .75800E+00  .94000E+02  .15550E+04  .42000E+04
    H2           Enhanced by   2.000E+00
    H2O          Enhanced by   6.000E+00
    CH4          Enhanced by   2.000E+00
    CO           Enhanced by   1.500E+00
    CO2          Enhanced by   2.000E+00
```

```
    C2H6          Enhanced by   3.000E+00
58. H+CH2O<=>HCO+H2                        5.74E+07   1.9    2742.0
59. H+CH2OH(+M)<=>CH3OH(+M)                1.06E+12   .5      86.0
  Low pressure limit:  .43600E+32 -.46500E+01  .50800E+04
  TROE centering:      .60000E+00  .10000E+03  .90000E+05  .10000E+05
    H2          Enhanced by   2.000E+00
    H2O         Enhanced by   6.000E+00
    CH4         Enhanced by   2.000E+00
    CO          Enhanced by   1.500E+00
    CO2         Enhanced by   2.000E+00
    C2H6        Enhanced by   3.000E+00
60. H+CH2OH<=>H2+CH2O                      2.00E+13   .0      .0
61. H+CH2OH<=>OH+CH3                       1.65E+11   .7    -284.0
62. H+CH2OH<=>CH2(S)+H2O                   3.28E+13  -.1     610.0
63. H+CH3O(+M)<=>CH3OH(+M)                 2.43E+12   .5      50.0
  Low pressure limit:  .46600E+42 -.74400E+01  .14080E+05
  TROE centering:      .70000E+00  .10000E+03  .90000E+05  .10000E+05
    H2          Enhanced by   2.000E+00
    H2O         Enhanced by   6.000E+00
    CH4         Enhanced by   2.000E+00
    CO          Enhanced by   1.500E+00
    CO2         Enhanced by   2.000E+00
    C2H6        Enhanced by   3.000E+00
64. H+CH3O<=>H+CH2OH                       4.15E+07   1.6    1924.0
65. H+CH3O<=>H2+CH2O                       2.00E+13   .0      .0
66. H+CH3O<=>OH+CH3                        1.50E+12   .5    -110.0
67. H+CH3O<=>CH2(S)+H2O                    2.62E+14  -.2    1070.0
68. H+CH3OH<=>CH2OH+H2                     1.70E+07   2.1    4870.0
69. H+CH3OH<=>CH3O+H2                      4.20E+06   2.1    4870.0
70. H+C2H(+M)<=>C2H2(+M)                   1.00E+17  -1.0     .0
  Low pressure limit:  .37500E+34 -.48000E+01  .19000E+04
  TROE centering:      .64640E+00  .13200E+03  .13150E+04  .55660E+04
    H2          Enhanced by   2.000E+00
    H2O         Enhanced by   6.000E+00
    CH4         Enhanced by   2.000E+00
    CO          Enhanced by   1.500E+00
    CO2         Enhanced by   2.000E+00
    C2H6        Enhanced by   3.000E+00
    AR          Enhanced by   7.000E-01
71. H+C2H2(+M)<=>C2H3(+M)                  5.60E+12   .0    2400.0
  Low pressure limit:  .38000E+41 -.72700E+01  .72200E+04
  TROE centering:      .75070E+00  .98500E+02  .13020E+04  .41670E+04
    H2          Enhanced by   2.000E+00
```

```
     H2O          Enhanced by    6.000E+00
     CH4          Enhanced by    2.000E+00
     CO           Enhanced by    1.500E+00
     CO2          Enhanced by    2.000E+00
     C2H6         Enhanced by    3.000E+00
     AR           Enhanced by    7.000E-01
72. H+C2H3(+M)<=>C2H4(+M)                  6.08E+12    .3     280.0
   Low pressure limit:  .14000E+31 -.38600E+01  .33200E+04
   TROE centering:      .78200E+00  .20750E+03  .26630E+04  .60950E+04
     H2           Enhanced by    2.000E+00
     H2O          Enhanced by    6.000E+00
     CH4          Enhanced by    2.000E+00
     CO           Enhanced by    1.500E+00
     CO2          Enhanced by    2.000E+00
     C2H6         Enhanced by    3.000E+00
     AR           Enhanced by    7.000E-01
73. H+C2H3<=>H2+C2H2                    3.00E+13    .0       .0
74. H+C2H4(+M)<=>C2H5(+M)                  5.40E+11    .5    1820.0
   Low pressure limit:  .60000E+42 -.76200E+01  .69700E+04
   TROE centering:      .97530E+00  .21000E+03  .98400E+03  .43740E+04
     H2           Enhanced by    2.000E+00
     H2O          Enhanced by    6.000E+00
     CH4          Enhanced by    2.000E+00
     CO           Enhanced by    1.500E+00
     CO2          Enhanced by    2.000E+00
     C2H6         Enhanced by    3.000E+00
     AR           Enhanced by    7.000E-01
75. H+C2H4<=>C2H3+H2                    1.33E+06    2.5   12240.0
76. H+C2H5(+M)<=>C2H6(+M)                  5.21E+17   -1.0   1580.0
   Low pressure limit:  .19900E+42 -.70800E+01  .66850E+04
   TROE centering:      .84220E+00  .12500E+03  .22190E+04  .68820E+04
     H2           Enhanced by    2.000E+00
     H2O          Enhanced by    6.000E+00
     CH4          Enhanced by    2.000E+00
     CO           Enhanced by    1.500E+00
     CO2          Enhanced by    2.000E+00
     C2H6         Enhanced by    3.000E+00
     AR           Enhanced by    7.000E-01
77. H+C2H5<=>H2+C2H4                    2.00E+12    .0       .0
78. H+C2H6<=>C2H5+H2                    1.15E+08    1.9    7530.0
79. H+HCCO<=>CH2(S)+CO                  1.00E+14    .0       .0
80. H+CH2CO<=>HCCO+H2                   5.00E+13    .0    8000.0
81. H+CH2CO<=>CH3+CO                    1.13E+13    .0    3428.0
```

```
82. H+HCCOH<=>H+CH2CO                      1.00E+13   .0       .0
83. H2+CO(+M)<=>CH2O(+M)                   4.30E+07   1.5    79600.0
   Low pressure limit:  .50700E+28 -.34200E+01  .84350E+05
   TROE centering:      .93200E+00  .19700E+03  .15400E+04  .10300E+05
     H2          Enhanced by   2.000E+00
     H2O         Enhanced by   6.000E+00
     CH4         Enhanced by   2.000E+00
     CO          Enhanced by   1.500E+00
     CO2         Enhanced by   2.000E+00
     C2H6        Enhanced by   3.000E+00
     AR          Enhanced by   7.000E-01
84. OH+H2<=>H+H2O                          2.16E+08   1.5    3430.0
85. 2OH(+M)<=>H2O2(+M)                     7.40E+13   -.4       .0
   Low pressure limit:  .23000E+19 -.90000E+00 -.17000E+04
   TROE centering:      .73460E+00  .94000E+02  .17560E+04  .51820E+04
     H2          Enhanced by   2.000E+00
     H2O         Enhanced by   6.000E+00
     CH4         Enhanced by   2.000E+00
     CO          Enhanced by   1.500E+00
     CO2         Enhanced by   2.000E+00
     C2H6        Enhanced by   3.000E+00
     AR          Enhanced by   7.000E-01
86. 2OH<=>O+H2O                            3.57E+04   2.4    -2110.0
87. OH+HO2<=>O2+H2O                        1.45E+13   .0     -500.0
   Declared duplicate reaction...
88. OH+H2O2<=>HO2+H2O                      2.00E+12   .0      427.0
   Declared duplicate reaction...
89. OH+H2O2<=>HO2+H2O                      1.70E+18   .0    29410.0
   Declared duplicate reaction...
90. OH+C<=>H+CO                            5.00E+13   .0       .0
91. OH+CH<=>H+HCO                          3.00E+13   .0       .0
92. OH+CH2<=>H+CH2O                        2.00E+13   .0       .0
93. OH+CH2<=>CH+H2O                        1.13E+07   2.0    3000.0
94. OH+CH2(S)<=>H+CH2O                     3.00E+13   .0       .0
95. OH+CH3(+M)<=>CH3OH(+M)                 2.79E+18  -1.4    1330.0
   Low pressure limit:  .40000E+37 -.59200E+01  .31400E+04
   TROE centering:      .41200E+00  .19500E+03  .59000E+04  .63940E+04
     H2          Enhanced by   2.000E+00
     H2O         Enhanced by   6.000E+00
     CH4         Enhanced by   2.000E+00
     CO          Enhanced by   1.500E+00
     CO2         Enhanced by   2.000E+00
     C2H6        Enhanced by   3.000E+00
```

```
 96. OH+CH3<=>CH2+H2O                  5.60E+07  1.6   5420.0
 97. OH+CH3<=>CH2(S)+H2O               6.44E+17 -1.3   1417.0
 98. OH+CH4<=>CH3+H2O                  1.00E+08  1.6   3120.0
 99. OH+CO<=>H+CO2                     4.76E+07  1.2     70.0
100. OH+HCO<=>H2O+CO                   5.00E+13  .0      .0
101. OH+CH2O<=>HCO+H2O                 3.43E+09  1.2   -447.0
102. OH+CH2OH<=>H2O+CH2O               5.00E+12  .0      .0
103. OH+CH3O<=>H2O+CH2O                5.00E+12  .0      .0
104. OH+CH3OH<=>CH2OH+H2O              1.44E+06  2.0   -840.0
105. OH+CH3OH<=>CH3O+H2O               6.30E+06  2.0   1500.0
106. OH+C2H<=>H+HCCO                   2.00E+13  .0      .0
107. OH+C2H2<=>H+CH2CO                 2.18E-04  4.5  -1000.0
108. OH+C2H2<=>H+HCCOH                 5.04E+05  2.3  13500.0
109. OH+C2H2<=>C2H+H2O                 3.37E+07  2.0  14000.0
110. OH+C2H2<=>CH3+CO                  4.83E-04  4.0  -2000.0
111. OH+C2H3<=>H2O+C2H2                5.00E+12  .0      .0
112. OH+C2H4<=>C2H3+H2O                3.60E+06  2.0   2500.0
113. OH+C2H6<=>C2H5+H2O                3.54E+06  2.1    870.0
114. OH+CH2CO<=>HCCO+H2O               7.50E+12  .0   2000.0
115. 2HO2<=>O2+H2O2                    1.30E+11  .0  -1630.0
   Declared duplicate reaction...
116. 2HO2<=>O2+H2O2                    4.20E+14  .0  12000.0
   Declared duplicate reaction...
117. HO2+CH2<=>OH+CH2O                 2.00E+13  .0      .0
118. HO2+CH3<=>O2+CH4                  1.00E+12  .0      .0
119. HO2+CH3<=>OH+CH3O                 3.78E+13  .0      .0
120. HO2+CO<=>OH+CO2                   1.50E+14  .0  23600.0
121. HO2+CH2O<=>HCO+H2O2               5.60E+06  2.0  12000.0
122. C+O2<=>O+CO                       5.80E+13  .0    576.0
123. C+CH2<=>H+C2H                     5.00E+13  .0      .0
124. C+CH3<=>H+C2H2                    5.00E+13  .0      .0
125. CH+O2<=>O+HCO                     6.71E+13  .0      .0
126. CH+H2<=>H+CH2                     1.08E+14  .0   3110.0
127. CH+H2O<=>H+CH2O                   5.71E+12  .0   -755.0
128. CH+CH2<=>H+C2H2                   4.00E+13  .0      .0
129. CH+CH3<=>H+C2H3                   3.00E+13  .0      .0
130. CH+CH4<=>H+C2H4                   6.00E+13  .0      .0
131. CH+CO(+M)<=>HCCO(+M)              5.00E+13  .0      .0
   Low pressure limit:  .26900E+29 -.37400E+01  .19360E+04
   TROE centering:      .57570E+00  .23700E+03  .16520E+04  .50690E+04
     H2          Enhanced by   2.000E+00
     H2O         Enhanced by   6.000E+00
     CH4         Enhanced by   2.000E+00
```

```
      CO          Enhanced by   1.500E+00
      CO2         Enhanced by   2.000E+00
      C2H6        Enhanced by   3.000E+00
      AR          Enhanced by   7.000E-01
132. CH+CO2<=>HCO+CO                        1.90E+14   .0   15792.0
133. CH+CH2O<=>H+CH2CO                      9.46E+13   .0    -515.0
134. CH+HCCO<=>CO+C2H2                      5.00E+13   .0       .0
135. CH2+O2=>OH+H+CO                        5.00E+12   .0    1500.0
136. CH2+H2<=>H+CH3                         5.00E+05  2.0    7230.0
137. 2CH2<=>H2+C2H2                         1.60E+15   .0   11944.0
138. CH2+CH3<=>H+C2H4                       4.00E+13   .0       .0
139. CH2+CH4<=>2CH3                         2.46E+06  2.0    8270.0
140. CH2+CO(+M)<=>CH2CO(+M)                 8.10E+11   .5    4510.0
   Low pressure limit:  .26900E+34 -.51100E+01  .70950E+04
   TROE centering:      .59070E+00  .27500E+03  .12260E+04  .51850E+04
      H2          Enhanced by   2.000E+00
      H2O         Enhanced by   6.000E+00
      CH4         Enhanced by   2.000E+00
      CO          Enhanced by   1.500E+00
      CO2         Enhanced by   2.000E+00
      C2H6        Enhanced by   3.000E+00
      AR          Enhanced by   7.000E-01
141. CH2+HCCO<=>C2H3+CO                     3.00E+13   .0       .0
142. CH2(S)+N2<=>CH2+N2                     1.50E+13   .0     600.0
143. CH2(S)+AR<=>CH2+AR                     9.00E+12   .0     600.0
144. CH2(S)+O2<=>H+OH+CO                    2.80E+13   .0       .0
145. CH2(S)+O2<=>CO+H2O                     1.20E+13   .0       .0
146. CH2(S)+H2<=>CH3+H                      7.00E+13   .0       .0
147. CH2(S)+H2O(+M)<=>CH3OH(+M)             4.82E+17 -1.2    1145.0
   Low pressure limit:  .18800E+39 -.63600E+01  .50400E+04
   TROE centering:      .60270E+00  .20800E+03  .39220E+04  .10180E+05
      H2          Enhanced by   2.000E+00
      H2O         Enhanced by   6.000E+00
      CH4         Enhanced by   2.000E+00
      CO          Enhanced by   1.500E+00
      CO2         Enhanced by   2.000E+00
      C2H6        Enhanced by   3.000E+00
148. CH2(S)+H2O<=>CH2+H2O                   3.00E+13   .0       .0
149. CH2(S)+CH3<=>H+C2H4                    1.20E+13   .0    -570.0
150. CH2(S)+CH4<=>2CH3                      1.60E+13   .0    -570.0
151. CH2(S)+CO<=>CH2+CO                     9.00E+12   .0       .0
152. CH2(S)+CO2<=>CH2+CO2                   7.00E+12   .0       .0
153. CH2(S)+CO2<=>CO+CH2O                   1.40E+13   .0       .0
```

```
154. CH2(S)+C2H6<=>CH3+C2H5                 4.00E+13   .0   -550.0
155. CH3+O2<=>O+CH3O                        3.56E+13   .0  30480.0
156. CH3+O2<=>OH+CH2O                       2.31E+12   .0  20315.0
157. CH3+H2O2<=>HO2+CH4                     2.45E+04  2.5   5180.0
158. 2CH3(+M)<=>C2H6(+M)                    6.77E+16 -1.2    654.0
   Low pressure limit:  .34000E+42 -.70300E+01  .27620E+04
   TROE centering:      .61900E+00  .73200E+02  .11800E+04  .99990E+04
     H2          Enhanced by   2.000E+00
     H2O         Enhanced by   6.000E+00
     CH4         Enhanced by   2.000E+00
     CO          Enhanced by   1.500E+00
     CO2         Enhanced by   2.000E+00
     C2H6        Enhanced by   3.000E+00
     AR          Enhanced by   7.000E-01
159. 2CH3<=>H+C2H5                          6.84E+12   .1  10600.0
160. CH3+HCO<=>CH4+CO                       2.65E+13   .0      .0
161. CH3+CH2O<=>HCO+CH4                     3.32E+03  2.8   5860.0
162. CH3+CH3OH<=>CH2OH+CH4                  3.00E+07  1.5   9940.0
163. CH3+CH3OH<=>CH3O+CH4                   1.00E+07  1.5   9940.0
164. CH3+C2H4<=>C2H3+CH4                    2.27E+05  2.0   9200.0
165. CH3+C2H6<=>C2H5+CH4                    6.14E+06  1.7  10450.0
166. HCO+H2O<=>H+CO+H2O                     1.50E+18 -1.0  17000.0
167. HCO+M<=>H+CO+M                         1.87E+17 -1.0  17000.0
     H2          Enhanced by   2.000E+00
     H2O         Enhanced by   0.000E+00
     CH4         Enhanced by   2.000E+00
     CO          Enhanced by   1.500E+00
     CO2         Enhanced by   2.000E+00
     C2H6        Enhanced by   3.000E+00
168. HCO+O2<=>HO2+CO                        1.35E+13   .0    400.0
169. CH2OH+O2<=>HO2+CH2O                    1.80E+13   .0    900.0
170. CH3O+O2<=>HO2+CH2O                     4.28E-13  7.6  -3530.0
171. C2H+O2<=>HCO+CO                        1.00E+13   .0   -755.0
172. C2H+H2<=>H+C2H2                        5.68E+10   .9   1993.0
173. C2H3+O2<=>HCO+CH2O                     4.58E+16 -1.4   1015.0
174. C2H4(+M)<=>H2+C2H2(+M)                 8.00E+12   .4  86770.0
   Low pressure limit:  .15800E+52 -.93000E+01  .97800E+05
   TROE centering:      .73450E+00  .18000E+03  .10350E+04  .54170E+04
     H2          Enhanced by   2.000E+00
     H2O         Enhanced by   6.000E+00
     CH4         Enhanced by   2.000E+00
     CO          Enhanced by   1.500E+00
     CO2         Enhanced by   2.000E+00
```

```
     C2H6          Enhanced by   3.000E+00
     AR            Enhanced by   7.000E-01
175. C2H5+O2<=>HO2+C2H4                    8.40E+11    .0    3875.0
176. HCCO+O2<=>OH+2CO                      3.20E+12    .0     854.0
177. 2HCCO<=>2CO+C2H2                      1.00E+13    .0       .0
178. N+NO<=>N2+O                           2.70E+13    .0     355.0
179. N+O2<=>NO+O                           9.00E+09   1.0    6500.0
180. N+OH<=>NO+H                           3.36E+13    .0     385.0
181. N2O+O<=>N2+O2                         1.40E+12    .0   10810.0
182. N2O+O<=>2NO                           2.90E+13    .0   23150.0
183. N2O+H<=>N2+OH                         3.87E+14    .0   18880.0
184. N2O+OH<=>N2+HO2                       2.00E+12    .0   21060.0
185. N2O(+M)<=>N2+O(+M)                    7.91E+10    .0   56020.0
   Low pressure limit:  .63700E+15  .00000E+00  .56640E+05
     H2            Enhanced by   2.000E+00
     H2O           Enhanced by   6.000E+00
     CH4           Enhanced by   2.000E+00
     CO            Enhanced by   1.500E+00
     CO2           Enhanced by   2.000E+00
     C2H6          Enhanced by   3.000E+00
     AR            Enhanced by   6.250E-01
186. HO2+NO<=>NO2+OH                       2.11E+12    .0    -480.0
187. NO+O+M<=>NO2+M                        1.06E+20   -1.4      .0
     H2            Enhanced by   2.000E+00
     H2O           Enhanced by   6.000E+00
     CH4           Enhanced by   2.000E+00
     CO            Enhanced by   1.500E+00
     CO2           Enhanced by   2.000E+00
     C2H6          Enhanced by   3.000E+00
     AR            Enhanced by   7.000E-01
188. NO2+O<=>NO+O2                         3.90E+12    .0    -240.0
189. NO2+H<=>NO+OH                         1.32E+14    .0     360.0
190. NH+O<=>NO+H                           4.00E+13    .0       .0
191. NH+H<=>N+H2                           3.20E+13    .0     330.0
192. NH+OH<=>HNO+H                         2.00E+13    .0       .0
193. NH+OH<=>N+H2O                         2.00E+09   1.2       .0
194. NH+O2<=>HNO+O                         4.61E+05   2.0    6500.0
195. NH+O2<=>NO+OH                         1.28E+06   1.5     100.0
196. NH+N<=>N2+H                           1.50E+13    .0       .0
197. NH+H2O<=>HNO+H2                       2.00E+13    .0   13850.0
198. NH+NO<=>N2+OH                         2.16E+13   -.2       .0
199. NH+NO<=>N2O+H                         3.65E+14   -.5       .0
200. NH2+O<=>OH+NH                         3.00E+12    .0       .0
```

```
201. NH2+O<=>H+HNO                      3.90E+13   .0       .0
202. NH2+H<=>NH+H2                      4.00E+13   .0    3650.0
203. NH2+OH<=>NH+H2O                    9.00E+07   1.5    -460.0
204. NNH<=>N2+H                         3.30E+08   .0       .0
205. NNH+M<=>N2+H+M                     1.30E+14   -.1    4980.0
     H2          Enhanced by   2.000E+00
     H2O         Enhanced by   6.000E+00
     CH4         Enhanced by   2.000E+00
     CO          Enhanced by   1.500E+00
     CO2         Enhanced by   2.000E+00
     C2H6        Enhanced by   3.000E+00
     AR          Enhanced by   7.000E-01
206. NNH+O2<=>HO2+N2                    5.00E+12   .0       .0
207. NNH+O<=>OH+N2                      2.50E+13   .0       .0
208. NNH+O<=>NH+NO                      7.00E+13   .0       .0
209. NNH+H<=>H2+N2                      5.00E+13   .0       .0
210. NNH+OH<=>H2O+N2                    2.00E+13   .0       .0
211. NNH+CH3<=>CH4+N2                   2.50E+13   .0       .0
212. H+NO+M<=>HNO+M                     4.48E+19   -1.3     740.0
     H2          Enhanced by   2.000E+00
     H2O         Enhanced by   6.000E+00
     CH4         Enhanced by   2.000E+00
     CO          Enhanced by   1.500E+00
     CO2         Enhanced by   2.000E+00
     C2H6        Enhanced by   3.000E+00
     AR          Enhanced by   7.000E-01
213. HNO+O<=>NO+OH                      2.50E+13   .0       .0
214. HNO+H<=>H2+NO                      9.00E+11   .7     660.0
215. HNO+OH<=>NO+H2O                    1.30E+07   1.9    -950.0
216. HNO+O2<=>HO2+NO                    1.00E+13   .0   13000.0
217. CN+O<=>CO+N                        7.70E+13   .0       .0
218. CN+OH<=>NCO+H                      4.00E+13   .0       .0
219. CN+H2O<=>HCN+OH                    8.00E+12   .0    7460.0
220. CN+O2<=>NCO+O                      6.14E+12   .0    -440.0
221. CN+H2<=>HCN+H                      2.95E+05   2.5    2240.0
222. NCO+O<=>NO+CO                      2.35E+13   .0       .0
223. NCO+H<=>NH+CO                      5.40E+13   .0       .0
224. NCO+OH<=>NO+H+CO                   2.50E+12   .0       .0
225. NCO+N<=>N2+CO                      2.00E+13   .0       .0
226. NCO+O2<=>NO+CO2                    2.00E+12   .0   20000.0
227. NCO+M<=>N+CO+M                     3.10E+14   .0   54050.0
     H2          Enhanced by   2.000E+00
     H2O         Enhanced by   6.000E+00
```

```
      CH4          Enhanced by   2.000E+00
      CO           Enhanced by   1.500E+00
      CO2          Enhanced by   2.000E+00
      C2H6         Enhanced by   3.000E+00
      AR           Enhanced by   7.000E-01
228. NCO+NO<=>N2O+CO                      1.90E+17  -1.5     740.0
229. NCO+NO<=>N2+CO2                      3.80E+18  -2.0     800.0
230. HCN+M<=>H+CN+M                       1.04E+29  -3.3  126600.0
      H2           Enhanced by   2.000E+00
      H2O          Enhanced by   6.000E+00
      CH4          Enhanced by   2.000E+00
      CO           Enhanced by   1.500E+00
      CO2          Enhanced by   2.000E+00
      C2H6         Enhanced by   3.000E+00
      AR           Enhanced by   7.000E-01
231. HCN+O<=>NCO+H                        2.03E+04   2.6    4980.0
232. HCN+O<=>NH+CO                        5.07E+03   2.6    4980.0
233. HCN+O<=>CN+OH                        3.91E+09   1.6   26600.0
234. HCN+OH<=>HOCN+H                      1.10E+06   2.0   13370.0
235. HCN+OH<=>HNCO+H                      4.40E+03   2.3    6400.0
236. HCN+OH<=>NH2+CO                      1.60E+02   2.6    9000.0
237. H+HCN(+M)<=>H2CN(+M)                 3.30E+13    .0       .0
   Low pressure limit:  .14000E+27 -.34000E+01  .19000E+04
      H2           Enhanced by   2.000E+00
      H2O          Enhanced by   6.000E+00
      CH4          Enhanced by   2.000E+00
      CO           Enhanced by   1.500E+00
      CO2          Enhanced by   2.000E+00
      C2H6         Enhanced by   3.000E+00
      AR           Enhanced by   7.000E-01
238. H2CN+N<=>N2+CH2                      6.00E+13    .0     400.0
239. C+N2<=>CN+N                          6.30E+13    .0   46020.0
240. CH+N2<=>HCN+N                        3.12E+09    .9   20130.0
241. CH+N2(+M)<=>HCNN(+M)                 3.10E+12    .1       .0
   Low pressure limit:  .13000E+26 -.31600E+01  .74000E+03
   TROE centering:      .66700E+00  .23500E+03  .21170E+04  .45360E+04
      H2           Enhanced by   2.000E+00
      H2O          Enhanced by   6.000E+00
      CH4          Enhanced by   2.000E+00
      CO           Enhanced by   1.500E+00
      CO2          Enhanced by   2.000E+00
      C2H6         Enhanced by   3.000E+00
      AR           Enhanced by   1.000E+00
```

```
242. CH2+N2<=>HCN+NH                      1.00E+13    .0   74000.0
243. CH2(S)+N2<=>NH+HCN                   1.00E+11    .0   65000.0
244. C+NO<=>CN+O                          1.90E+13    .0       .0
245. C+NO<=>CO+N                          2.90E+13    .0       .0
246. CH+NO<=>HCN+O                        4.10E+13    .0       .0
247. CH+NO<=>H+NCO                        1.62E+13    .0       .0
248. CH+NO<=>N+HCO                        2.46E+13    .0       .0
249. CH2+NO<=>H+HNCO                      3.10E+17   -1.4    1270.0
250. CH2+NO<=>OH+HCN                      2.90E+14   -.7     760.0
251. CH2+NO<=>H+HCNO                      3.80E+13   -.4     580.0
252. CH2(S)+NO<=>H+HNCO                   3.10E+17   -1.4    1270.0
253. CH2(S)+NO<=>OH+HCN                   2.90E+14   -.7     760.0
254. CH2(S)+NO<=>H+HCNO                   3.80E+13   -.4     580.0
255. CH3+NO<=>HCN+H2O                     9.60E+13    .0   28800.0
256. CH3+NO<=>H2CN+OH                     1.00E+12    .0   21750.0
257. HCNN+O<=>CO+H+N2                     2.20E+13    .0       .0
258. HCNN+O<=>HCN+NO                      2.00E+12    .0       .0
259. HCNN+O2<=>O+HCO+N2                   1.20E+13    .0       .0
260. HCNN+OH<=>H+HCO+N2                   1.20E+13    .0       .0
261. HCNN+H<=>CH2+N2                      1.00E+14    .0       .0
262. HNCO+O<=>NH+CO2                      9.80E+07   1.4    8500.0
263. HNCO+O<=>HNO+CO                      1.50E+08   1.6   44000.0
264. HNCO+O<=>NCO+OH                      2.20E+06   2.1   11400.0
265. HNCO+H<=>NH2+CO                      2.25E+07   1.7    3800.0
266. HNCO+H<=>H2+NCO                      1.05E+05   2.5   13300.0
267. HNCO+OH<=>NCO+H2O                    3.30E+07   1.5    3600.0
268. HNCO+OH<=>NH2+CO2                    3.30E+06   1.5    3600.0
269. HNCO+M<=>NH+CO+M                     1.18E+16    .0   84720.0
     H2          Enhanced by   2.000E+00
     H2O         Enhanced by   6.000E+00
     CH4         Enhanced by   2.000E+00
     CO          Enhanced by   1.500E+00
     CO2         Enhanced by   2.000E+00
     C2H6        Enhanced by   3.000E+00
     AR          Enhanced by   7.000E-01
270. HCNO+H<=>H+HNCO                      2.10E+15   -.7    2850.0
271. HCNO+H<=>OH+HCN                      2.70E+11    .2    2120.0
272. HCNO+H<=>NH2+CO                      1.70E+14   -.8    2890.0
273. HOCN+H<=>H+HNCO                      2.00E+07   2.0    2000.0
274. HCCO+NO<=>HCNO+CO                    9.00E+12    .0       .0
275. CH3+N<=>H2CN+H                       6.10E+14   -.3     290.0
276. CH3+N<=>HCN+H2                       3.70E+12    .1     -90.0
277. NH3+H<=>NH2+H2                       5.40E+05   2.4    9915.0
```

```
278. NH3+OH<=>NH2+H2O                    5.00E+07   1.6     955.0
279. NH3+O<=>NH2+OH                      9.40E+06   1.9    6460.0
280. NH+CO2<=>HNO+CO                     1.00E+13    .0   14350.0
281. CN+NO2<=>NCO+NO                     6.16E+15   -.8     345.0
282. NCO+NO2<=>N2O+CO2                   3.25E+12    .0    -705.0
283. N+CO2<=>NO+CO                       3.00E+12    .0   11300.0
284. O+CH3=>H+H2+CO                      3.37E+13    .0       .0
285. O+C2H4<=>H+CH2CHO                   6.70E+06   1.8     220.0
286. O+C2H5<=>H+CH3CHO                   1.10E+14    .0       .0
287. OH+HO2<=>O2+H2O                     5.00E+15    .0   17330.0
   Declared duplicate reaction...
288. OH+CH3=>H2+CH2O                     8.00E+09    .5   -1755.0
289. CH+H2(+M)<=>CH3(+M)                 1.97E+12    .4    -370.0
   Low pressure limit:  .48200E+26 -.28000E+01  .59000E+03
   TROE centering:      .57800E+00  .12200E+03  .25350E+04  .93650E+04
     H2          Enhanced by   2.000E+00
     H2O         Enhanced by   6.000E+00
     CH4         Enhanced by   2.000E+00
     CO          Enhanced by   1.500E+00
     CO2         Enhanced by   2.000E+00
     C2H6        Enhanced by   3.000E+00
     AR          Enhanced by   7.000E-01
290. CH2+O2=>2H+CO2                      5.80E+12    .0    1500.0
291. CH2+O2<=>O+CH2O                     2.40E+12    .0    1500.0
292. CH2+CH2=>2H+C2H2                    2.00E+14    .0   10989.0
293. CH2(S)+H2O=>H2+CH2O                 6.82E+10    .3    -935.0
294. C2H3+O2<=>O+CH2CHO                  3.03E+11    .3      11.0
295. C2H3+O2<=>HO2+C2H2                  1.34E+06   1.6    -384.0
296. O+CH3CHO<=>OH+CH2CHO                2.92E+12    .0    1808.0
297. O+CH3CHO=>OH+CH3+CO                 2.92E+12    .0    1808.0
298. O2+CH3CHO=>HO2+CH3+CO               3.01E+13    .0   39150.0
299. H+CH3CHO<=>CH2CHO+H2                2.05E+09   1.2    2405.0
300. H+CH3CHO=>CH3+H2+CO                 2.05E+09   1.2    2405.0
301. OH+CH3CHO=>CH3+H2O+CO               2.34E+10    .7   -1113.0
302. HO2+CH3CHO=>CH3+H2O2+CO             3.01E+12    .0   11923.0
303. CH3+CH3CHO=>CH3+CH4+CO              2.72E+06   1.8    5920.0
304. H+CH2CO(+M)<=>CH2CHO(+M)            4.87E+11    .4   -1755.0
   Low pressure limit:  .10120E+43 -.76300E+01  .38540E+04
   TROE centering:      .46500E+00  .20100E+03  .17730E+04  .53330E+04
     H2          Enhanced by   2.000E+00
     H2O         Enhanced by   6.000E+00
     CH4         Enhanced by   2.000E+00
     CO          Enhanced by   1.500E+00
```

```
      CO2          Enhanced by    2.000E+00
      C2H6         Enhanced by    3.000E+00
      AR           Enhanced by    7.000E-01
305. O+CH2CHO=>H+CH2+CO2                    1.50E+14    .0       .0
306. O2+CH2CHO=>OH+CO+CH2O                  1.81E+10    .0       .0
307. O2+CH2CHO=>OH+2HCO                     2.35E+10    .0       .0
308. H+CH2CHO<=>CH3+HCO                     2.20E+13    .0       .0
309. H+CH2CHO<=>CH2CO+H2                    1.10E+13    .0       .0
310. OH+CH2CHO<=>H2O+CH2CO                  1.20E+13    .0       .0
311. OH+CH2CHO<=>HCO+CH2OH                  3.01E+13    .0       .0
312. CH3+C2H5(+M)<=>C3H8(+M)                9.43E+12    .0       .0
   Low pressure limit:  .27100E+75 -.16820E+02  .13065E+05
   TROE centering:      .15270E+00  .29100E+03  .27420E+04  .77480E+04
      H2           Enhanced by    2.000E+00
      H2O          Enhanced by    6.000E+00
      CH4          Enhanced by    2.000E+00
      CO           Enhanced by    1.500E+00
      CO2          Enhanced by    2.000E+00
      C2H6         Enhanced by    3.000E+00
      AR           Enhanced by    7.000E-01
313. O+C3H8<=>OH+C3H7                       1.93E+05    2.7     3716.0
314. H+C3H8<=>C3H7+H2                       1.32E+06    2.5     6756.0
315. OH+C3H8<=>C3H7+H2O                     3.16E+07    1.8      934.0
316. C3H7+H2O2<=>HO2+C3H8                   3.78E+02    2.7     1500.0
317. CH3+C3H8<=>C3H7+CH4                    9.03E-01    3.6     7154.0
318. CH3+C2H4(+M)<=>C3H7(+M)                2.55E+06    1.6     5700.0
   Low pressure limit:  .30000E+64 -.14600E+02  .18170E+05
   TROE centering:      .18940E+00  .27700E+03  .87480E+04  .78910E+04
      H2           Enhanced by    2.000E+00
      H2O          Enhanced by    6.000E+00
      CH4          Enhanced by    2.000E+00
      CO           Enhanced by    1.500E+00
      CO2          Enhanced by    2.000E+00
      C2H6         Enhanced by    3.000E+00
      AR           Enhanced by    7.000E-01
319. O+C3H7<=>C2H5+CH2O                     9.64E+13    .0       .0
320. H+C3H7(+M)<=>C3H8(+M)                  3.61E+13    .0       .0
   Low pressure limit:  .44200E+62 -.13545E+02  .11357E+05
   TROE centering:      .31500E+00  .36900E+03  .32850E+04  .66670E+04
      H2           Enhanced by    2.000E+00
      H2O          Enhanced by    6.000E+00
      CH4          Enhanced by    2.000E+00
      CO           Enhanced by    1.500E+00
```

```
     CO2          Enhanced by   2.000E+00
     C2H6         Enhanced by   3.000E+00
     AR           Enhanced by   7.000E-01
321. H+C3H7<=>CH3+C2H5                      4.06E+06   2.2     890.0
322. OH+C3H7<=>C2H5+CH2OH                     2.41E+13    .0       .0
323. HO2+C3H7<=>O2+C3H8                     2.55E+10    .3    -943.0
324. HO2+C3H7=>OH+C2H5+CH2O                   2.41E+13    .0       .0
325. CH3+C3H7<=>2C2H5                     1.93E+13   -.3       .0
```

NOTE: A units mole-cm-sec-K, E units cal/mole

B.3 Warnatz mechanism

```
CHEMKIN INTERPRETER OUTPUT: CHEMKIN-II Version 3.1 Feb. 1993
                 DOUBLE PRECISION

                 -------------------------------
                 ELEMENTS     ATOMIC
                 CONSIDERED   WEIGHT
                 -------------------------------
                  1. C              12.0112
                  2. H              1.00797
                  3. O              15.9994
                  4. N              14.0067
                 -------------------------------

--------------------------------------------------------------------------------
                   C
                  P H
                  H A
                  A R
SPECIES          S G MOLEC    TEMPERATURE   ELEMENT COUNT
CONSIDERED       E E WEIGHT   LOW   HIGH      C H O N
--------------------------------------------------------------------------------
  1. H2          G 0  2.01594  300.0 5000.0  0 2 0 0
  2. O2          G 0 31.99880  300.0 5000.0  0 0 2 0
  3. O           G 0 15.99940  300.0 5000.0  0 0 1 0
  4. OH          G 0 17.00737  300.0 5000.0  0 1 1 0
  5. H2O         G 0 18.01534  300.0 5000.0  0 2 1 0
  6. H           G 0  1.00797  300.0 5000.0  0 1 0 0
  7. HO2         G 0 33.00677  300.0 5000.0  0 1 2 0
  8. H2O2        G 0 34.01474  300.0 5000.0  0 2 2 0
  9. CH4         G 0 16.04303  300.0 5000.0  1 4 0 0
 10. CO          G 0 28.01055  300.0 5000.0  1 0 1 0
```

```
11. CO2          G 0  44.00995  300.0 5000.0  1  0  2  0
12. CH2O          G 0  30.02649  300.0 5000.0  1  2  1  0
13. CHO          G 0  29.01852  300.0 5000.0  1  1  1  0
14. CH2OH         G 0  31.03446  250.0 4000.0  1  3  1  0
15. CH3OH         G 0  32.04243  300.0 5000.0  1  4  1  0
16. CH3          G 0  15.03506  300.0 5000.0  1  3  0  0
17. CH3O          G 0  31.03446  300.0 3000.0  1  3  1  0
18. CH           G 0  13.01912  300.0 5000.0  1  1  0  0
19. CH2          G 0  14.02709  250.0 4000.0  1  2  0  0
20. CH2(S)        G 0  14.02709  300.0 4000.0  1  2  0  0
21. C2H2         G 0  26.03824  300.0 5000.0  2  2  0  0
22. C2H3         G 0  27.04621  300.0 5000.0  2  3  0  0
23. C2H4         G 0  28.05418  300.0 5000.0  2  4  0  0
24. C2H5         G 0  29.06215  300.0 5000.0  2  5  0  0
25. C2H6         G 0  30.07012  300.0 4000.0  2  6  0  0
26. CH3O2         G 0  47.03386  300.0 5000.0  1  3  2  0
27. CH3O2H        G 0  48.04183  298.1 5000.0  1  4  2  0
28. C2H          G 0  25.03027  300.0 5000.0  2  1  0  0
29. HCCO          G 0  41.02967  300.0 4000.0  2  1  1  0
30. CH2CO         G 0  42.03764  300.0 5000.0  2  2  1  0
31. CH2CHO         G 0  43.04561  300.0 5000.0  2  3  1  0
32. CH3CO         G 0  43.04561  300.0 5000.0  2  3  1  0
33. CH3CHO         G 0  44.05358  300.0 5000.0  2  4  1  0
34. N2          G 0  28.01340  300.0 5000.0  0  0  0  2
35. NH3          G 0  17.03061  300.0 5000.0  0  3  0  1
36. NH2          G 0  16.02264  300.0 5000.0  0  2  0  1
37. NH           G 0  15.01467  300.0 5000.0  0  1  0  1
38. HNO          G 0  31.01407  300.0 5000.0  0  1  1  1
39. NO           G 0  30.00610  300.0 5000.0  0  0  1  1
40. N           G 0  14.00670  300.0 5000.0  0  0  0  1
41. N2H          G 0  29.02137  250.0 4000.0  0  1  0  2
42. N2O          G 0  44.01280  300.0 5000.0  0  0  1  2
43. HCN          G 0  27.02582  300.0 5000.0  1  1  0  1
44. CN           G 0  26.01785  300.0 5000.0  1  0  0  1
45. H2CN          G 0  28.03379  300.0 4000.0  1  2  0  1
46. HNO2          G 0  47.01347  300.0 4000.0  0  1  2  1
47. HCNO          G 0  43.02522  250.0 4000.0  1  1  1  1
48. NCO          G 0  42.01725  300.0 5000.0  1  0  1  1
49. HNCO          G 0  43.02522  300.0 4000.0  1  1  1  1
50. C2N2         G 0  52.03570  300.0 5000.0  2  0  0  2
51. C           G 0  12.01115  300.0 5000.0  1  0  0  0
52. NO2          G 0  46.00550  300.0 5000.0  0  0  2  1
----------------------------------------------------------------------------
```

REACTIONS CONSIDERED	(k = A T**b exp(-E/RT)) A	b	E
1. O2+H=OH+O	8.70E+13	.0	60300.0
2. H2+O=OH+H	5.06E+04	2.7	26300.0
3. H2+OH=H2O+H	1.00E+08	1.6	13800.0
4. OH+OH=H2O+O	1.50E+09	1.1	420.0
5. H+H+M=H2+M	1.80E+18	-1.0	.0
H2 Enhanced by	1.000E+00		
H2O Enhanced by	6.500E+00		
O2 Enhanced by	4.000E-01		
N2 Enhanced by	4.000E-01		
CO Enhanced by	7.500E-01		
CO2 Enhanced by	1.500E+00		
CH4 Enhanced by	3.000E+00		
6. O+O+M=O2+M	2.90E+17	-1.0	.0
H2 Enhanced by	1.000E+00		
H2O Enhanced by	6.500E+00		
O2 Enhanced by	4.000E-01		
N2 Enhanced by	4.000E-01		
CO Enhanced by	7.500E-01		
CO2 Enhanced by	1.500E+00		
CH4 Enhanced by	3.000E+00		
7. H+OH+M=H2O+M	2.20E+22	-2.0	.0
H2 Enhanced by	1.000E+00		
H2O Enhanced by	6.500E+00		
O2 Enhanced by	4.000E-01		
N2 Enhanced by	4.000E-01		
CO Enhanced by	7.500E-01		
CO2 Enhanced by	1.500E+00		
CH4 Enhanced by	3.000E+00		
8. H+O2+M=HO2+M	2.30E+18	-.8	.0
H2 Enhanced by	1.000E+00		
H2O Enhanced by	6.500E+00		
O2 Enhanced by	4.000E-01		
N2 Enhanced by	4.000E-01		
CO Enhanced by	7.500E-01		
CO2 Enhanced by	1.500E+00		
CH4 Enhanced by	3.000E+00		
9. HO2+H=OH+OH	1.50E+14	.0	4200.0
10. HO2+H=H2+O2	2.50E+13	.0	2900.0
11. HO2+H=H2O+O	3.00E+13	.0	7200.0

```
12. HO2+O=OH+O2                       1.80E+13    .0   -1700.0
13. HO2+OH=H2O+O2                      6.00E+13    .0       .0
14. HO2+HO2=H2O2+O2                    2.50E+11    .0   -5200.0
15. OH+OH+M=H2O2+M                     3.25E+22  -2.0       .0
      H2          Enhanced by  1.000E+00
      H2O         Enhanced by  6.500E+00
      O2          Enhanced by  4.000E-01
      N2          Enhanced by  4.000E-01
      CO          Enhanced by  7.500E-01
      CO2         Enhanced by  1.500E+00
      CH4         Enhanced by  3.000E+00
16. H2O2+H=H2+HO2                     1.70E+12    .0   15700.0
17. H2O2+H=H2O+OH                      1.00E+13    .0   15000.0
18. H2O2+O=OH+HO2                      2.80E+13    .0   26800.0
19. H2O2+OH=H2O+HO2                    5.40E+12    .0    4200.0
20. CO+OH=CO2+H                       4.76E+07   1.2     290.0
21. CO+HO2=CO2+OH                      1.50E+14    .0   98700.0
22. CO+O+M=CO2+M                       7.10E+13    .0  -19000.0
      H2          Enhanced by  1.000E+00
      H2O         Enhanced by  6.500E+00
      O2          Enhanced by  4.000E-01
      N2          Enhanced by  4.000E-01
      CO          Enhanced by  7.500E-01
      CO2         Enhanced by  1.500E+00
      CH4         Enhanced by  3.000E+00
23. CO+O2=CO2+O                       2.50E+12    .0  200000.0
24. CH+O=CO+H                         4.00E+13    .0       .0
25. CH+O2=CHO+O                        3.00E+13    .0       .0
26. CH+CO2=CHO+CO                      3.40E+12    .0    2900.0
27. CH+OH=CHO+H                        3.00E+13    .0       .0
28. CH+H2O=CH2O+H                      4.56E+12    .0   -3200.0
29. CH+H2O=CH2+OH                      1.14E+12    .0   -3200.0
30. CHO+M=CO+H+M                       7.10E+14    .0   70300.0
      H2          Enhanced by  1.000E+00
      H2O         Enhanced by  6.500E+00
      O2          Enhanced by  4.000E-01
      N2          Enhanced by  4.000E-01
      CO          Enhanced by  7.500E-01
      CO2         Enhanced by  1.500E+00
      CH4         Enhanced by  3.000E+00
31. CHO+H=CO+H2                       9.00E+13    .0       .0
32. CHO+O=CO+OH                        3.00E+13    .0       .0
33. CHO+O=CO2+H                        3.00E+13    .0       .0
```

34. CHO+OH=CO+H2O 1.00E+14 .0 .0
35. CHO+O2=CO+HO2 3.00E+12 .0 .0
36. CHO+CHO=CH2O+CO 3.00E+13 .0 .0
37. CH2+H=CH+H2 6.00E+12 .0 -7500.0
38. CH2+O=>CO+H+H 8.40E+12 .0 .0
39. CH2+CH2=C2H2+H2 1.20E+13 .0 3400.0
40. CH2+CH2=C2H2+H+H 1.10E+14 .0 3400.0
41. CH2+CH3=C2H4+H 4.20E+13 .0 .0
42. CH2+O2=CO+OH+H 1.30E+13 .0 6200.0
43. CH2+O2=CO2+H2 1.20E+13 .0 6200.0
44. CH2(S)+M=CH2+M 1.20E+13 .0 .0
    H2 Enhanced by 1.000E+00
    H2O Enhanced by 6.500E+00
    O2 Enhanced by 4.000E-01
    N2 Enhanced by 4.000E-01
    CO Enhanced by 7.500E-01
    CO2 Enhanced by 1.500E+00
    CH4 Enhanced by 3.000E+00
45. CH2(S)+O2=CO+OH+H 3.10E+13 .0 .0
46. CH2(S)+H2=CH3+H 7.20E+13 .0 .0
47. CH2(S)+CH3=C2H4+H 1.60E+13 .0 -2380.0
48. CH2O+M=CHO+H+M 5.00E+16 .0 320000.0
    H2 Enhanced by 1.000E+00
    H2O Enhanced by 6.500E+00
    O2 Enhanced by 4.000E-01
    N2 Enhanced by 4.000E-01
    CO Enhanced by 7.500E-01
    CO2 Enhanced by 1.500E+00
    CH4 Enhanced by 3.000E+00
49. CH2O+H=CHO+H2 2.30E+10 1.1 13700.0
50. CH2O+O=CHO+OH 4.15E+11 .6 11600.0
51. CH2O+OH=CHO+H2O 3.40E+09 1.2 -1900.0
52. CH2O+HO2=CHO+H2O2 3.00E+12 .0 54700.0
53. CH2O+CH3=CHO+CH4 1.00E+11 .0 25500.0
54. CH2O+O2=CHO+HO2 6.00E+13 .0 170700.0
55. CH3+M=CH2+H+M 1.00E+16 .0 379000.0
    H2 Enhanced by 1.000E+00
    H2O Enhanced by 6.500E+00
    O2 Enhanced by 4.000E-01
    N2 Enhanced by 4.000E-01
    CO Enhanced by 7.500E-01
    CO2 Enhanced by 1.500E+00
    CH4 Enhanced by 3.000E+00

```
56. CH3+M=CH+H2+M                    6.90E+14    .0   345030.0
    H2          Enhanced by   1.000E+00
    H2O         Enhanced by   6.500E+00
    O2          Enhanced by   4.000E-01
    N2          Enhanced by   4.000E-01
    CO          Enhanced by   7.500E-01
    CO2         Enhanced by   1.500E+00
    CH4         Enhanced by   3.000E+00
57. CH3+O=CH2O+H                   8.43E+13    .0       .0
58. CH3+H=CH4                    1.93E+36   -7.0   38000.0
59. CH3+OH=>CH3O+H                 2.26E+14    .0   64800.0
60. CH3O+H=>CH3+OH                 4.75E+16   -.1   88000.0
61. CH3+OH=>CH2(S)+H2O              2.30E+13    .0       .0
62. CH2(S)+H2O=>CH3+OH              7.90E+13    .0       .0
63. CH3+O2=>CH2O+OH                3.30E+11    .0   37400.0
64. CH3+HO2=CH3O+OH                1.80E+13    .0       .0
65. CH3+HO2=CH4+O2                 3.60E+12    .0       .0
66. CH3+CH3=>C2H4+H2               1.00E+16    .0  134000.0
67. CH3+CH3=C2H6                 1.69E+53  -12.0   81240.0
68. CH3O+M=CH2O+H+M                5.00E+13    .0  105000.0
    H2          Enhanced by   1.000E+00
    H2O         Enhanced by   6.500E+00
    O2          Enhanced by   4.000E-01
    N2          Enhanced by   4.000E-01
    CO          Enhanced by   7.500E-01
    CO2         Enhanced by   1.500E+00
    CH4         Enhanced by   3.000E+00
69. CH3O+H=CH2O+H2                 1.80E+13    .0       .0
70. CH3O+O2=CH2O+HO2               4.00E+10    .0    8900.0
71. CH2O+CH3O=>CH3OH+CHO               6.00E+11    .0   13800.0
72. CH3OH+CHO=>CH2O+CH3O               6.50E+09    .0   57200.0
73. CH3O+O=O2+CH3                1.10E+13    .0       .0
74. CH3O+O=OH+CH2O                 1.40E+12    .0       .0
75. CH2OH+M=CH2O+H+M               5.00E+13    .0  105000.0
    H2          Enhanced by   1.000E+00
    H2O         Enhanced by   6.500E+00
    O2          Enhanced by   4.000E-01
    N2          Enhanced by   4.000E-01
    CO          Enhanced by   7.500E-01
    CO2         Enhanced by   1.500E+00
    CH4         Enhanced by   3.000E+00
76. CH2OH+H=CH2O+H2                3.00E+13    .0       .0
77. CH2OH+O2=CH2O+HO2              1.00E+13    .0   30000.0
```

78. CH3O2+M=>CH3+O2+M 7.24E+16 .0 111100.0
H2 Enhanced by 1.000E+00
H2O Enhanced by 6.500E+00
O2 Enhanced by 4.000E-01
N2 Enhanced by 4.000E-01
CO Enhanced by 7.500E-01
CO2 Enhanced by 1.500E+00
CH4 Enhanced by 3.000E+00
79. CH3+O2+M=>CH3O2+M 1.41E+16 .0 -4600.0
H2 Enhanced by 1.000E+00
H2O Enhanced by 6.500E+00
O2 Enhanced by 4.000E-01
N2 Enhanced by 4.000E-01
CO Enhanced by 7.500E-01
CO2 Enhanced by 1.500E+00
CH4 Enhanced by 3.000E+00
80. CH3O2+CH2O=>CH3O2H+CHO 1.30E+11 .0 37700.0
81. CH3O2H+CHO=>CH3O2+CH2O 2.50E+10 .0 42300.0
82. CH3O2+CH3=>CH3O+CH3O 3.80E+12 .0 -5000.0
83. CH3O+CH3O=>CH3O2+CH3 2.00E+10 .0 .0
84. CH3O2+HO2=>CH3O2H+O2 4.60E+10 .0 -10900.0
85. CH3O2H+O2=>CH3O2+HO2 3.00E+12 .0 163300.0
86. CH3O2+CH3O2=>CH2O+CH3OH+O2 1.80E+12 .0 .0
87. CH3O2+CH3O2=>CH3O+CH3O+O2 3.70E+12 .0 9200.0
88. CH4+H=H2+CH3 1.30E+04 3.0 33600.0
89. CH4+O=OH+CH3 6.92E+08 1.6 35500.0
90. CH4+OH=H2O+CH3 1.60E+07 1.8 11600.0
91. CH4+HO2=H2O2+CH3 1.10E+13 .0 103100.0
92. CH4+CH=C2H4+H 3.00E+13 .0 -1700.0
93. CH4+CH2=CH3+CH3 1.30E+13 .0 39900.0
94. CH3OH=CH3+OH 9.51E+29 -4.3 404100.0
95. CH3OH+H=CH2OH+H2 4.00E+13 .0 25500.0
96. CH3OH+O=CH2OH+OH 1.00E+13 .0 19600.0
97. CH3OH+OH=CH2OH+H2O 1.00E+13 .0 7100.0
98. CH3OH+HO2=>CH2OH+H2O2 6.20E+12 .0 81100.0
99. CH2OH+H2O2=>HO2+CH3OH 1.00E+07 1.7 47900.0
100. CH3OH+CH3=CH4+CH2OH 9.00E+12 .0 41100.0
101. CH3O+CH3OH=>CH2OH+CH3OH 2.00E+11 .0 29300.0
102. CH2OH+CH3OH=>CH3O+CH3OH 2.20E+04 1.7 45400.0
103. CH3OH+CH2O=>CH3O+CH3O 1.53E+12 .0 333200.0
104. CH3O+CH3O=>CH3OH+CH2O 3.00E+13 .0 .0
105. CH3O2H=CH3O+OH 4.00E+15 .0 180500.0
106. OH+CH3O2H=H2O+CH3O2 2.60E+12 .0 .0

```
107. C2H+O=CO+CH                          1.00E+13   .0      .0
108. C2H+O2=HCCO+O                        3.00E+12   .0      .0
109. HCCO+H=CH2+CO                        1.50E+14   .0      .0
110. HCCO+O=>CO+CO+H                      9.60E+13   .0      .0
111. HCCO+CH2=C2H3+CO                     3.00E+13   .0      .0
112. C2H2+M=C2H+H+M                       3.60E+16   .0  446000.0
     H2          Enhanced by  1.000E+00
     H2O         Enhanced by  6.500E+00
     O2          Enhanced by  4.000E-01
     N2          Enhanced by  4.000E-01
     CO          Enhanced by  7.500E-01
     CO2         Enhanced by  1.500E+00
     CH4         Enhanced by  3.000E+00
113. C2H2+O2=HCCO+OH                      2.00E+08   1.5 126000.0
114. C2H2+H=C2H+H2                        6.02E+13   .0  116400.0
115. C2H2+O=CH2+CO                        2.17E+06   2.1   6570.0
116. C2H2+O=HCCO+H                        5.06E+06   2.1   6570.0
117. C2H2+OH=H2O+C2H                      6.00E+13   .0    54200.0
118. CH2CO+M=CH2+CO+M                     1.00E+16   .0   248000.0
     H2          Enhanced by  1.000E+00
     H2O         Enhanced by  6.500E+00
     O2          Enhanced by  4.000E-01
     N2          Enhanced by  4.000E-01
     CO          Enhanced by  7.500E-01
     CO2         Enhanced by  1.500E+00
     CH4         Enhanced by  3.000E+00
119. CH2CO+H=CH3+CO                       3.60E+13   .0    14100.0
120. CH2CO+O=CHO+CHO                      2.30E+12   .0    5700.0
121. CH2CO+OH=CH2O+CHO                    1.00E+13   .0      .0
122. C2H3=C2H2+H                       4.73E+40  -8.8  194500.0
123. C2H3+OH=C2H2+H2O                     5.00E+13   .0      .0
124. C2H3+H=C2H2+H2                       1.20E+13   .0      .0
125. C2H3+O=C2H2+OH                       1.00E+13   .0      .0
126. C2H3+O=CH3+CO                        1.00E+13   .0      .0
127. C2H3+O=CHO+CH2                       1.00E+13   .0      .0
128. C2H3+O2=CH2O+CHO                     3.00E+12  -.1   -3324.0
129. C2H3+O2=CH2CHO+O                     2.46E+15  -.8   13120.0
130. CH3CO=CH3+CO                      2.32E+26  -5.0   75120.0
131. CH3CO+H=CH2CO+H2                     2.00E+13   .0      .0
132. CH2CHO+H=CH2CO+H2                    2.00E+13   .0      .0
133. C2H4+M=C2H2+H2+M                     7.50E+17   .0  332000.0
     H2          Enhanced by  1.000E+00
     H2O         Enhanced by  6.500E+00
```

```
      O2          Enhanced by   4.000E-01
      N2          Enhanced by   4.000E-01
      CO          Enhanced by   7.500E-01
      CO2         Enhanced by   1.500E+00
      CH4         Enhanced by   3.000E+00
134. C2H4+M=C2H3+H+M                      8.50E+17    .0  404000.0
      H2          Enhanced by   1.000E+00
      H2O         Enhanced by   6.500E+00
      O2          Enhanced by   4.000E-01
      N2          Enhanced by   4.000E-01
      CO          Enhanced by   7.500E-01
      CO2         Enhanced by   1.500E+00
      CH4         Enhanced by   3.000E+00
135. C2H4+H=C2H3+H2                     5.40E+14    .0   62900.0
136. C2H4+O=CH2CHO+H                    1.02E+06   2.1       .0
137. C2H4+O=CHO+CH3                     2.42E+06   2.1       .0
138. C2H4+OH=C2H3+H2O                   2.20E+13    .0   24900.0
139. CH3CHO+M=CH3+CHO+M                    7.00E+15    .0  342800.0
      H2          Enhanced by   1.000E+00
      H2O         Enhanced by   6.500E+00
      O2          Enhanced by   4.000E-01
      N2          Enhanced by   4.000E-01
      CO          Enhanced by   7.500E-01
      CO2         Enhanced by   1.500E+00
      CH4         Enhanced by   3.000E+00
140. CH3CHO+H=CH3CO+H2                    2.10E+09   1.2   10100.0
141. CH3CHO+H=CH2CHO+H2                   2.00E+09   1.2   10100.0
142. CH3CHO+O=CH3CO+OH                    5.00E+12    .0    7600.0
143. CH3CHO+O=CH2CHO+OH                   8.00E+11    .0    7600.0
144. CH3CHO+O2=CH3CO+HO2                  4.00E+13    .0  164300.0
145. CH3CHO+OH=CH3CO+H2O                  2.30E+10    .7   -4700.0
146. CH3CHO+HO2=CH3CO+H2O2                3.00E+12    .0   50000.0
147. CH3CHO+CH2=CH3CO+CH3                 2.50E+12    .0   15900.0
148. CH3CHO+CH3=CH3CO+CH4                 2.00E-06   5.6   10300.0
149. C2H5=C2H4+H                       1.02E+43  -9.1  224150.0
150. C2H5+H=CH3+CH3                     3.00E+13    .0       .0
151. C2H5+O=CH3CHO+H                    5.00E+13    .0       .0
152. C2H5+O=CH2O+CH3                    1.00E+13    .0       .0
153. C2H5+O2=C2H4+HO2                   1.10E+10    .0   -6300.0
154. C2H5+CH3=C2H4+CH4                  1.14E+12    .0       .0
155. C2H5+C2H5=C2H4+C2H6                1.40E+12    .0       .0
156. C2H6+H=C2H5+H2                     1.40E+09   1.5   31100.0
157. C2H6+O=C2H5+OH                     1.00E+09   1.5   24400.0
```

158. C2H6+OH=C2H5+H2O 7.20E+06 2.0 3600.0
159. C2H6+HO2=C2H5+H2O2 1.70E+13 .0 85900.0
160. C2H6+O2=C2H5+HO2 6.00E+13 .0 217000.0
161. C2H6+CH2=C2H5+CH3 2.20E+13 .0 36300.0
162. C2H6+CH3=C2H5+CH4 1.50E-07 6.0 25400.0
163. NH3+H=NH2+H2 6.36E+05 2.4 42560.0
164. NH3+O=NH2+OH 1.10E+06 2.1 21780.0
165. NH3+OH=NH2+H2O 2.14E+06 2.0 1405.0
166. NH3+M=NH2+H+M 1.40E+16 .1 379060.0
H2 Enhanced by 1.000E+00
H2O Enhanced by 6.500E+00
O2 Enhanced by 4.000E-01
N2 Enhanced by 4.000E-01
CO Enhanced by 7.500E-01
CO2 Enhanced by 1.500E+00
CH4 Enhanced by 3.000E+00
167. NH2+H=NH+H2 6.03E+12 .0 .0
168. NH2+O=NH+OH 7.00E+12 .0 .0
169. NH2+O=HNO+H 4.50E+13 .0 .0
170. NH2+O=NO+H2 5.00E+12 .0 .0
171. NH2+OH=NH+H2O 9.00E+07 1.5 -1912.0
172. NH2+NH2=NH3+NH 6.30E+12 .0 41800.0
173. NH2+O2=HNO+OH 4.50E+12 .0 104600.0
174. NH2+O2=NH+HO2 1.00E+14 .0 209190.0
175. NH2+HO2=NH3+O2 4.53E+13 .0 .0
176. NH2+N=N2+H+H 7.20E+13 .0 .0
177. NH+H=N+H2 1.02E+13 .0 .0
178. NH+O=NO+H 7.00E+13 .0 .0
179. NH+OH=HNO+H 4.00E+13 .0 .0
180. NH+OH=NO+H2 2.40E+13 .0 .0
181. NH+OH=N+H2O 2.00E+09 1.2 25.0
182. NH+O2=HNO+O 4.61E+05 2.0 27170.0
183. NH+O2=NO+OH 1.00E+13 -.2 20080.0
184. NH+NH=N2+H+H 2.54E+13 .0 400.0
185. N+NH=N2+H 3.00E+13 .0 .0
186. N2H+OH=N2+H2O 3.00E+13 .0 .0
187. N2H+M=N2+H+M 1.70E+12 .0 59860.0
H2 Enhanced by 1.000E+00
H2O Enhanced by 6.500E+00
O2 Enhanced by 4.000E-01
N2 Enhanced by 4.000E-01
CO Enhanced by 7.500E-01
CO2 Enhanced by 1.500E+00

```
     CH4          Enhanced by   3.000E+00
188. N2H+NO=N2+HNO                    5.00E+13    .0       .0
189. N2H+O=N2O+H                      1.00E+14    .0       .0
190. N2H+O=NO+NH                      1.00E+13    .0       .0
191. N+OH=NO+H                        3.80E+13    .0       .0
192. N+O2=NO+O                        6.40E+09   1.0   26100.0
193. N+NO=N2+O                        3.27E+12    .3       .0
194. C2H2+N=HCN+CH                    1.04E+15   -.5       .0
195. C2H3+N=HCN+CH2                   2.00E+13    .0       .0
196. N+CO2=NO+CO                      1.90E+11    .0   14210.0
197. CH+N=CN+H                        1.30E+12    .0       .0
198. CH2+N=HCN+H                      5.00E+13    .0       .0
199. N+CH3=H2CN+H                     7.10E+13    .0       .0
200. HCCO+N=HCN+CO                    5.00E+13    .0       .0
201. NO+NH2=N2+H2O                    2.00E+20  -2.6    3870.0
202. NO+NH2=N2H+OH                    3.97E+11    .0   -1630.0
203. NO+NH2=N2+H+OH                   4.76E+15  -1.1     815.0
204. NO+NH=N2+OH                      2.16E+13   -.2       .0
205. NO+NH=N2O+H                      1.00E+14   -.3    -831.0
206. NO+OH+M=HNO2+M                   5.08E+12  -2.5     280.0
     H2           Enhanced by   1.000E+00
     H2O          Enhanced by   6.500E+00
     O2           Enhanced by   4.000E-01
     N2           Enhanced by   4.000E-01
     CO           Enhanced by   7.500E-01
     CO2          Enhanced by   1.500E+00
     CH4          Enhanced by   3.000E+00
207. NO+CH=HCN+O                      1.20E+14    .0       .0
208. NO+CH2=HCNO+H                    2.59E+12    .0   25000.0
209. NO+CH2=OH+HCN                    5.01E+11    .0   12000.0
210. NO+CH2(S)=HCN+OH                 2.00E+13    .0       .0
211. NO+CH3=HCN+H2O                   1.50E+12    .0   91000.0
212. NO+CH3=H2CN+OH                   1.00E+12    .0   91000.0
213. NO+CHO=CO+HNO                    7.20E+12    .0       .0
214. NO+C2H=HCN+CO                    2.11E+13    .0       .0
215. N2O+M=O+N2+M                     7.23E+17   -.7  262720.0
     H2           Enhanced by   1.000E+00
     H2O          Enhanced by   6.500E+00
     O2           Enhanced by   4.000E-01
     N2           Enhanced by   4.000E-01
     CO           Enhanced by   7.500E-01
     CO2          Enhanced by   1.500E+00
     CH4          Enhanced by   3.000E+00
```

```
216. N2O+H=OH+N2                          9.64E+13    .0   63140.0
217. N2O+OH=HO2+N2                         2.00E+12    .0   41840.0
218. N2O+O=NO+NO                          6.60E+13    .0  111410.0
219. N2O+O=N2+O2                          1.02E+14    .0  117230.0
220. N2O+CO=N2+CO2                         1.25E+12    .0   72310.0
221. NO2+M=NO+O+M                          1.10E+16    .0     275.9
     H2          Enhanced by   1.000E+00
     H2O         Enhanced by   6.500E+00
     O2          Enhanced by   4.000E-01
     N2          Enhanced by   4.000E-01
     CO          Enhanced by   7.500E-01
     CO2         Enhanced by   1.500E+00
     CH4         Enhanced by   3.000E+00
222. NO2+O=NO+O2                          1.00E+13    .0    2510.0
223. NO2+H=NO+OH                          3.50E+14    .0    6270.0
224. NO2+N=N2+O2                          1.81E+12    .0       .0
225. NO2+NO2=NO+NO+O2                          1.60E+12    .0  109190.0
226. NO+HO2=NO2+OH                         2.10E+12    .0   -2010.0
227. NO2+CHO=H+CO2+NO                         8.40E+15   -.8    8070.0
228. NO2+CHO=CO+HNO2                         2.10E+00   3.3    9820.0
229. CH3+NO2=CH3O+NO                         1.30E+13    .0       .0
230. CH2+NO2=CH2O+NO                         5.90E+13    .0       .0
231. CH+NO2=CHO+NO                         5.90E+13    .0       .0
232. NO2+CO=NO+CO2                         1.20E+14    .0  132090.0
233. HCCO+NO2=NCO+CO+OH                          5.00E+13    .0       .0
234. HCCO+NO2=HNCO+CO2                         5.00E+12    .0       .0
235. HCCO+NO2=HCN+CO2+O                         5.00E+12    .0       .0
236. HNO+H=NO+H2                          1.81E+13    .0    4157.0
237. HNO+OH=NO+H2O                         1.33E+07   1.9   -4000.0
238. HNO+N=NO+NH                          1.00E+13    .0    8300.0
239. HNO+NH2=NO+NH3                         5.00E+13    .0    4200.0
240. HNO+M=NO+H+M                          1.50E+16    .0  203480.0
     H2          Enhanced by   1.000E+00
     H2O         Enhanced by   6.500E+00
     O2          Enhanced by   4.000E-01
     N2          Enhanced by   4.000E-01
     CO          Enhanced by   7.500E-01
     CO2         Enhanced by   1.500E+00
     CH4         Enhanced by   3.000E+00
241. HNO+HNO=N2O+H2O                         3.90E+12    .0  209200.0
242. HNO+NO=N2O+OH                         2.00E+12    .0  108784.0
243. HNO+NO2=HNO2+NO                         6.02E+11    .0    8314.0
244. HNO+O2=NO+HO2                         3.16E+12    .0   12550.0
```

```
245. HNO2+H=NO2+H2                    1.20E+13    .0   30720.0
246. HNO2+O=NO2+OH                    1.20E+13    .0   25080.0
247. HNO2+OH=NO2+H2O                  1.30E+10   1.0     560.0
248. HCN+O=NCO+H                      1.11E+06   2.1   25570.0
249. HCN+O=NH+CO                      2.77E+05   2.1   25570.0
250. HCN+O=CN+OH                      2.70E+09   1.6  111190.0
251. HCN+OH=HNCO+H                    4.77E+11    .0   91450.0
252. H2CN+N=N2+CH2                    2.00E+13    .0       .0
253. H2CN+M=HCN+H+M                   3.00E+14    .0   91960.0
     H2          Enhanced by  1.000E+00
     H2O         Enhanced by  6.500E+00
     O2          Enhanced by  4.000E-01
     N2          Enhanced by  4.000E-01
     CO          Enhanced by  7.500E-01
     CO2         Enhanced by  1.500E+00
     CH4         Enhanced by  3.000E+00
254. CN+H2=HCN+H                      3.10E+05   2.5    9300.0
255. CN+O=CO+N                        1.00E+13    .0       .0
256. CN+OH=NCO+H                      6.00E+13    .0       .0
257. CN+O2=NCO+O                      6.60E+12    .0   -1700.0
258. CN+H2O=HCN+OH                    7.83E+12    .0   31120.0
259. CN+CH4=HCN+CH3                   9.03E+12    .0    7820.0
260. CN+NO2=NCO+NO                    3.00E+13    .0       .0
261. CN+NO=N2+CO                      1.07E+14    .0   33440.0
262. CN+NO=NCO+N                      9.64E+13    .0  176260.0
263. CN+HCN=C2N2+H                    2.00E+13    .0       .0
264. CN+N=N2+C                        1.04E+15   -.5       .0
265. CN+N2O=NCO+N2                    1.00E+13    .0       .0
266. C2N2+O=NCO+CN                    4.57E+12    .0   37120.0
267. NCO+H2=HNCO+H                    7.60E+02   3.0   16720.0
268. NCO+H=NH+CO                      5.24E+13    .0       .0
269. NCO+O=NO+CO                      4.20E+13    .0       .0
270. NCO+N=N2+CO                      2.00E+13    .0       .0
271. NCO+M=N+CO+M                     1.02E+15    .0  195400.0
     H2          Enhanced by  1.000E+00
     H2O         Enhanced by  6.500E+00
     O2          Enhanced by  4.000E-01
     N2          Enhanced by  4.000E-01
     CO          Enhanced by  7.500E-01
     CO2         Enhanced by  1.500E+00
     CH4         Enhanced by  3.000E+00
272. NCO+NO=N2O+CO                    6.20E+17  -1.7    3190.0
273. NCO+NO=N2+CO2                    7.80E+17  -1.7    3190.0
```

274. NCO+OH=CHO+NO	5.00E+12	.0	62700.0
275. NCO+O2=NO+CO2	2.00E+12	.0	83600.0
276. NCO+CHO=HNCO+CO	3.60E+13	.0	.0
277. NCO+NO2=CO+NO+NO	1.30E+13	.0	.0
278. NCO+NO2=CO2+N2O	5.40E+12	.0	.0
279. NCO+HNO=HNCO+NO	1.80E+13	.0	.0
280. NCO+NCO=N2+CO+CO	1.80E+13	.0	.0
281. N2+CH=HCN+N	1.57E+12	.0	75080.0
282. N2+CH2=HCN+NH	4.82E+12	.0	149650.0
283. HNCO+H=NH2+CO	2.25E+07	1.7	15900.0
284. HNCO+OH=NCO+H2O	6.40E+05	2.0	10700.0
285. HNCO+O2=HNO+CO2	1.00E+12	.0	146300.0
286. HNCO+O=NH+CO2	9.60E+07	1.4	35610.0
287. HNCO+O=NCO+OH	2.20E+06	2.1	47780.0
288. HNCO+O=HNO+CO	1.50E+08	1.6	184000.0
289. HNCO+NH2=NCO+NH3	5.00E+12	.0	25920.0
290. HNCO+NH=NCO+NH2	3.03E+13	.0	99070.0
291. HNO2+NCO=HNCO+NO2	3.60E+12	.0	.0
292. HNCO+HO2=NCO+H2O2	3.00E+11	.0	121220.0
293. HNCO+M=NH+CO+M	1.10E+16	.0	359480.0
H2 Enhanced by 1.000E+00			
H2O Enhanced by 6.500E+00			
O2 Enhanced by 4.000E-01			
N2 Enhanced by 4.000E-01			
CO Enhanced by 7.500E-01			
CO2 Enhanced by 1.500E+00			
CH4 Enhanced by 3.000E+00			
294. NO+HCCO=HCNO+CO	1.30E+13	.0	.0
295. HCNO+H=HCN+OH	1.00E+14	.0	50160.0
296. HCNO+H=HNCO+H	5.00E+10	.0	.0
297. C+NO=CN+O	6.60E+13	.0	.0
298. CH+H=C+H2	1.50E+14	.0	.0
299. C+O2=CO+O	5.00E+13	.0	.0

NOTE: E units Joules/mole, A units mole-cm-sec-K